Geothermal Resources of the Western Arm of the Black Rock Desert, Northwestern Nevada:

Part II, Aqueous Geochemistry and Hydrology

By Alan H. Welch and Alan M. Preissler

U.S. GEOLOGICAL SURVEY

Water-Resources Investigations Report 87-4062

Carson City, Nevada
1990

DEPARTMENT OF THE INTERIOR

MANUEL LUJAN, JR., Secretary

U.S. GEOLOGICAL SURVEY

Dallas L. Peck, Director

For additional information
write to:

U.S. Geological Survey
Room 227, Federal Building
705 North Plaza Street
Carson City, NV 89701

Copies of this report may be
purchased from:

U.S. Geological Survey
Books and Open-File Reports Section
Federal Center, Building 810
Box 25425
Denver, CO 80225

CONTENTS

ILLUSTRATIONS

TABLES

APPENDICES

CONVERSION FACTORS AND ABBREVIATIONS

Metric (International System) units of measure used in this report may be converted to "inch-pound" units by using the following factors:

Multiply	*By*	*To obtain*
Centimeters (cm)	0.3937	Inches (in.)
Cubic hectometers (hm^3)	810.7	Acre-feet (acre-ft)
Cubic meters per minute (m^3/min)	35.31	Cubic feet per minute (ft^3/min)
Kilometers (km)	0.6214	Miles (mi)
Liters per minute (L/min)	0.2642	Gallons per minute (gal/min)
Liters per second (L/s)	15.85	Gallons per minute (gal/min)
Meters (m)	3.281	Feet (ft)
Meters per meter (m/m)	1.000	Feet per foot (ft/ft)
Millimeters (mm)	0.03937	Inches (in.)
Square kilometers (km^2)	0.3861	Square miles (mi^2)
Square meters (m^2)	10.76	Square feet (ft^2)

For temperature, degrees Celsius (°C) can be converted to degrees Fahrenheit (°F) by using the formula °F = [(1.8)(°C)] + 32.

SEA LEVEL

In this report, "sea level" refers to the National Geodetic Vertical Datum of 1929 (NGVD of 1929), which is derived from a general adjustment of the first-order leveling networks of both the United States and Canada (formerly called "Sea Level Datum of 1929").

Geothermal Resources of the Western Arm of the Black Rock Desert, Northwestern Nevada:

Part II, Aqueous Geochemistry and Hydrology

By Alan H. Welch and Alan M. Preissler

ABSTRACT

The western arm of the Black Rock Desert includes several hydrothermal systems, some of which exceed 150 degrees and may exceed 200 degrees Celsius at depth, determined on the basis of chemical geothermometry. Geochemical and isotopic data, in conjunction with hydrologic and geophysical information, indicate that the hydrologically distinct systems are recharged by local meteoric water.

The cation composition of the thermal water appears to be controlled by aluminosilicate minerals that are common in other active geothermal systems. Close agreement between estimates of the equilibrium temperatures at which some mineral pairs are stable, and the more commonly applied geothermometer estimates, indicates that thermodynamic data may be useful for estimating deep aquifer temperatures. Use of a chemical geothermometer with a thermodynamic foundation (rather than an empirical formula) allows incorporation of geologic and mineralogic information into the evaluation of a geothermal system. Disadvantages of chemical geothermometers can be inadequate thermodynamic data and, as is the case for the western Black Rock Desert, lack of mineralogic data.

Thermal water at Great Boiling and Mud Springs has a chloride concentration of about 2,000 milligrams per liter and a total dissolved-solids concentration of about 4,500 milligrams per liter; the thermal water appears to have been affected by shallow evapotranspiration in an adjacent playa prior to deep circulation. The conclusion that shallow evapotranspiration affects the thermal water is based on the isotopically evolved character of the water and the correspondence between stable-isotope compositions and chloride concentrations in the thermal and local nonthermal water. The hydrothermal system at Trego Hot Springs and, perhaps, Fly Ranch in Hualapai Flat also may be recharged by water that has been affected by shallow evapotranspiration prior to deep circulation.

INTRODUCTION

Purpose and Scope

This report describes the results of a study to examine the basic hydrologic and geochemical data and to evaluate the validity of integrated conceptual models of the geothermal resources in the western arm of the Black Rock Desert, northern Great Basin. The most significant aspects of the study were: (1) The hydrologic connection, if any, between and among the various known thermal areas; (2) probable recharge paths to these thermal areas; and (3) controls on the aqueous geochemistry that can be deduced from information derived from springs and shallow wells. A multi-disciplinary approach was used, with emphasis on geochemistry and isotopic hydrology. Such an approach incorporates hydrologic, geochemical, and isotopic analyses and, thus, constrains conceptual heat- and mass-flow models more effectively than a limited study.

The study was confined to the western arm of the Black Rock Desert. This area provided an opportunity not only to examine the relations between the shallow nonthermal water and the deeper thermal water, but also to explore the relations among several shallow thermal areas. Data collection was limited primarily to shallow ground water. Geology and geophysics were discussed in a previous report (Schaefer and others, 1983).

Geographic Setting

The western arm of the Black Rock Desert is an area of about 2,000 km^2 in parts of Humboldt, Pershing, and Washoe Counties, Nevada (fig. 1). The major towns in this area, Gerlach and Empire, have an aggregate population of fewer than 1,000. A major geographic feature of the western Black Rock Desert region is a central, flat ephemeral lakebed (playa) at an altitude of about 1,190 m above sea level. The Granite Range and Calico Mountains to the west of the playa rise abruptly, reaching an altitude of 2,760 m at Granite Peak, the highest point in northwestern Nevada. To the east and south of the basin floor are the Black Rock and Selenite Ranges, respectively. The Quinn River, the largest surface-water source in the study area, discharges onto a low area at the southern end of the Black Rock Range. Hualapai Flat, a relatively small basin, is separated from the playa by a low ridge extending south from the Calico Mountains.

Thermal water discharges from springs and flowing wells from Soldier Meadow to Gerlach. Springs along the margins of the basin discharge thermal water, primarily at Soldier Meadow, from Double Hot Springs to the southern end of the Black Rock Range, at Trego, and near Gerlach. The thermal springs are generally undeveloped except for bathing and minor irrigation.

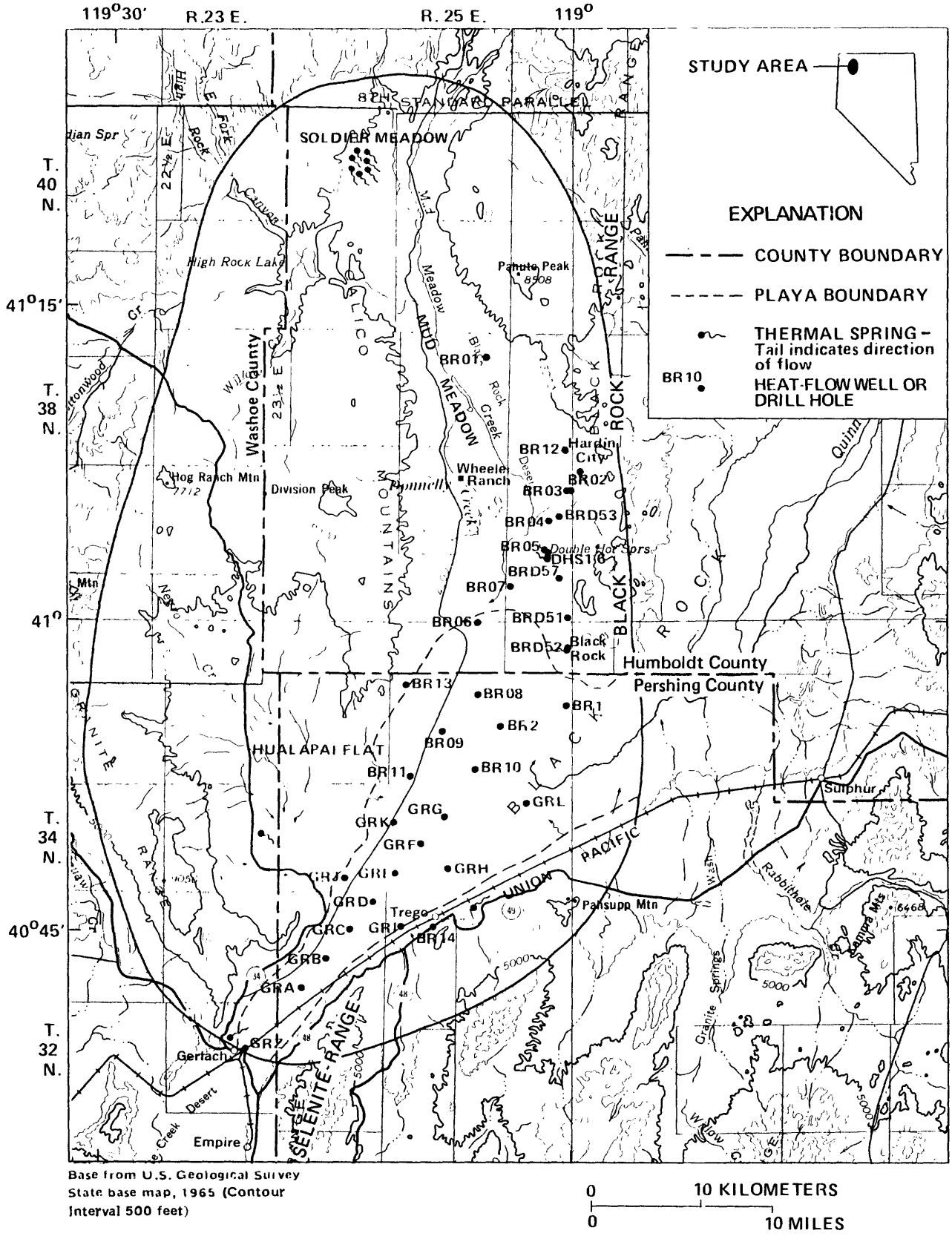

FIGURE 1.--Study area showing thermal springs, heat flow wells, and drill holes.

Previous Investigations

The geology and geophysics of the study area as related to the geothermal activity were discussed by Keller and Grose (1978a and b) and Schaefer and others (1983). Keller and Grose (1978a and b) presented results of geologic and geophysical investigations in the southern part of the study area and speculated on the nature of geothermal systems in the northern Basin and Range province. Schaefer and others (1983) discussed the geology and geophysics of a larger part of the western Black Rock Desert. Olmsted and others (1973), Keller and Grose (1978a and b), Garside and Schilling (1979), and Schaefer and others (1983) reviewed the main sources of information related to geothermal activity in this region. Sinclair (1963) conducted previous hydrologic studies on the Black Rock Desert, and Sinclair (1962) and Harrill (1969) provided basic information on Hualapai Flat, such as well locations, water-budget estimates, and some water-quality data. Olmsted and others (1975, p. 119-149) discussed the hydrology of the geothermal systems. Sanders and Miles (1974), Mariner and others (1974, 1975, and 1976), and Anderson (1977) presented analyses of thermal water.

The aqueous geochemistry and hydrology of other geothermal systems have been studied extensively. Results of previous work are discussed in appropriate sections as they apply to systems in the western Black Rock Desert.

Methods and Procedures

Geochemical sampling included field measurement and preservation of selected unstable parameters. Field procedures were similar to those outlined by Wood (1976).

Analyses for pH and alkalinity (reported as carbonate and bicarbonate) were done in the field. The pH measurements were made using Orion models 399A and 407A [1] portable meters. Measurements of pH were made after standardization using two buffers (with nominal pH values of 4, 7, or 10) that spanned the sample value. The standards were measured a second time after the field measurement. The standardization and measurement procedure was repeated until measured values for the separate standards before and after initial sample measurement agreed to within 0.2 pH units. The temperatures of the standards were brought to within 2 °C of the sample prior to measurement. Alkalinity was determined using the incremental method described by Wood (1976). The end point used for bicarbonate corresponded to the amount of acid added to reach the maximum rate of pH change per volume of titrant added.

Water temperature was measured using mercury-filled glass thermometers. Maximum reading thermometers were employed at thermal springs. The temperature measurements were taken as close to the source of the water as possible: flowing wells, at the top of the casing; and springs, as close as possible to areas with the greatest amount of flow.

Specific conductance measurements were made using a Yellow Springs Instrument Co. Model 33 m. Standards were measured that spanned the range of values measured in the field. The field values were corrected using the values measured for the standards and adjusted to a temperature of 25 °C.

---

[1] The use of trade names in this report is for identification purpose only and does not constitute endorsement by the U.S. Geological Survey.

Samples for cation and anion analysis were collected and filtered through 0.45 micrometer pore-size filters prior to placing in acid-washed polyethylene bottles. Doubly distilled nitric acid was added to samples collected for cation analysis to adjust the solution to a pH of about 2. Samples collected for anion analysis were not acidified. Samples collected for silica were diluted with deionized water when semi-quantitative field analysis indicated silica concentrations above 50 mg/L. The dilution was done to prevent polymerization of silica prior to analysis and is a commonly employed procedure for collection of geothermal samples. Samples collected for stable-isotope analysis were placed in 100-mL glass bottles with teflon-lined or polyseal caps. The caps were sealed with paraffin (generally within a week of collection) to guard against the loss of water vapor. All bottles and reagents were provided by the U.S. Geological Survey Central Laboratory in Arvada, Colo.

Gas samples were collected in an evacuated glass gas sampling tube. Samples were collected by placing an inverted funnel over areas in thermal springs that were evolving gas. The funnel and tubing that connected the funnel to the sampling tube were submerged so that they were initially full of water; the funnel then was placed over the rising gas. The water was displaced by the gas and a stopcock was opened to permit the gas to enter the sampling tube.

Most of the cations (calcium, magnesium, sodium, barium, lithium, manganese, strontium, and zinc) were analyzed using induction coupled plasma spectroscopy, unless the specific conductance was greater than 6,000 microsiemens per centimeter, in which case atomic absorption spectroscopy was used. All potassium analyses were done using atomic absorption spectroscopy. Chloride, silica, and boron concentrations were determined colorimetrically, and sulfate concentration was determined using a turbidimetric titration. An ion-selective electrode was used to analyze for fluoride. The stable-isotope analyses were determined using mass spectroscopy. Analyses of water are listed in appendixes 1 and 2. The gas analyses were done using chromatography.

Acknowledgments

Discussions with Frank Olmsted, U.S. Geological Survey, during the conduct of the study and the writing of this report were helpful and are gratefully acknowledged. Roger Jacobson, Desert Research Institute, Reno, Nev., provided some insight on the isotopic evolution of geothermal water in the Black Rock Desert.

HYDROLOGY

Climate

Climate in the western Black Rock Desert is typified by low rainfall, warm summers, and cold winters with large diurnal temperature changes. Average annual precipitation on the basin floor for the period 1931-57 is about 140 mm, on the basis of data collected in the Gerlach-Empire area (R. Olson, U.S. Weather Service, oral commun., 1985). Although higher altitude precipitation data are not available for northwestern Nevada, Sinclair (1963, table 1), using information from a map by Hardman (1936), estimated that areas above 2,130 m in altitude receive 380-510 mm of precipitation annually. Most of the precipitation falls during the non-summer months from storms moving westward over the Sierra Nevada.

Potential evaporation rates are high, although exact values have not been determined for the study area. The closest station where evaporation data have been collected is Rye Patch Dam, about 90 km east of Gerlach. About 760 mm was measured for the period June to September 1983; this represents several times the average annual precipitation rate. The rapid disappearance of a lake that generally forms during the winter

or early spring on the local playa gives a qualitative indication that actual evaporation rates can be high. The lake, which can cover an area of tens of square kilometers with depths reaching a meter or more, can evaporate over a few months' time and often is completely gone by early summer.

Water Budget

Approximate hydrographic boundaries are shown in figure 2. With the exception of the boundaries extending from the southern end of the Black Rock Range southward to Pahsupp Mountain and from the Granite Mountains to the Selenite Range, the limits of the ground-water system correspond with the approximate hydrologic boundaries determined by Sinclair (1963). Although some flow probably moves across some segments of the boundary, the volumes are probably small compared with the total flow in the system.

The development of a water budget for the western Black Rock Desert is made difficult by large uncertainties in several of the major components. Collection of data that would allow formulation of an accurate budget would require years of streamflow measurement--an effort beyond the scope of this study. Such a budget would be useful in constraining hydrologic models of the geothermal system. The following discussion is presented to document major problems associated with formulation of a water budget for the entire hydrographic area.

A water budget for the western Black Rock Desert can be represented by the formula:

$$Q_{riv} + Q_{prec} + Q_{if} = Q_{et} + Q_{phr} + Q_{of} \qquad (1)$$

where Q_{riv} = inflow from the Quinn River,

Q_{prec} = precipitation in the budget area,

Q_{if} = contribution from ground-water inflow,

Q_{et} = evaporation of surface and ground water from the playa,

Q_{phr} = evapotranspiration from phreatophytes and evaporation from thermal-spring pools, and

Q_{of} = ground-water outflow from the budget area.

Surface water supplied by the Quinn River is a major component of inflow to the study area; unfortunately, data are insufficient to accurately determine the average annual contribution from this source. The nearest surface-water gage (about 130 km northeast of Gerlach and about 110 river km upstream from the boundary of the study area on the Quinn River) has been operated for only 8 years (1964-67, 1978-81) and average discharge is about 3.2 m^3/min (U.S. Geological Survey, 1982, p. 332). The period of record does not include years of high flow, such as the 1983-84 water year, which may make the average much lower than the true average discharge (Otto Moosburner, U.S. Geological Survey, oral commun., 1985). Recharge from precipitation in the study area, on the basis of previous estimates, is about 70 m^3/min (table 1).

Inflow of ground water from basin-fill sediments between the southern end of the Black Rock Range and Pahsupp Mountain is difficult to estimate. The hydraulic gradient and the hydraulic conductivities are probably low and similar to those in basin-fill sediments farther west. The rate of inflow may be small relative to other components in the water budget.

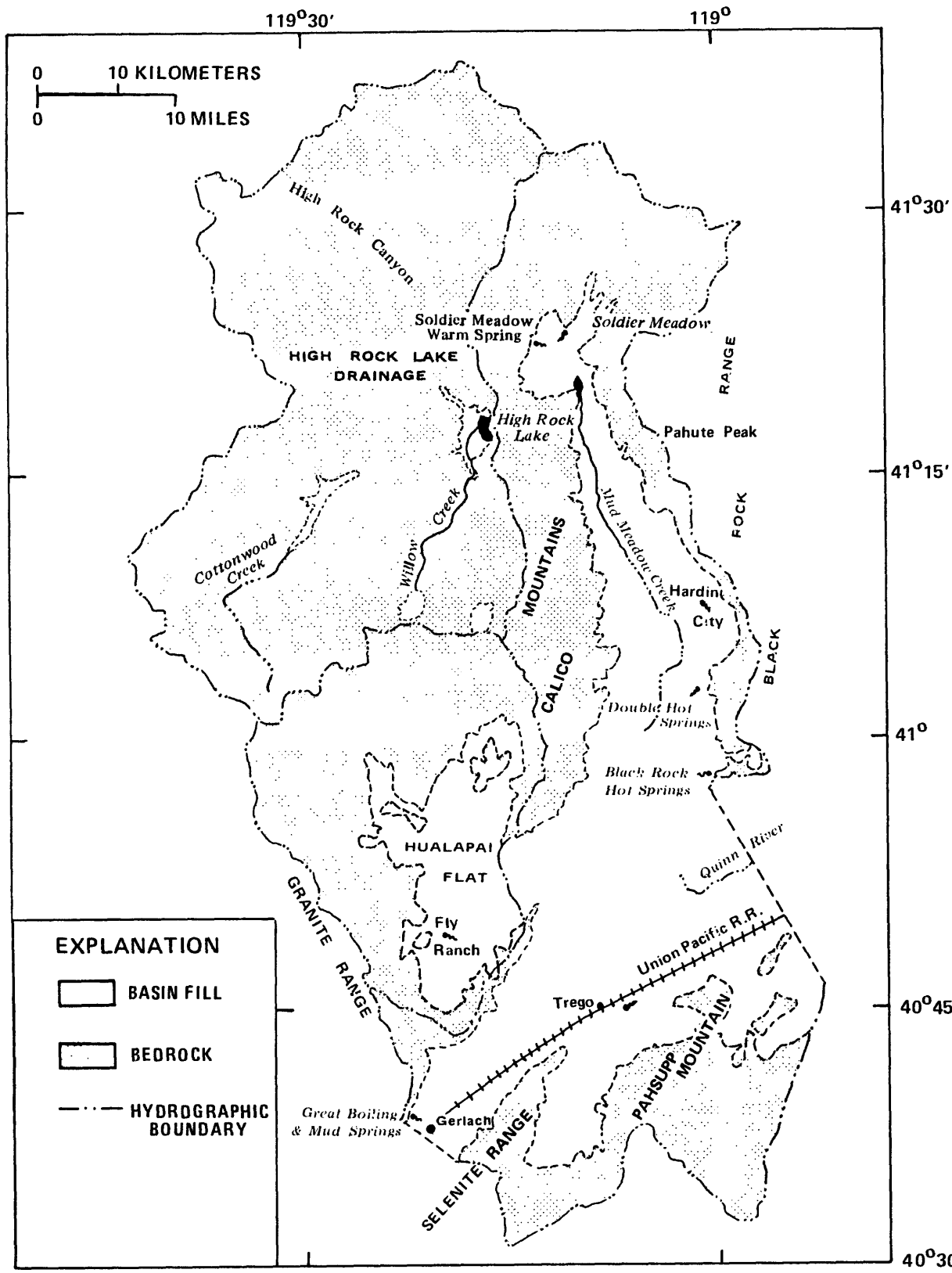

FIGURE 2.--Hydrographic boundaries in the western arm of the Black Rock Desert.

TABLE 1.--*Estimates of recharge from local precipitation*

[All values are from Sinclair (1963, table 1), except as noted.]

Area	Estimated recharge (cubic meters per minute)
Granite basin	5
Watershed south of the Union Pacific Railroad	[a]1
Hualapai Flat (Harrill, 1969, table 4)	16
West side of the Black Rock Range and the Calico Mountains	19
High Rock Lake drainage	30

[a] This value compares with 5 cubic meters per minute from Sinclair (1963). The lower value used here is estimated recharge from the Selenite Range and Pahsupp Mountain.

None of the components of the water budget that represent outflow from the system is well constrained. Evaporation of surface water from the playa is difficult to quantify because the average areal extent and depth of the ephemeral lake have not been measured. In some years the lake may cover an area of as much as 900 km^2. The depth of the lake is variable but may be 1 m or more. If the average depth were 8 cm, evaporation of the volume of water represented by the lake (72 hm^3) would be the largest discharge component in the budget for a year. This estimate, which corresponds to an average annual rate of about 140 m^3/min, is presented only to indicate a general order of magnitude for evaporation to allow comparison with other components in the budget. This value (140 m^3/min) is greater than all the other discharge components combined. A large error in this value prevents the formulation of a well-constrained budget. The other outflow components are probably much less than the amount of evaporation from the playa.

Evaporation of ground water from the playa can be estimated from vertical hydraulic conductivity and gradient data by employing Darcy's Law. On the basis of potentiometric measurements at paired wells in the playa, an average vertical hydraulic gradient is estimated to be about 0.01 m/m in the upper 100 m of sediment. Because available data are limited, this estimate is considered to be accurate only within a factor of about 3. The vertical intrinsic permeability of clay given by Morris and Johnson (1967, table 12) is $1x10^{-15}$ m^2 and is probably a reasonable estimate for the near-surface sediments. A 900-km^2 area would discharge about 0.22 hm^3/yr (assuming a density of 1 g/cm^3 and a viscosity corresponding to a temperature of 25 °C for the purpose of converting the intrinsic permeability to hydraulic conductivity), or about 0.4 m^3/min. This discharge is much less than the rough estimate for surface-water evaporation (140 m^3/min).

The rate of evapotranspiration from areas other than the central playa is probably much less than the direct evaporation rate for the playa. Estimates are not available for the entire study area. Available estimates for the various areas are shown in table 2. The procedure for estimating evapotranspiration consisted of combining either spring-flow data or phreatophyte mapping with estimates of evaporation from open water at the largest thermal springs (table 2). Areas of phreatophyte mapping conducted along the base of the Black Rock Range are shown in figure 3. Spring-flow data cannot be rigorously defended as an accurate measure of evapotranspiration--adoption of this approach was dictated by availability of existing data and the amount of effort required to obtain a better estimate. When flow data are used as a measure of evapotranspiration, the

TABLE 2.--*Estimates of evapotranspiration rates in the western arm of the Black Rock Desert, excluding the central playa*

Location (see figure 2)	Evapotranspiration rate (cubic meters per minute)	Method used for estimate	Reference
Great Boiling and Mud Springs	3.3	Phreatophyte mapping and estimate of lateral flow	Olmsted and others (1975, p. 145)
Trego Hot Springs	.075	Not specified	Waring (1965, p. 34)
Hualapai Flat	14.7	Phreatophyte mapping	Harrill (1969, table 9)
Fly Ranch	.5	Not specified	Brook and others (1979, p. 77)
Black Rock Hot Springs	.2	Not specified	Sinclair (1963, table 3)
Double Hot Springs	.9	Not specified	Sinclair (1963, table 3)
Base of Black Rock Range	1.9	Phreatophyte mapping	This study
Mud Meadow	6.0	Flow measurement	This study
Soldier Meadows	5.9	Flow measurement	This study
High Rock Lake drainage	8.2-9.4	Phreatophyte mapping and estimate of lake-surface evaporation	Sinclair (1963)

assumption is made that all the flow is lost to the atmosphere. In the case where spring flow supplies groundwater recharge, the evapotranspiration estimate will be too great. In areas where evapotranspiration is supplied by ground water, the estimate will be too low. Although phreatophyte mapping is not available for the entire area, such as the the eastern part of Soldier Meadow, most of the water that does discharge at the surface as a result of evapotranspiration is represented in table 2 (except for the playa, which is considered as a separate component).

Evaporation from the surfaces of thermal-spring pools contributes to the total discharge from the study area. Estimates of evaporation from thermal water are considered to represent only general magnitudes. The approach of Olmsted and others (1975, p. 71-72) is adopted for use here. Their approach is based on a quasi-empirical mass-transfer equation presented by Harbeck (1962). Data from Olmsted and others (1975, p. 70), based on weather data for Winnemucca (about 150 km east of Gerlach), were used to estimate evaporation rates for the thermal pools (table 3). Both the surface areas and temperatures are estimates. The temperatures were estimated using the measured temperatures (which represent maximum values for the pools) and arbitrarily subtracting 15 °C. The lower temperature is believed to more closely represent the temperature at the air-water interface, which is the value required by the adopted procedure.

The total evapotranspiration for the areas listed in table 2 is about 42 m^3/min. As noted above, this total probably represents most of the evapotranspiration for the western Black Rock Desert, except for evaporation directly from the playa. In comparison with the rough estimate of surface-water evaporation from the playa (140 m^3/min), the estimated evapotranspiration from the remaining part of the area is a considerably smaller component of the total discharge.

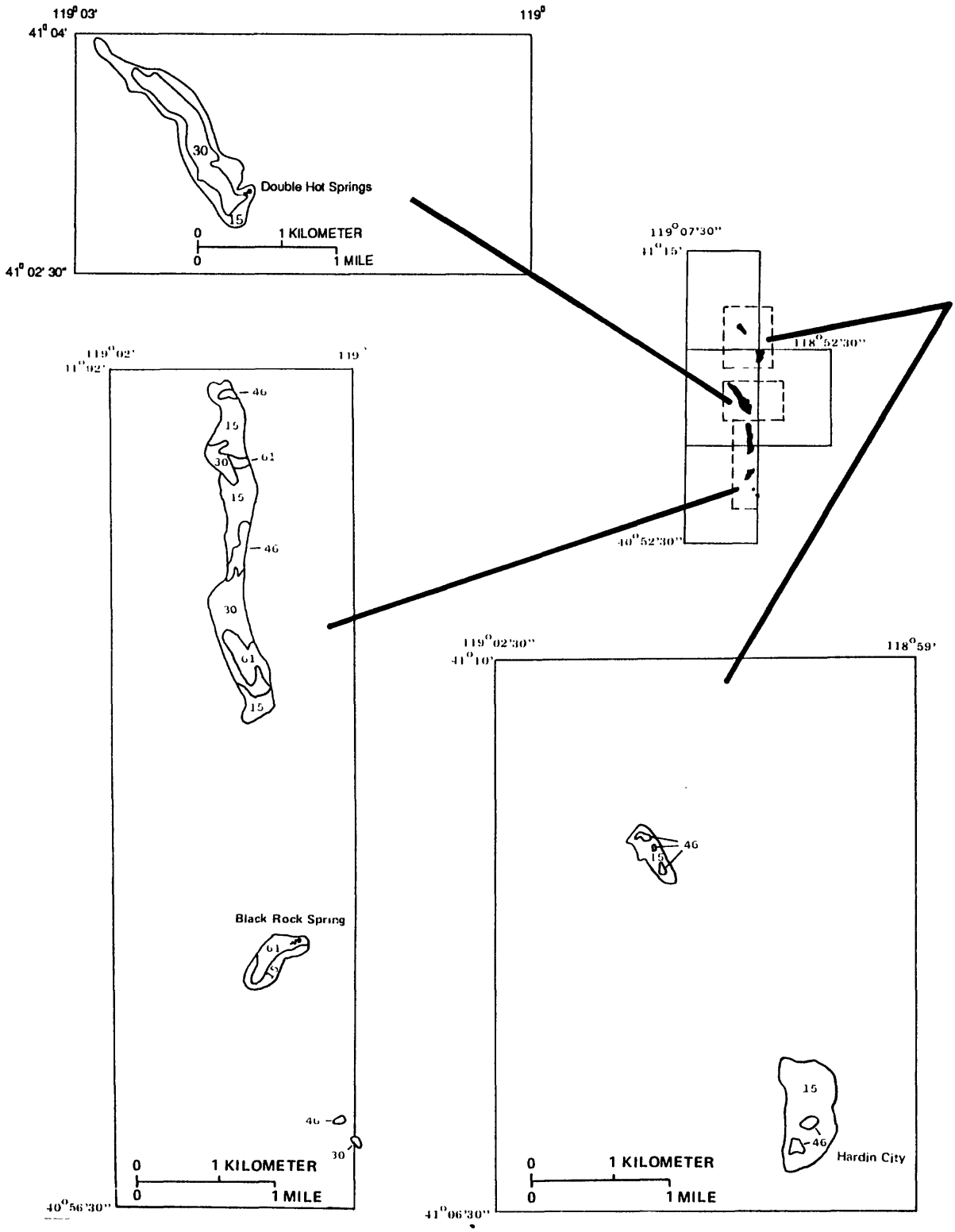

FIGURE 3.--Phreatophytes along the western flank of the Black Rock Range. (Values are estimated evapotranspiration based on vegetation type and density, in centimeters per year. Mapping was done by Patrick A. Glancy, U.S. Geological Survey, in 1983.)

TABLE 3.--*Estimates of evaporation from thermal pools*

[Evaporation rates are modified from Olmsted and others (1975, p. 72)]

Location	Surface area (square meters)	Surface temperature (degrees Celsius)	Evaporation rate (meters per year)	Total evaporation (liters per minute)
Pool at the southern end of the Black Rock Range	180	77	76	25
Double Hot Springs				
Orifice 4	260	45	18	9.1
Orifice 5	110	63	316	21

The amount of outflow from the western Black Rock Desert through the Gerlach-Empire area probably is small, as noted by Sinclair (1963, p. 15) because the horizontal hydraulic gradient in basin-fill sediments in the southern part of the area is small. On the basis of hydraulic head measurements in shallow (about 6 m) and intermediate (about 100 m) depth wells (appendix 3), the maximum difference in head in the playa is less than about 6 m. The low horizontal gradient indicates little horizontal flow in the playa sediments. Additionally, sediments in the Gerlach-Empire area are probably predominantly lacustrine deposits with a low hydraulic conductivity.

The estimated average annual ground-water recharge (assuming negligible ground-water inflow) is about 73 m^3/min, which is derived predominantly from local precipitation (70 m^3/min). The outflow estimate is dominated by two components--evaporation of surface water on the central playa (140 m^3/min) and from phreatophyte areas (42 m^3/min). The large apparent imbalance between inflow and outflow (73 compared with 180 m^3/min, respectively) is believed to reflect uncertainties in the estimates, rather than a real change in ground-water storage or the existence of a major, unaccounted for source of recharge (such as inflow through surrounding mountain blocks). Playa evaporation, which is the value with the greatest magnitude, probably is the primary cause of the imbalance, as the estimate is poorly constrained. Estimates of local precipitation-derived recharge and phreatophyte evaporation are probably more accurate and, thus, are the best indicators of the amount of water moving through the study area.

Shallow Ground-Water Flow

Movement of nonthermal water in the shallow subsurface cannot be fully described on the basis of available information. In general, ground water moves through consolidated sedimentary, igneous, and metamorphic rocks in the mountain blocks. Fracturing and faulting caused by multiple periods of tectonic activity and cooling (in the case of igneous volcanic rocks) have resulted in enhanced vertical hydraulic conductivity that may allow localized deep movement and recharge of geothermal systems. Ground-water movement in the basin-fill deposits is primarily intergranular.

In general, the shallow ground water moves from areas of higher to lower altitude. In the western Black Rock Desert, movement is generally north to south from Soldier Meadow through Mud Meadow to the playa. Some ground water also moves eastward from the High Rock Lake drainage, Granite basin, and Hualapai Flat. The ground-water system is recharged by precipitation in the mountains and from infiltration of streamflow through alluvial fans along the flanks of the mountains. Due to higher infiltration capacities recharge from infiltration of streamflow probably is more important in mountainous areas composed of low-hydraulic conductivity rock types such as the Granite Range than for areas such as the northern Calico Mountains which are underlain by fractured volcanic rocks.

Test holes were drilled in the western Black Rock Desert to collect geochemical, hydrologic, and heat-flow data. Drilling sites, shown in figure 1, are primarily on the playa and along the western base of the Black Rock Range. At some of the sites on the playa, two wells were drilled to compare hydraulic head at two different altitudes. Test holes were drilled along the base of the Black Rock Range to better define thermal discharge in that area. Some of the wells were pumped or allowed to flow for brief periods (generally less than 4 hours) to estimate the hydraulic conductivity, using the computational procedure of Brown (1963) and the Thiem (Thiem, 1906) equation.

Water-level contours are available for Hualapai Flat (Harrill, 1969, pl. 1) and the thermal area near Gerlach (Olmsted and others, 1975, fig. 20A). On the basis of water-level data collected during this study (appendix 3), notable hydrologic features of the area are the low hydraulic gradient in the playa sediments and the upward gradient beneath much of the valley floor.

As mentioned in the previous section, the apparently low hydraulic gradients in the playa deposits at the boundaries of the study area (south of the Black Rock Range and near Gerlach) indicate that little water is moving beneath these boundaries. Additionally, the horizontal hydraulic conductivity of these deposits is low, as indicated by brief aquifer tests at some of the flowing wells in the playa, conducted by using the procedure described by Jacob and Lohman (1952). The horizontal hydraulic conductivity of the playa sediments at a depth of about 100 m below land surface is estimated (from aquifer tests) to be $5x10^{-14}$ to $5x10^{-16}$ m^2. This range is in reasonable agreement with the value $1x10^{-1}$ m^2 for clay (Morris and Johnson, 1967, table 12). The hydraulic conductivity of the sediments can reasonably be expected to decrease with depth as a result of compaction, which would thereby further decrease the amount of flow at greater depths. Depths to bedrock south of the Black Rock Range appear to be less than about 300 m below land surface--much less than depths to bedrock beneath the playa farther to the west (Schaefer and others, 1983, pl. 4). Depths to bedrock between Gerlach and the Selenite Range appear to be between 300 and 600 m.

An upward hydraulic gradient in the upper 100 m of sediments (as indicated by data in appendix 3 for wells at sites GRB, D, I, and L and BR10) causes an upward component of flow. Low heat-flow values may indicate that recharge to a deep geothermal system is taking place beneath the playa (Mase and Sass, 1980). As will be discussed in a later section of the report, any downward flow in the playa sediments must be at depths greater than about 100 m below land surface.

Thermal Ground Water

Information on thermal ground water is limited to direct measurements at various thermal springs and a few shallow wells. Geophysical, geochemical, and isotopic data can be used indirectly to provide some information on the system. Nonetheless, lack of direct access to the deeper parts of the system prevents a complete description of the geothermal system. Integration of geophysical, geochemical, and hydrologic data will be considered in the "Summary and Conclusions" section; hydrologic aspects are discussed in this section.

For the purpose of discussion, water with a measured temperature of less than 25 °C is considered nonthermal, whereas water with a temperature greater than 25 °C is described as "thermal." The volume of thermal water moving through the study area is equivalent to a significant part (about one-third) of the local precipitation-derived recharge. Although the thermal water is not necessarily derived solely from precipitation in the local hydrologic basin, the quantity of thermal water appears to represent a significant part of total

ground-water flow in the area. The quantity of thermal ground water estimated to be discharging from the area is based on measured flows from springs and wells and on estimated evapotranspiration rates (as indicated by phreatophyte mapping and estimated evaporation from spring pools).

Hydraulic head relations among the various geothermal areas, as deduced from spring-pool altitudes and water levels in shallow wells (depths less than about 100 m), are similar to heads in the nonthermal system. In general, hydraulic head decreases southward from Soldier Meadow; heads in Great Boiling and Mud Springs are the lowest. Although the head relations indicate potential for a general southward flow, hydraulic connection between the various known thermal discharge areas cannot be demonstrated. The differing geochemical and isotopic compositions of the water, as discussed in the section on the aqueous geochemistry, indicate that the various major discharge areas do not represent upflow from a single geothermal system, at least not without significant recharge between the discharge areas.

AQUEOUS GEOCHEMISTRY

Major Constituents

A major part of the field work conducted in support of this project consisted of collecting and analyzing ground-water samples for major and minor chemical constituents and stable isotopes (locations shown in fig. 4). Results of previous analytical work are in appendix 1; chemical analyses obtained during this study are in appendix 2.

Major Element Evolution

The major element chemistry of water in the western Black Rock Desert varies primarily from a mixed cation-bicarbonate or mixed cation and anion type to a sodium-chloride-bicarbonate type (fig. 5). The more dilute mixed-cation water is generally from the higher altitudes--Soldier Meadow and Hualapai Flat (fields R, S, and U, respectively, in fig. 4). Increasing salinity in both thermal and nonthermal water roughly corresponds to increasing distance along the general shallow, ground-water flowpath (primarily from north to south). Salinity in the thermal water ranges from fairly dilute in Soldier Meadow (S) (dissolved-solids concentration about 250 mg/L) to moderate near Gerlach (G) (dissolved-solids concentration about 4,500 mg/L). Ranges of total dissolved solids in the nonthermal water are greater; water from higher altitudes (R) is more dilute than any of the thermal water and the saline water in the playa sediments (P) have the highest salinity. The anion chemistry of the thermal water generally shows an increasing chloride predominance with decreasing latitude (fig. 5 and appendixes 1 and 2). The predominance of chloride roughly correlates with the flow direction of the nonthermal water. This trend also generally correlates with an increase in dissolved-solids concentration. Thermal springs with higher dissolved-solids and chloride concentrations are near the playa.

The evolution of the geochemistry is similar to that in other closed basins (see Eugster and Hardie, 1978, and Eugster and Jones, 1979, for overviews of this subject). Although most of these previous investigations have centered on chemical evolution of surface water, methods used to examine processes responsible for geochemical evolution are applicable to this study. For this reason, a brief introduction is presented to provide a framework for understanding aqueous geochemistry in the western Black Rock Desert.

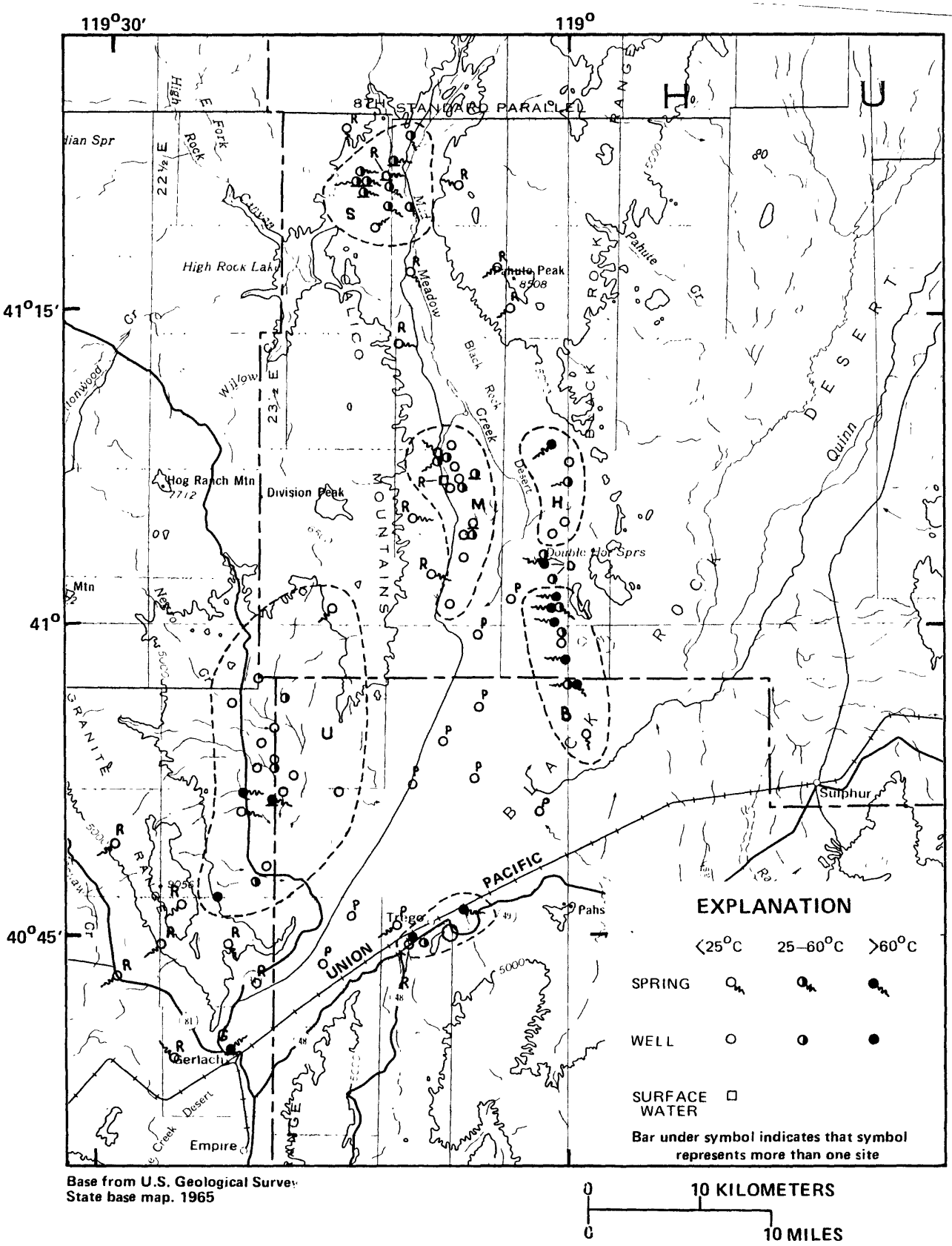

FIGURE 4.--Ground-water sampling locations. The letters indicate the sampling locality and generally from north to south are: S = Soldier Meadow, H = Hardin City, M = Mud Meadow, B = southern Black Rock Range, U = Hualapai Flat, P = playa, O = Trego Hot Springs and McClellen Ranch, G = Great Boiling and Mud Springs, and R = recharge (primarily upper altitude cold springs).

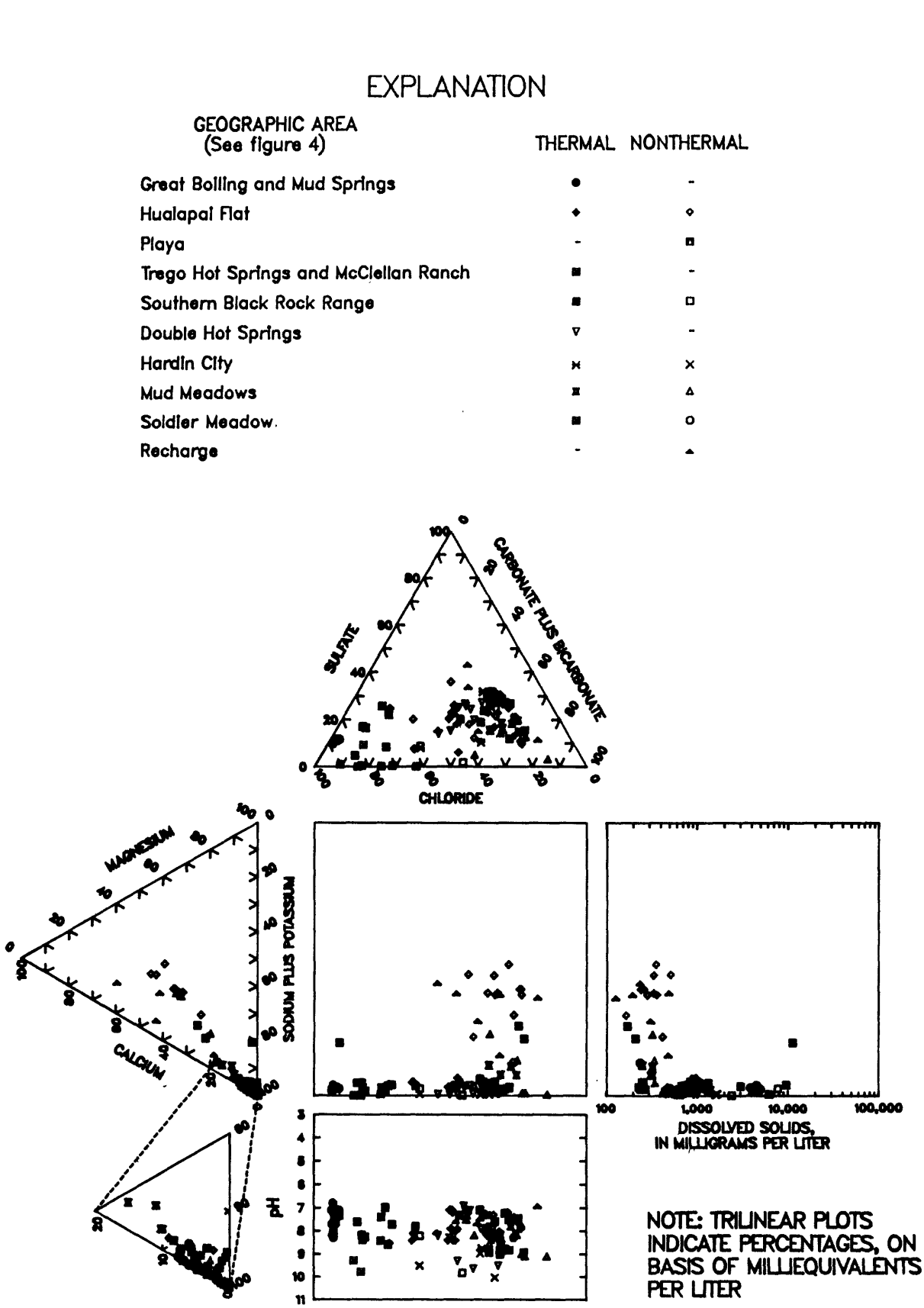

FIGURE 5.--Chemical types of ground water in the western arm of the Black Rock Desert. Sampling sites are shown in figure 4.

A change in predominant cations and anions corresponding to a general increase in salinity is a typical feature of ground-water systems affected by dissolution reactions or evaporative concentration, or both (Freeze and Cherry, 1979, p. 237-302). A typical anion sequence consists of the change from an initial carbonate plus bicarbonate-dominated water to a mixed anion and eventually a chloride-dominated water. Within the final chloride dominated type and commonly within the other types, the chloride concentration also can be used as an indicator of the geochemical "maturity." This increase in chloride has been used as an indicator of the general degree of evaporative concentration in closed basins (Eugster and Jones, 1979, p. 615). In the western Black Rock Desert, chloride becomes increasingly predominant from the Soldier Meadow-Mud Meadow area southward to Trego Hot Springs and to Great Boiling and Mud Springs. Sodium is typically the predominant cation in thermal water, as is the case for the water in this study area.

Chloride ions in natural water are usually conservative, neither removed from nor added to the aqueous phase by other processes over a wide range in concentration. Plotting the molar concentration of a solute versus chloride can assist in the examination of solute behavior in response to evaporative concentration (Eugster and Jones, 1979, p. 614, 615). Assuming that chloride concentrations provide a measure of evaporative concentration, then conservative solutes will plot along a path with a slope of 1. If solutes are removed from solution by other processes, the water will evolve along a path with a slope of less than 1. Solute addition from other processes that also do not supply chloride will result in an evolutionary path with a slope greater than 1. Processes that provide constant proportions of both the solute of interest and chloride will evolve along a path that asymptotically approaches a line with a slope equal to 1. For example, dissolution of halite (NaCl) will result in a path that approaches a line with a slope of 1 (as shown in fig. 6A) and an intercept of 0 on a plot of log (sodium) versus log (chloride).

The relation between sodium and chloride concentrations for ground water in the study area is shown in figure 6A. In general, sodium and chloride approach equal concentrations with increasing mineralization. The anion composition is less than 40 percent chloride in the more dilute water (the recharge, Soldier Meadow, and Hualapai Flat samples--fields R, S, and U, respectively). As chloride increasingly dominates the anion composition, the ratio of sodium to chloride approaches 1:1 at concentrations above about 1.5 log-millimole units (about 1,000 mg/L for sodium or chloride). The apparent asymptotic approach to equal concentrations of sodium and chloride could result from either evaporative concentration or dissolution of a mineral that contains equal proportions of these two elements. Because halite can be deposited in closed basins such as the Black Rock Desert, dissolution may be occurring. As will be discussed in the section on stable isotopes, the water in the playa and at Great Boiling and Mud Springs (the P and G samples, respectively) has been affected by evaporation. Water with intermediate chloride concentrations (about 100 to 1,000 mg/L--or about 0.45 to 1.5 log-millimole units) may be affected by evaporative concentration, halite dissolution, and mixing of water with varying concentrations. Except for Hualapai Flat (which is, in part, underlain by playa sediments), the geographic areas that yield water with low sodium and chloride concentrations (less than about 100 mg/L, or about 0.45 log-millimole units) do not appear to contain strata that are likely to contain halite.

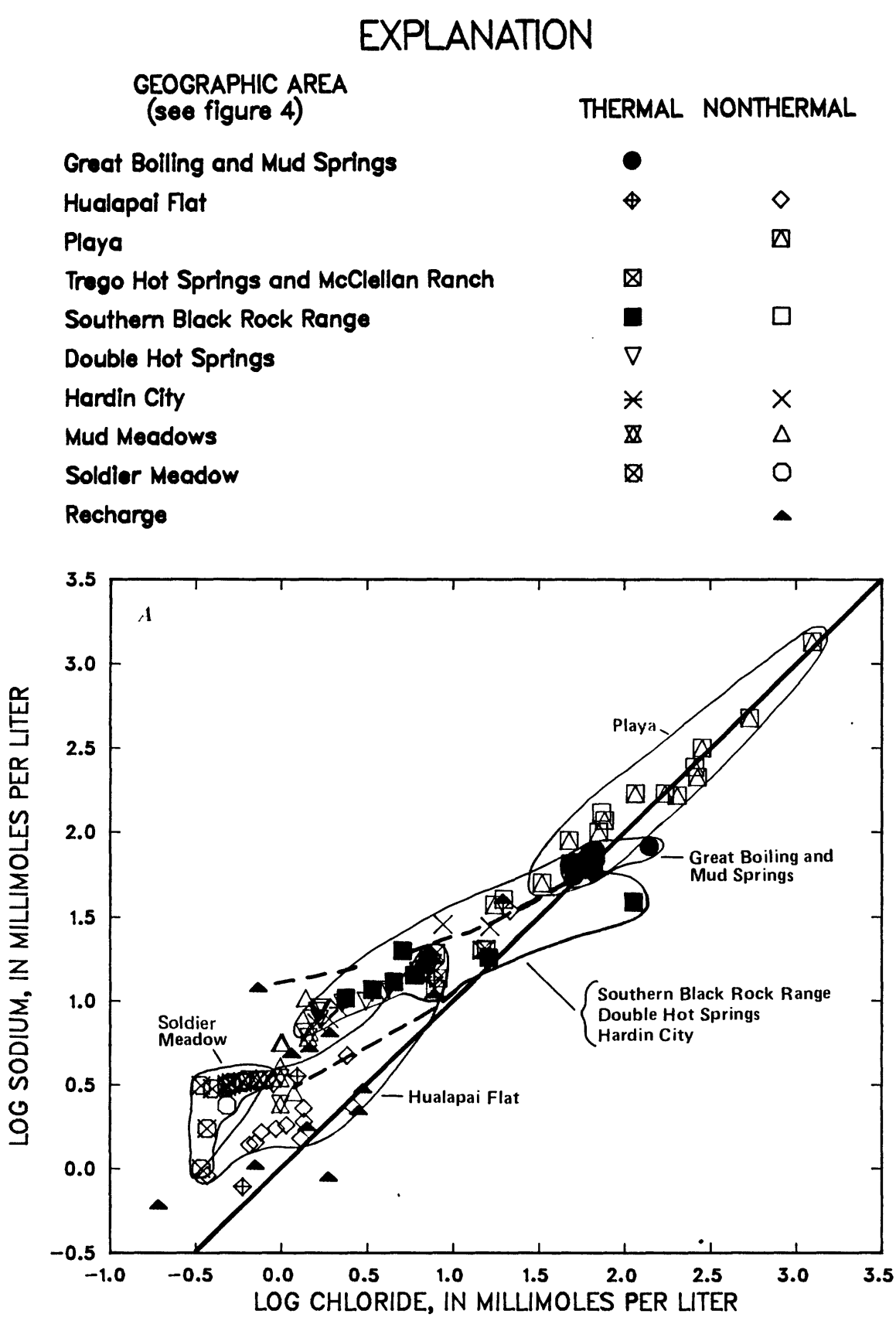

FIGURE 6.--Relations between chloride and *(A)* sodium, *(B)* potassium, *(C)* calcium, *(D)* magnesium, *(E)* sulfate, *(F)* total carbonate, and *(G)* carbonate alkalinity. The lines represent the slope that would result from conservation of the plotted constituents. The dashed line indicates the evolution resulting from dissolution of halite on figure 6A. Sampling sites are shown on figure 4.

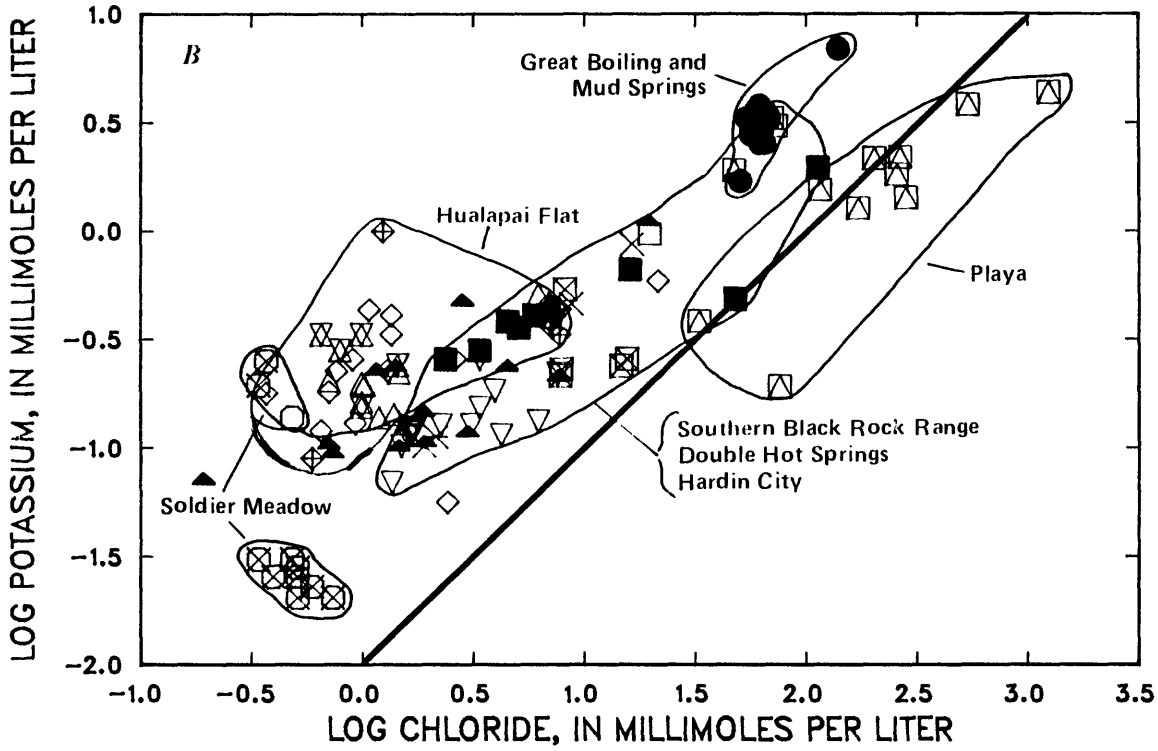

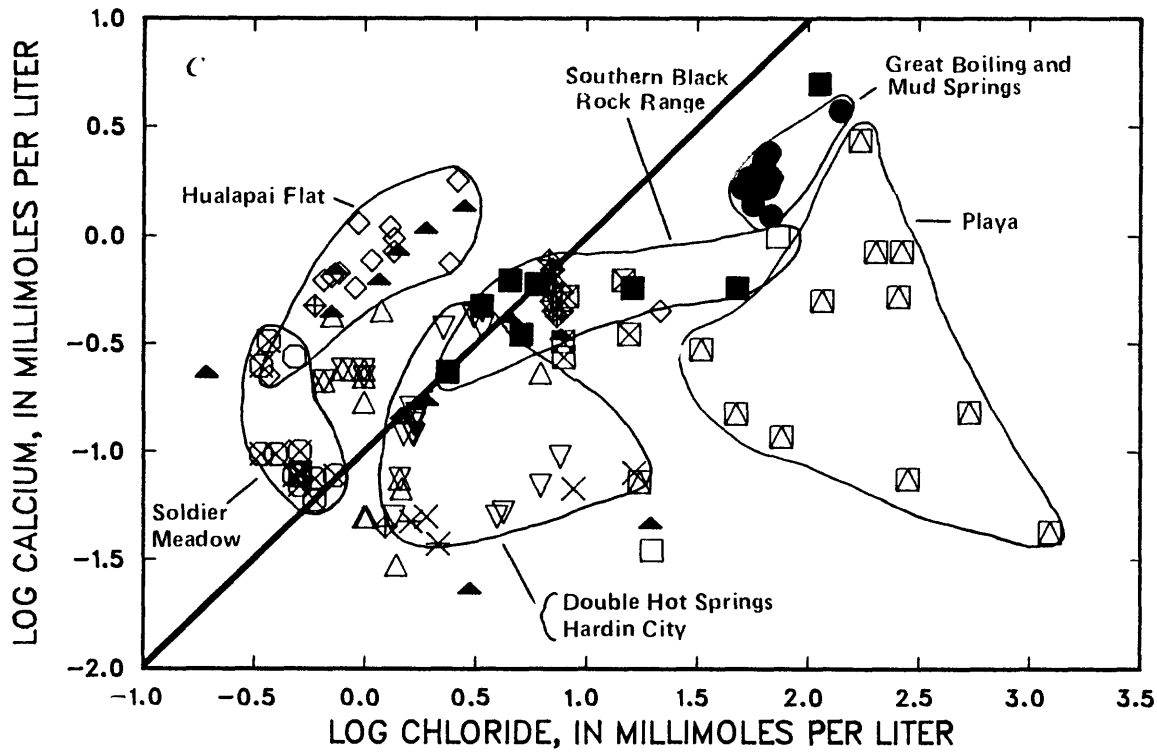

FIGURE 6.--Continued.

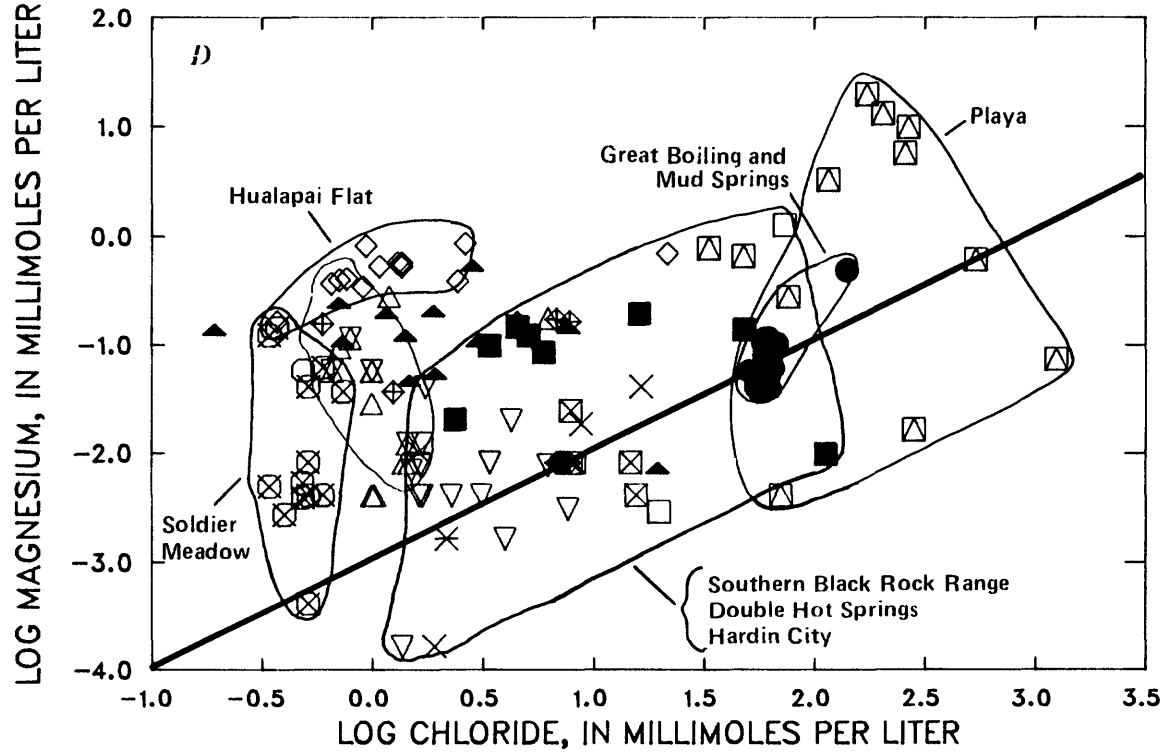

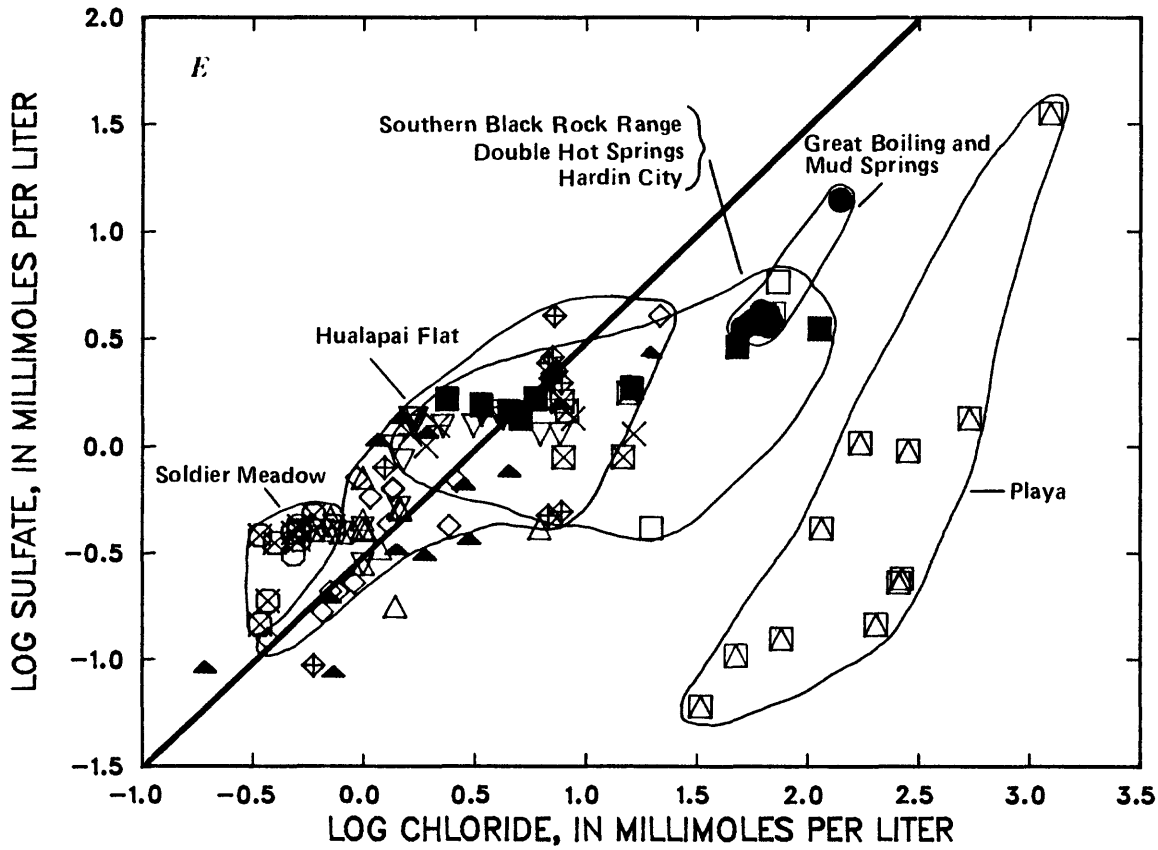

FIGURE 6.--Continued.

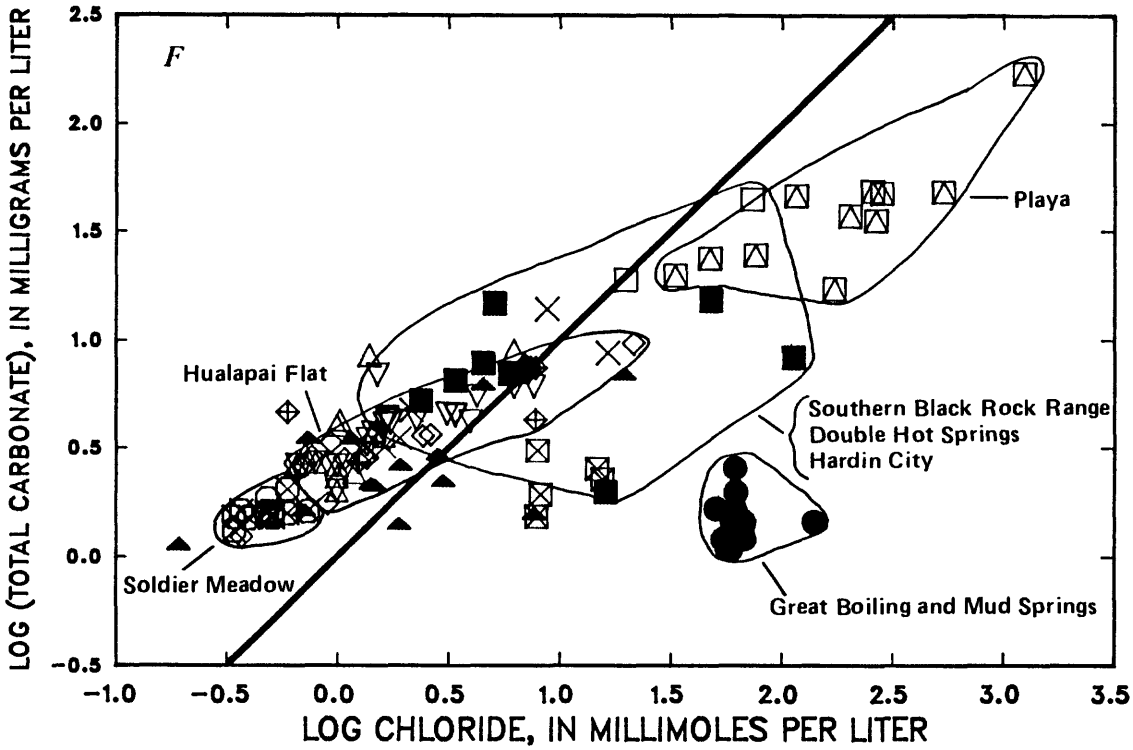

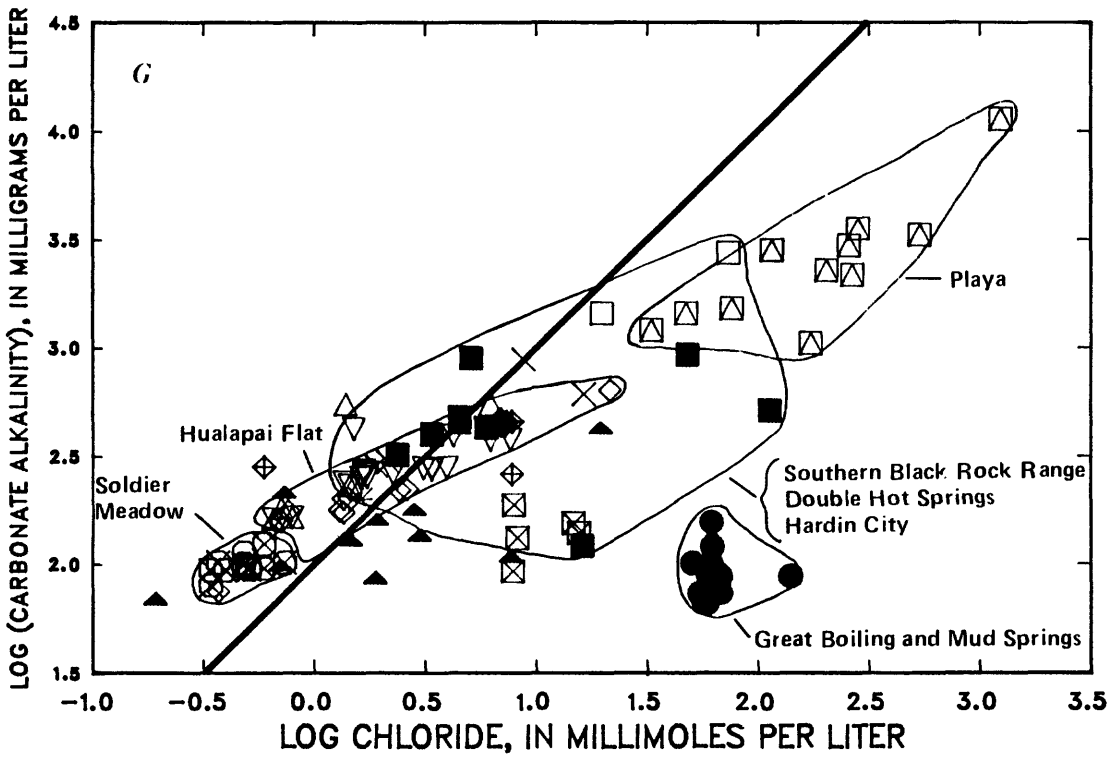

FIGURE 6.--Continued.

The potassium concentrations relative to those of chloride are shown in figure 6B. Potassium concentrations vary widely for samples with log (Cl) values of less than about 1.0. The samples from Soldier Meadow plot in two groups in figure 6B. The samples with the lower potassium concentrations have measured temperatures of 35 °C or greater, with the exception of a sample from a large pool that undoubtedly has been affected by conductive heat loss. A generally conservative trend is indicated by thermal water sampled at Soldier Meadow, along the western base of Black Rock Range (Hardin City, Double Hot Springs, and Black Rock area), Trego Hot Springs, and Great Boiling-Mud Springs. Potassium concentrations in the thermal water appear to be controlled by temperature-dependent reactions in the deeper parts of the geothermal systems as discussed in the geothermometry section. The samples from Hualapai Flat with source temperatures greater than 30 °C also plot along this conservative trend. The samples from wells drilled in playa sediments (the P samples) appear to define a second trend, although with lower potassium to chloride ratios, perhaps as a result of potassium removal by clays (as documented for saline Lake Abert by Jones and Weir, 1983) in the playa sediments.

The calcium and magnesium concentrations show considerable variation with respect to increasing chloride (figs. 6C and D). The plotting positions of the lower temperature water in Soldier Meadow and Hualapai Flat generally indicate conservation of calcium and magnesium. The thermal water samples show considerable scatter and water samples from the playa sediments show the greatest variation of any of the groups of samples.

The distinctly lower sulfate to chloride ratio in water from the playa than in other water in the study area indicates that there may be a sink for sulfate in the playa sediments. Bacterial reduction of sulfate to form hydrogen sulfide or iron sulfides is a mechanism for sulfate loss in other closed basins (see Eugster and Jones, 1979, p. 626, for a general discussion of this topic). The black muds penetrated during drilling on the playa in the Black Rock Desert form a suitable geochemical environment for the reduction of sulfate. All samples are well undersaturated with respect to gypsum; thus, precipitation of gypsum does not appear to be responsible for the apparent decrease in sulfate. Eugster and Jones (1979, p. 626) suggested that sulfate sorption also may be an important process in saline environments. The sulfate-to-chloride ratio in the sample from well GRL′, which contains the greatest chloride concentration, is greater than in the other playa samples. This indicates that the sulfate may be, at least in part, a result of oxidation of sulfide minerals. Dissolution of halite also would result in the lower sulfate-to-chloride ratio. Stable-isotope data, as discussed in a later section, indicate that evaporation rather than dissolution is probably the primary control on the chloride concentrations.

The effect of increasing mineralization on the total carbonate ($HCO_3^- + CO_3^{2-}$) and carbonate alkalinity ($HCO_3^- + 2CO_3^{2-}$) is indicated by figures 6F and 6G. A nonconservative trend with a slope less than 1 is formed by most of the points in both these figures. The decrease in inorganic carbon concentrations could be the result of outgassing or mineral precipitation. Because carbonate alkalinity is unaffected by carbon dioxide outgassing, the nonequilibrium trend indicated for the water in figure 6F may be the result of carbonate precipitation. Thermodynamic calculations made by using a modified version of the program SOLMNEQ (Kharaka and Barnes, 1973) indicate that almost all the water with source temperatures of about 50 °C or greater is at or near saturation with respect to calcite [considering the values of log (AP/K) in the range of ±0.5 to be in equilibrium as suggested by Paces, 1972]. The saturation indices for calcite are displayed in figure 7. Analyses that result in apparent oversaturation may be a result of shallow outgassing prior to the pH measurement. The relation between calcium and inorganic carbon in the playa sediments is consistent with evaporative concentration of these solutes resulting in calcite precipitation.

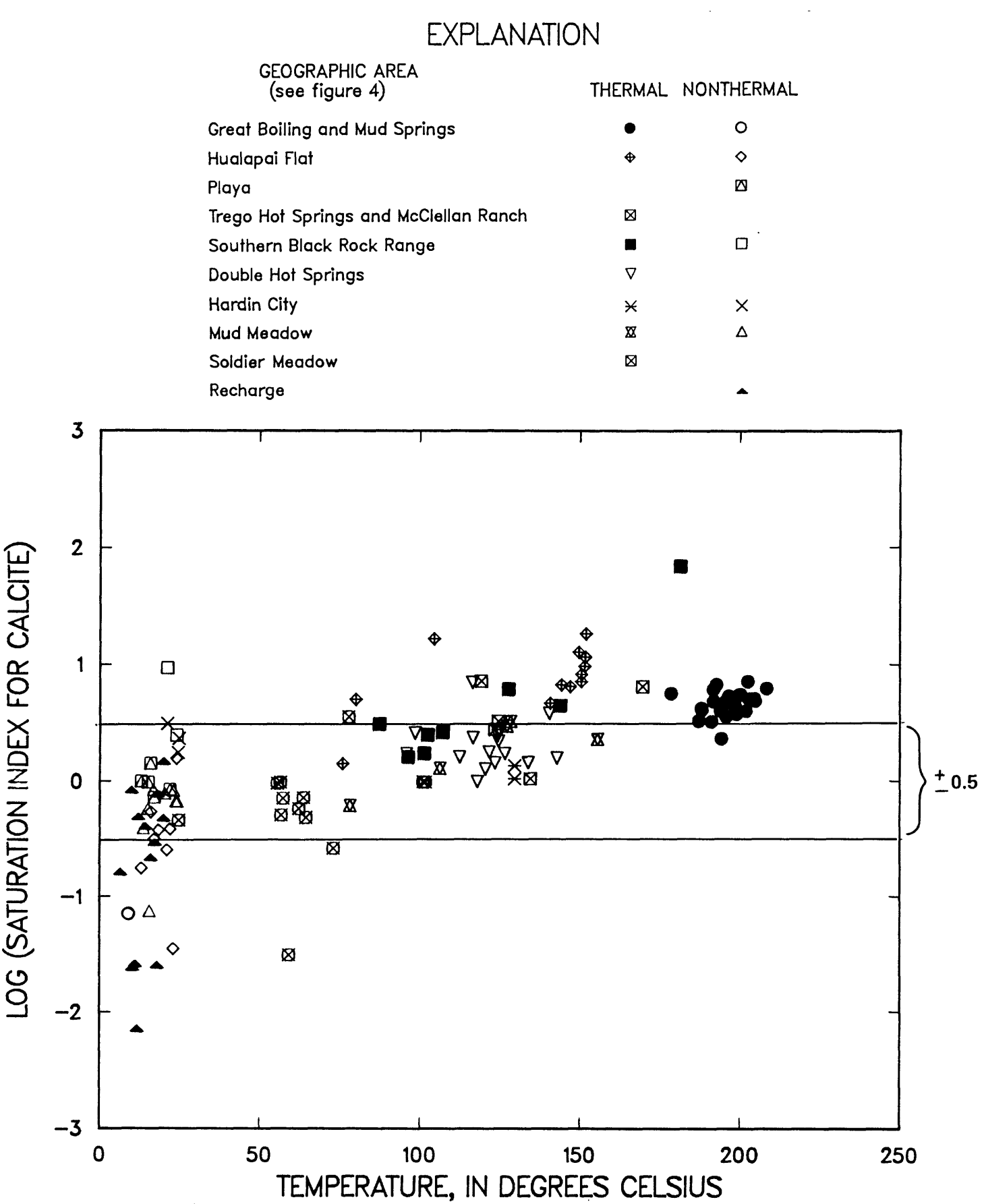

FIGURE 7.--Relation between the saturation index for calcite and temperature. The magnesium-corrected cation estimates are used for water with a source temperature greater than 25 °C; otherwise, the measured temperature is employed. Sampling sites are shown in figure 4.

Relations among major constituents with respect to increasin chloride concentrations are varied. Sodium and chloride concentrations approach equality with increasing mineralization, which appears to be a result of evaporative concentration (as indicated by the evolution of the stable isotopes) and, perhaps, some halite dissolution. Potassium concentrations show a generally nonconservative trend which, for the thermal water, is probably a result of temperature-dependent reactions at depth (as discussed in the section on geothermometry). Sulfate concentrations appear to be nonconservative in water with higher chloride concentrations, probably owing to the formation of mineral sulfides or the evolution of H_2S in the playa sediments.

Thermodynamic Controls

Activity diagrams can be used to evaluate thermodynamic controls on major cations. Plots of the activities of species in solution on an activity diagram can be compared to phase relations shown by idealized activity diagrams based on thermodynamic data. Sources of error associated with calculating the activities of species include the analytical methods (and associated sampling problems), the method of calculating the activities of the various species, and the thermodynamic data used in the aqueous model.

For this study, a modified version of the program SOLMNEQ (Kharaka and Barnes, 1973; Kharaka and Mariner, 1977) was used to calculate the activities. The activities were calculated for all the complete analyses and for the thermal water, the activities were calculated at magnesium-corrected Na-K-Ca temperature (Fournier and Potter, 1979). The calculations using the higher temperature more closely approximate conditions in the deep thermal aquifer. The thermodynamic data used in the calculations have been updated by Y.K. Kharaka to include more recent work by Helgeson and others (1974, 1978, 1981); the improved thermodynamic data have been used for the calculations. All activities and saturation indices presented in this report result from these calculations.

Problems associated with producing a theoretical activity diagram include the selection of appropriate phases and their corresponding thermodynamic data. Phase selection is complicated by the lack of lithologic information on the deep aquifers. In this study, slopes formed by the calculated activities and the occurrence of minerals in other hydrothermal systems were used to identify appropriate phases. The selection of thermodynamic data is a problem in spite of major advances in evaluating existing data at 25 °C and elevated temperatures (Helgeson, 1969; Helgeson and others, 1974, 1978, 1981; Robie and others, 1978). Despite these problems, activity diagrams appear to be useful in indicating the possible controlling phases.

The generalized summary of phases present in active geothermal systems (fig. 8) was used as a guide in selecting phases for consideration. The temperature range of about 100-200 °C is considered reasonable for the systems in the western Black Rock Desert. Phases considered as possibly stable (at equilibrium) include calcite, quartz, montmorillonite, albite, laumontite, and wairakite for the system $Ca\text{-}Na\text{-}K\text{-}CO_2\text{-}Si\text{-}H_20$. Magnesium was not considered because adequate thermodynamic data were lacking for magnesium-bearing minerals.

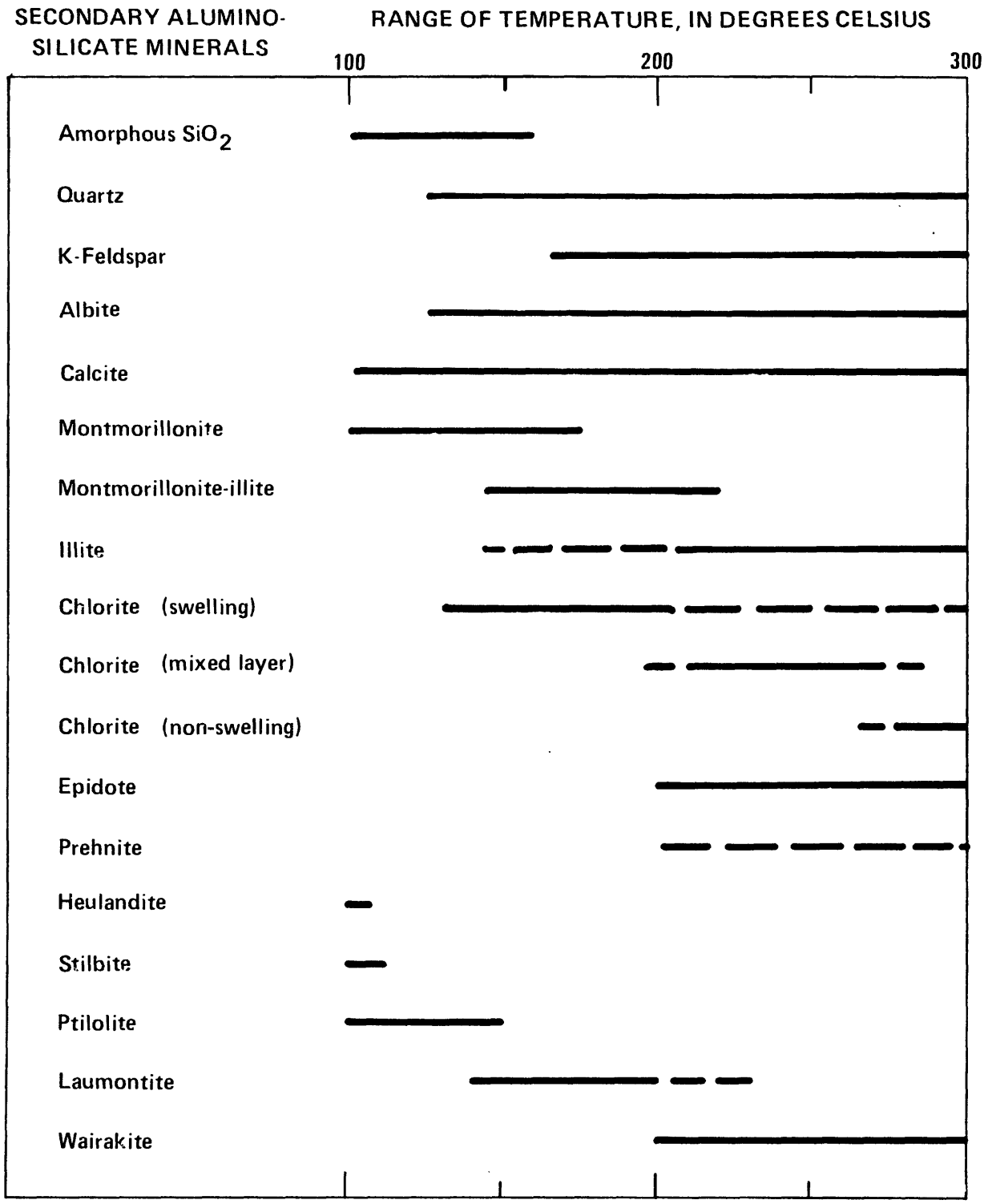

FIGURE 8.--Temperatures over which secondary aluminosilicate minerals have been observed in active geothermal systems. Solid lines indicate the most commonly observed temperature ranges. The three chlorite stability ranges indicate swelling, mixed layer, and non-swelling chlorite with increasing temperature. Modified after Henly and Ellis (1983).

Data plotted in figure 9A indicate that: (1) the sodium-to-potassium activity ratio is different for the geothermal areas consisting of Soldier Meadow, Hardin City-Double Hot Springs-southern Black Rock Range, Hualapai Flat, and Great Boiling and Mud Springs; and (2) each of the above areas plots on a slope of 1. A slope formed by plotting activity ratios is a strong indication that some mineral phases are controlling the relative activities. Furthermore, the slope can be a useful indicator of phases that may be controlling the activities. In the case of the sodium-potasssium activities, the slope of 1 is consistent with either an albite-microcline or Na-montmorillonite-Ca-montmorillonite phase boundary. The associated controlling reactions can be derived from the reactions for the minerals as follows:

For Na-montmorillonite and K-montmorillonite:

$$\underset{\text{Na-montmorillonite}}{3\,Na_{0.33}Al_{2.33}Si_{3.67}O_{10}(OH)_2} + 30\,H_2O + 6\,OH^- = Na^+ + 7\,Al(OH)_4^- + 11\,H_4SiO_4^0 \qquad (2)$$

$$\underset{\text{K-montmorillonite}}{3\,K_{0.33}Al_{2.33}Si_{3.67}O_{10}(OH)_2} + 30\,H_2O + 6\,OH^- = K^+ + 7\,Al(OH)_4^- + 11\,H_4SiO_4^0 \qquad (3)$$

By subtracting the second reaction from the first, and adding a hydrogen ion to each side, the result is:

$$\underset{\text{Na-montmorillonite}}{3\,Na_{0.33}Al_{2.33}Si_{3.67}O_{10}(OH)_2} + K^+ + H^+ = \underset{\text{K-montmorillonite}}{3\,K_{0.33}Al_{2.33}Si_{3.67}O_{10}(OH)_2} + Na^+ + H^+ \qquad (4)$$

and the associated thermodynamic relation is:

$$\text{Log}\frac{[Na^+]}{[H^+]} - \log\frac{[K^+]}{[H^+]} = 3[\log K_T(\text{Na-montmorillonite}) - \text{Log}\,K_T(\text{K-montmorillonite})] \qquad (5)$$

where the brackets indicate activities and K_T is the temperature-dependent equilibrium constant for the indicated mineral.

Similarly for albite and microcline:

$$\underset{\text{Albite}}{NaAlSi_3O_8} + 8\,H_2O = Na^+ + Al(OH)_4^- + 3\,H_4SiO_4^0 \qquad (6)$$

$$\underset{\text{Microcline}}{KAlSi_3O_8} + 8\,H_2O = K^+ + Al(OH)_4^- + 3\,H_4SiO_4^0 \qquad (7)$$

By subtracting as before:

$$\underset{\text{Albite}}{NaAlSi_3O_8} + K^+ - H^+ = \underset{\text{Microcline}}{KAlSi_3O_8} + Na^+ - H^+ \qquad (8)$$

the associated thermodynamic relation is:

$$\text{Log}\frac{[Na^+]}{[H^+]} - \log\frac{[K^+]}{[H^+]} = \log K_T(\text{albite}) - \log K_T(\text{microcline}) \qquad (9)$$

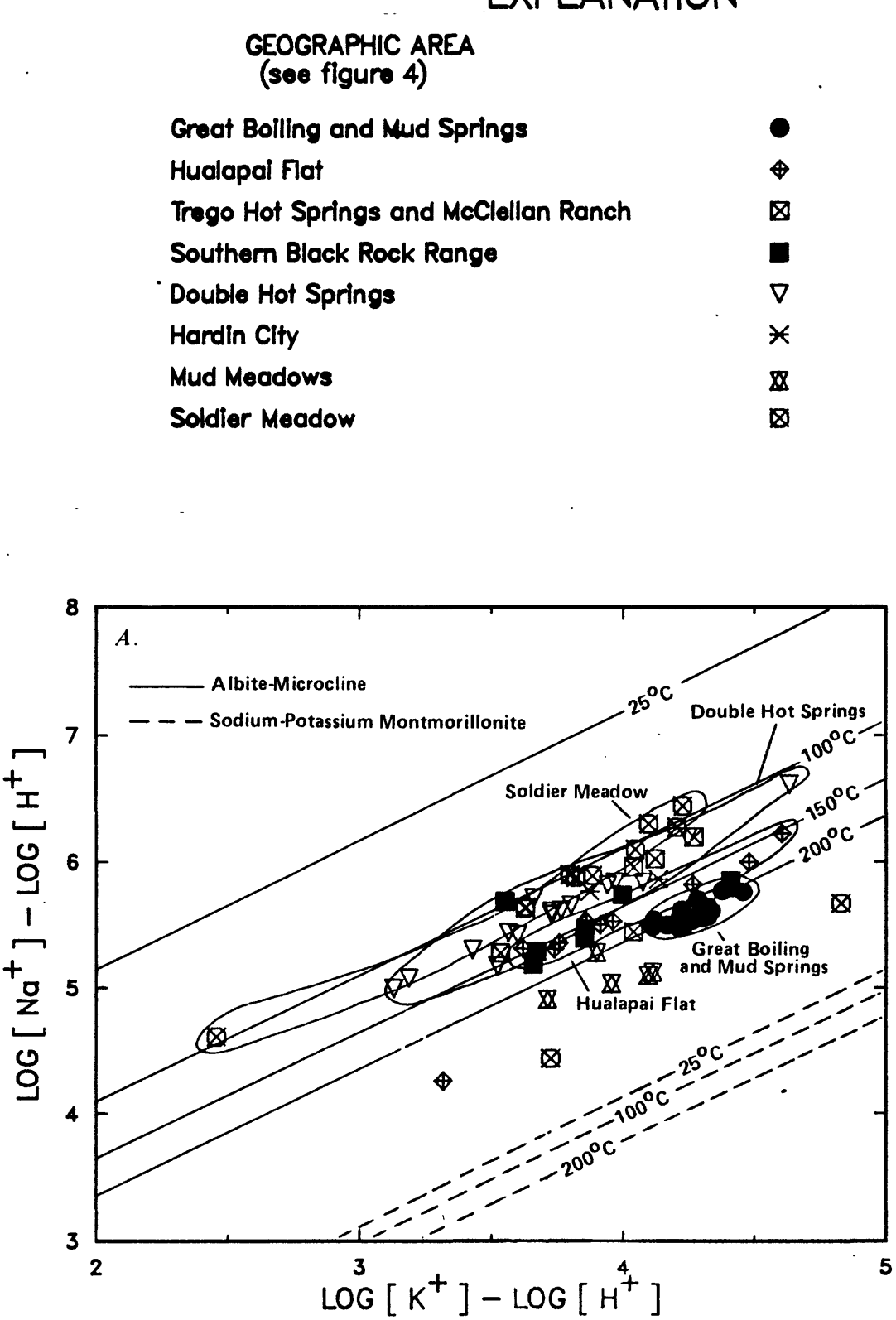

FIGURE 9.--Activity of: *A*, sodium and potassium; *B*, calcium and potassium; and *C*, calcium and sodium. Sampling sites are shown in figure 4.

The two thermodynamic expressions define a linear relation with a slope of 1 for log $[K^+/H^+]$ versus log $[Na^+/H^+]$ (which is exactly equivalent to the relation between log $[K^+]$ and log $[Na^+]$) where the position of the line is controlled by the equilibrium constants at a given temperature. For the position of the minerals being considered, the phase boundary on the activity diagram can be evaluated by using the polynomial expressions for K_T of the minerals presented by Arnorsson and others (1982, table 6). These expressions, which are based primarily on the work of Helgeson (1969) and Helgeson and others (1978), can be used to evaluate the log $[Na^+]$ - log $[K^+]$ relation as follows:

$$3 \log K_T(\text{Na-montmorillonite}) = 15273.90 + 1.7623T - 978782/T + 62805036/T^2 - 5366.18 \log T \quad (10)$$

$$3 \log K_T(\text{K-montmorillonite}) = 15075.11 + 1.7346T - 967127/T + 61985927/T^2 - 5294.72 \log T \quad (11)$$

Substitution of these two polynomial equations into the thermodynamic formula yields:

$$\text{Log}\frac{[Na^+]}{[H^+]} - \log\frac{[K^+]}{[H^+]} = 198.79 + 0.0277T - 11655/T + 819109/T^2 - 71.46 \log T \quad (12)$$

where T is in degrees Kelvin.

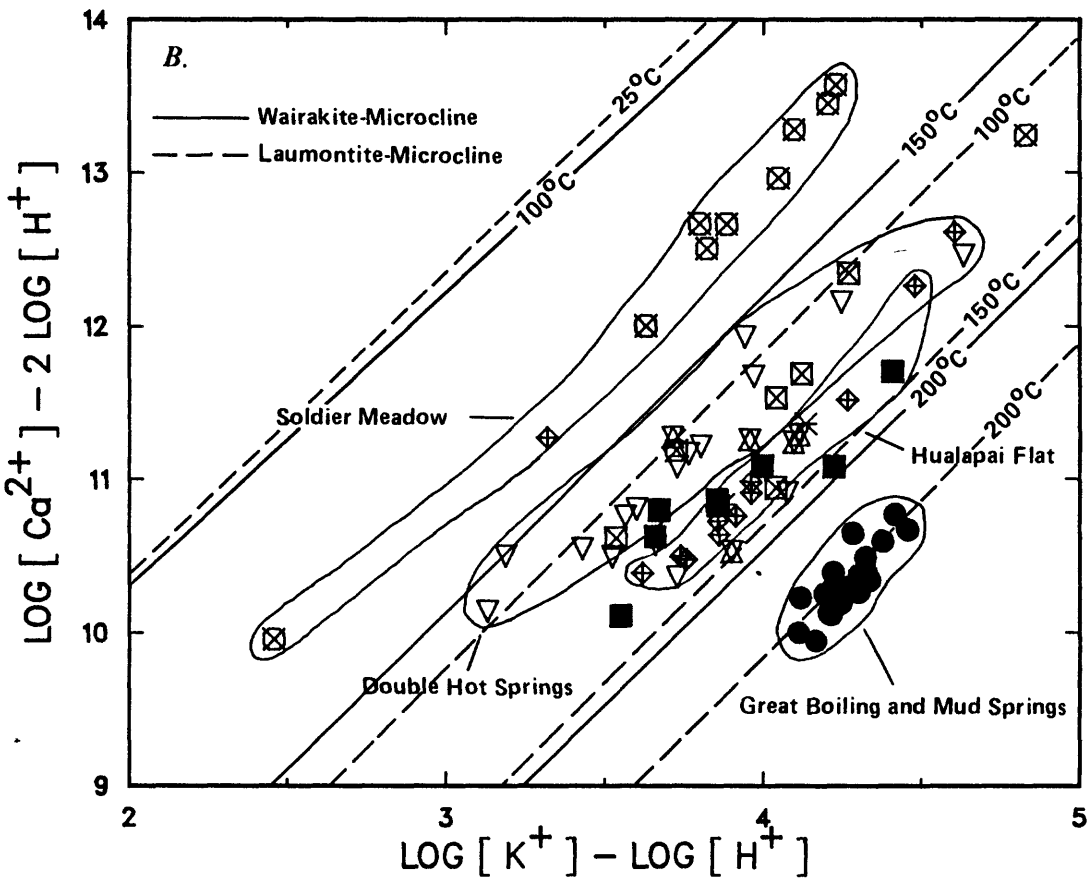

FIGURE 9.--Continued.

Similarly for albite and microcline:

$$\text{Log } K_T(\text{albite}) = 36.83 - 0.0439T - 16474/T + 1004631/T^2 \quad (13)$$

$$\text{Log } K_T(\text{microcline}) = 44.55 - 0.0498T - 19883/T + 1214019/T^2 \quad (14)$$

by substitution into the thermodynamic equation yields:

$$\text{Log } \frac{[Na^+]}{[H^+]} - \log \frac{[K^+]}{[H^+]} = -7.72 + 0.0059T + 3409/T - 209388/T^2 \quad (15)$$

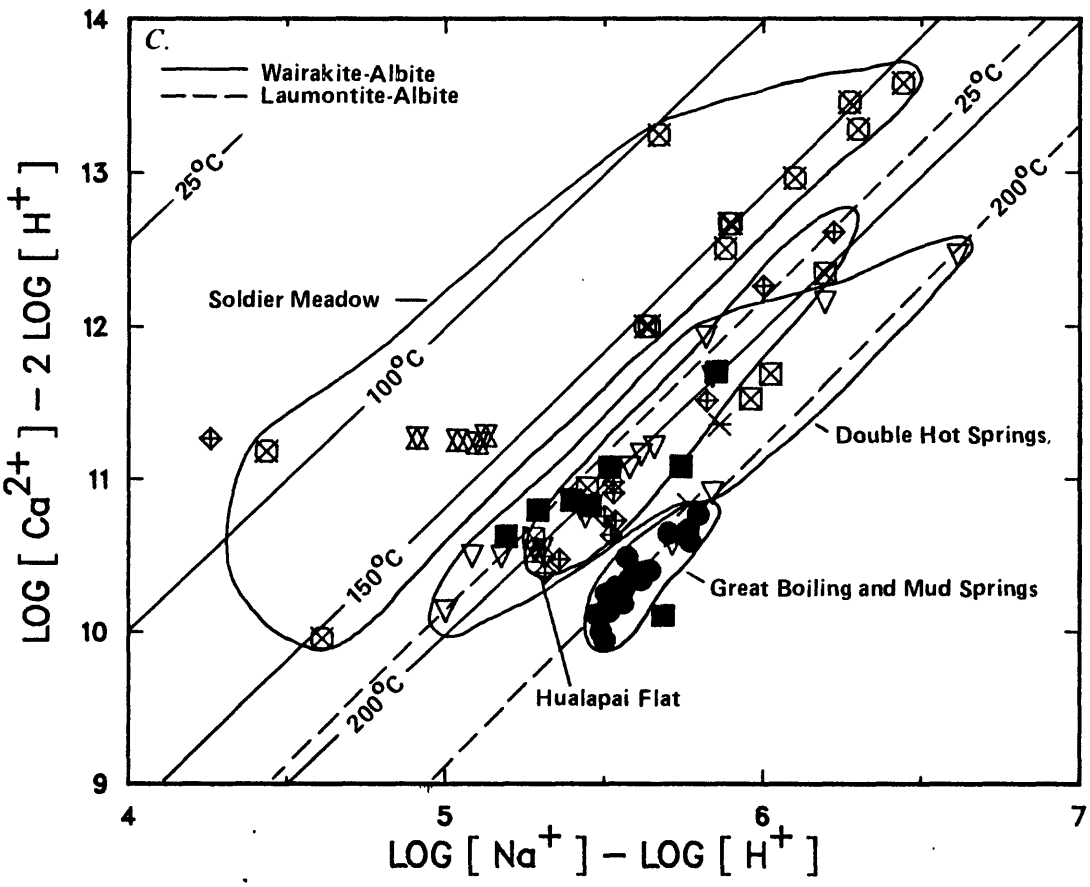

FIGURE 9.--Continued.

The equations for log $[Na^+/H^+]$ - log $[K^+/H^+]$ define the lines plotted in figure 9A. Data for the several geothermal areas support the contention that the aqueous geochemistry is controlled by the albite-microcline phase boundary over the temperature range of 100-200 °C. The temperature-dependent relations seem to be fairly consistent with the temperatures estimated using some of the commonly applied geothermometers. Polynomial equations for the albite-microcline and other reactions discussed in this section were used to calculate the temperature at which the aqueous solutions would be in equilibrium. Results of the calculations allow comparison of the thermodynamic based estimates with standard geothermometers. The suggestion that albite and microcline control the sodium and potassium activities in thermal water is not new. Ellis (1970) postulated that this control is the reason that the sodium-potassium geothermometer has proved to be accurate in many areas.

Arnorsson and others (1983) compared log $[Na^+/K^+]$ values for water from drill holes in Iceland with equilibrium values calculated for the albite-microcline reaction and found good agreement in the temperature range of about 50-250 °C. Thus, at least for basalt aquifers (the predominant aquifer type in Iceland), the albite microcline reaction appears to be controlling the sodium-to-potassium ratio.

The apparent poor correlation of the montmorillonite boundaries shown in figure 9A indicates that sodium and potassium are not controlled by these minerals.

Much of the data plotted in figure 9B indicates that the calcium and potassium activities are controlled by a temperature-dependent equilibrium. As is apparently the case for the potassium and sodium activities, the data define the same slope for each of the several geothermal areas. Although the slope is the same (in this case, 2:1) the data define different, parallel lines as a result of differing values of log $[Ca^{2+}]$ - 2log$[K^+]$ {which is equivalent to log $[Ca^{2+}/(H^+)^2]$ - 2log $[K^+/H^+]$} for the several geothermal areas.

The activities of calcium and potassium may be controlled by the minerals wairakite and microcline. The reaction can be written as:

$$2\,K^+ + \underset{\text{Wairakite}}{CaAl_2Si_4O_{12}\cdot 2H_2O} + 2\,H_4SiO_4^0 = \underset{\text{Microcline}}{2\,KAlSi_3O_8} + Ca^{2+} + 6\,H_2O \qquad (16)$$

Adopting the polynomial equations given by Arnorsson and others (1982, table 6), the corresponding thermodynamic relation is (assuming saturation with respect to quartz):

$$\text{Log}\,\frac{[Ca^{2+}]}{[H^+]^2} - 2\log\frac{[K^+]}{[H^+]} = -27.28 + 0.0149T + 12130/T - 626127/T^2 \qquad (17)$$

For the laumontite-microcline boundary, the corresponding polynomial expression is:

$$\text{Log}\,\frac{[Ca^{2+}]}{[H^+]^2} - 2\log\frac{[K^+]}{[H^+]} = -22.33 - 0.0168T + 8790/T - 511940/T^2 \qquad (18)$$

for the reaction:

$$2\,K^+ + \underset{\text{Laumontite}}{CaAl_2Si_4O_{12}\cdot 4H_2O} + 2\,H_4SiO_4^0 = \underset{\text{Microcline}}{2\,KAlSi_3O_8} + Ca^{2+} + 8\,H_2O \qquad (19)$$

The thermodynamic equations were used to calculate the phase boundaries plotted in figure 9B. The temperature-dependent phase boundaries appear to give a good indication of the deep aquifer temperature (as indicated by standard geothermometers). Data for Great Boiling and Mud Springs, Hualapai Flat, Trego Hot Springs, and the area from the southern end of the Black Rock Range to Double Hot Springs support the hypothesis that the laumontite-microcline reaction controls the aqueous geochemistry.

This conclusion is based on a comparison of the temperatures estimated using the magnesium-corrected cation geothermometer with the position of the plotted points relative to the phase boundaries indicated in figure 9B. For instance, the data for Great Boiling and Mud Springs lie along the 200 °C laumontite-microcline phase boundary, whereas geothermometry yields a range of 178-204 °C (appendix 4) which is near the upper temperature limit at which laumontite is found in active geothermal systems (Henley and others, 1984; also see fig. 8). If the wairakite-microcline reaction is controlling the geochemistry, then somewhat higher temperatures would be required for agreement with the thermodynamic data used here (fig. 9B and appendix 4).

The temperature-dependent equilibrium for the wairakite-albite phase boundary does not agree favorably with the values obtained using the magnesium-corrected geothermometer (table 4). The chemical reaction and associated polynomial equation for the wairakite-albite reaction are:

$$\overset{\text{Albite}}{Ca^{2+} + 2\,NaAlSi_3O_8 + 6\,H_2O} = \overset{\text{Wairakite}}{2\,Na^{+} + CaAl_2Si_4O_{12}\cdot 2\,H_2O + 2\,H_4SiO_4^0} \qquad (20)$$

and

$$\log \frac{[Ca^{2+}]}{[H^+]^2} - 2 \log \frac{[Na^+]}{[H^+]} = -11.84 + 0.0031T + 5321/T - 207351/T^2 \qquad (21)$$

For the laumontite-albite reaction:

$$\overset{\text{Albite}}{Ca^{2+} + NaAlSi_3O_8 + 8H_2O} = \overset{\text{Laumontite}}{2\,Na^{+} + CaAl_2Si_4O_{12}\cdot 4H_2O + 2H_4SiO^0} \qquad (22)$$

The polynomial expression is:

$$\text{Log} \frac{[Ca^{2+}]}{[H^+]^2} - 2 \log \frac{[Na^+]}{[H^+]} = -6.89 + 0.0050T + 1972/T - 93164/T^2 \qquad (23)$$

Data for the various geothermal areas plotted in figure 9C indicate a 2:1 slope, which is consistent with the slope for a wairakite-albite or laumontite-albite reaction. As noted above the albite-wairakite reaction does not appear to be controlling the sodium-calcium relation. For the Great Boiling-Mud Springs area, Trego Hot Springs, Hualapai Flat, and the Hardin City-Double Hot Spring-southern Black Rock Range areas, temperatures calculated using the cation geothermometer are less than those which are consistent with the phase boundary (appendix 4). The albite-laumontite boundary is more consistent with the cation values (with the exception of Double Hot Springs), although the range in values calculated using the polynomial equation for the albite-laumontite reaction is wider than that indicated by the cation estimates.

Stable Isotopes

Most of the stable-isotope data presented in this report are from analyses done in a U.S. Geological Survey Laboratory with some additional analyses done at the University of Arizona. Comparison of results for duplicate samples (table 4) indicates that results differ between the two laboratories. In the analysis of the data including calculations and in figures, all the University of Arizona data were adjusted by using the average differences. The original data, as received from the laboratories, are shown in appendix 2.

Measurements of the stable-isotope composition of thermal and nonthermal water commonly are useful in indicating the origin of the water and processes that control geochemical evolution. With few exceptions, the stable isotopes deuterium and oxygen-18 indicate that thermal water has been recharged by local meteoric water (Truesdell, 1976, p. lx). This conclusion is based on the observation that the deuterium content of water is essentially the same as that of the recharge water. In the case of Black Rock thermal water, local meteoric water is indicated as the recharge water. The difference in oxygen-isotope composition of thermal water, commonly termed an "oxygen shift," generally is attributed to exchange with the aquifer matrix. Another process that can affect the isotopic composition is evaporation, which can cause a change in both the deuterium and oxygen-18 concentrations. The evaporation trend shown in figure 10A indicates the general direction of the change caused by evaporation. (See Gat, 1971, for a discussion of effects of evaporation on the stable-isotope compositions.)

TABLE 4.--*Comparison of stable-isotope analyses performed by two laboratories*

[All units are permil relative to V-SMOW[1]]

Site name[2]	δD		$\delta^{18}O$		Difference between results from two laboratories	
	USGS[3]	University of Arizona[4]	USGS[3]	University of Arizona[4]	δD	$\delta^{18}O$
Mud Springs Orifice 2	- 99.5	- 95.5	-11.1	-10.8	4	0.3
Thermal Spring #1 Mud Meadow	-126	-124.0	-16.6	-16.5	2	.1
Fl WL AJRAN SOLCR	-121	-118.0	-15.6	-15.0	3	.6
WW 3922T1	-123	-116.0	-15.8	-15.7	7	.1
WW 3922T2	-123	-114.0	-15.8	-15.0	9	.8
WW 3922T3	-123	-115.0	-16.0	-15.7	8	.3
WW 3983T2	-121	-119.0	-15.9	-15.5	2	.4
WW 3983T1	-122	-115.0	-16.0	-15.7	7	.3
Flowing Well #3	-123	-117.0	-16.0	-16.4	6	-.4
3989T	-126	-124.0	-16.6	-16.0	2	.6
Wheeler Spring	-115	-114.0	-14.9	-14.6	1	.3
				AVERAGE	4.6	.3
				STANDARD DEVIATION	2.8	.3

[1] See Gonfiantini (1978) for a definition of the SMOW standards.
[2] See appendix 2 for location.
[3] Analyses performed under supervision of C. Kendell, U.S. Geological Survey, Reston, Va.
[4] Analyses performed at the Laboratory of Isotope Geochemistry, University of Arizona, Tucson, Ariz.

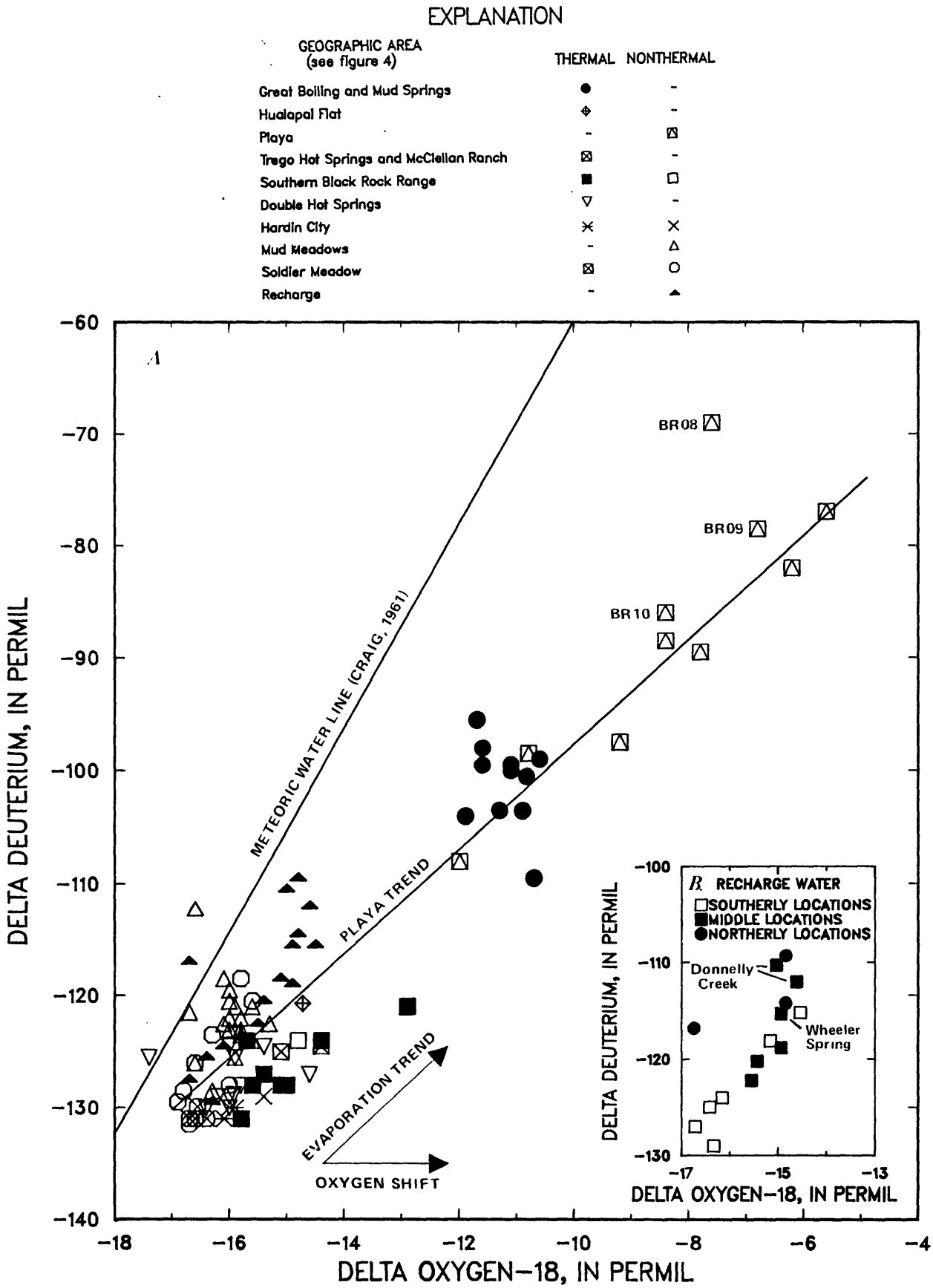

FIGURE 10.--Relation between stable isotopes of hydrogen and oxygen. Playa trend was determined by linear regression. Data for wells BR08, BR09, and BR10 probably do not represent potential recharge to deep ground-water system. Inset graph *B*: southern recharge samples are from Granite Range vicinity, middle samples are from Calico Mountains in townships 37 and 38 north, and northern samples are from townships 39 and 40 north. Sampling sites are shown in figure 4.

The isotopic composition of recharge water, as represented by upper-altitude springs and one spring runoff sample, appears to be generally lighter (more negative) with increasing latitude (fig. 10A). The isotopic composition of thermal water in Soldier Meadow is similar to that of the upper altitude springs in the area. Ground-water samples from the northern area (as defined in fig. 10) include the only available samples for the Black Rock Range. Isotopic composition of springs in the Black Rock Range is similar to that along the base of the mountains, although some samples contained a slightly heavier oxygen-isotope composition, which indicates that the water may have been affected by water-rock interaction (an oxygen shift) or evapotranspiration.

Thermal ground water in Mud Meadow is similar in composition to that in the upper-altitude springs in the Calico Range to the west. Water samples collected from Donnelly Creek (fig. 10B) display a distinctly heavier composition than samples from upper-altitude springs or from Mud Meadow. The sample from the creek was collected near the midpoint on an alluvial fan and may have been affected by evaporation prior to sampling; thus, this sample may not accurately represent the isotopic composition of recharge to Mud Meadow. Wheeler Spring is near the axis of the valley (east of Wheeler Ranch; fig. 1) and may be a mixture of direct recharge into the mountain block and surface water that has undergone evaporation.

Water from the Granite Range is isotopically heavier than other upper-altitude springs in the area but is distinctly lighter than water at Great Boiling and Mud Springs.

Isotopic Evolution

The deuterium concentration in lakes undergoing desiccation in an arid climate appears to be controlled by isotopic equilibrium between the liquid and vapor phases. Friedman and others (1976), for instance, in a study of Owens Lake in eastern California, determined that isotopic equilibrium controlled the deuterium concentration in the lake during a change from -120 to -20 permil. A change in the isotopic composition of water that proceeds under Rayleigh conditions (an equilibrium process with immediate removal of the vapor) can be described by the equation (Dansgaard, 1964):

$$\mathrm{Log}\frac{R}{R_o} = (\frac{1}{\alpha} - 1)\log\theta\,, \tag{24}$$

where R_o = initial deuterium concentration,

R = final deuterium concentration,

α = ratio of the deuterium concentration in the vapor to that in the liquid, and

θ = fraction of water remaining in the liquid phase relative to the initial volume.

An alpha value (α) can be calculated if the other parameters in the Rayleigh equation are known or can be estimated. The value of theta (θ) can be approximated for the Black Rock Desert by assuming that the chloride concentration is an indicator of evaporative concentration in the discussion of the major elements. If chloride acts conservatively in the aqueous phase (chloride is affected only by evaporation), then:

$$\theta = \frac{Cl_o}{Cl}\,, \tag{25}$$

where Cl_o = initial chloride concentration, and

Cl = final chloride concentration.

The term (R/R_o) can be converted to the δ notation using the definition:

$$\delta = \frac{R}{R_{std}} - 1 \times 1{,}000, \tag{26}$$

where R = ratio of the heavy to the light isotope in the sample, and
R_{std} = ratio of the heavy to the light isotope in the standard.

Use of this definition allows calculation of R/R_o by the equation:

$$\frac{R}{R_o} = \frac{(1{,}000 + \delta_i)}{(1{,}000 + \delta_f)}, \tag{27}$$

where δ_i = initial δ values, and
δ_f = final δ values.

The selection of the initial chloride concentration value can be made on the basis of analyzing water that represents recharge to the area of interest or selecting a value that creates a line on a plot of log (R/R_o) versus log θ that extrapolates to the origin on a log θ versus log (R/R_o) plot. The latter approach, extrapolation to the origin, was adopted. This approach was used in this study as an initial chloride value and cannot be ascertained on the basis of available hydrologic and geochemical data.

Two points on a δD versus chloride concentration graph--selected either on the basis of two data points or two points along a regression line fitted for a set of data--can be used to determine a Cl_o for a given δD_i, using the equation:

$$\text{Log } Cl_o = \frac{\log Cl_2 - \frac{\log R_2}{\log R_1} \log Cl_1}{1 - \frac{\log R_1}{\log R_2}}, \tag{28}$$

where Cl_1 = chloride concentrations for point 1,
Cl_2 = chloride concentrations for point 2,
R_1 = $(\delta D_i + 1{,}000)/(\delta D_1 + 1{,}000)$, and
R_2 = $(\delta D_i + 1{,}000)/(\delta D_2 + 1{,}000)$.

The above equations were used to calculate values for the initial chloride and alpha values from the data shown in table 5. The apparent alpha value for water from six of the playa wells is about 1.0079, the first apparent alpha value shown in table 5. The log (R/R_o) and log θ values plot along the same line in figure 11, indicating that the water at these sites could have evolved by evaporation from water with a similar initial chloride and deuterium concentration. Water that has evolved with a constant alpha from the same initial chloride and isotopic composition will plot along a line that passes through the origin on a log (R/R_o) versus log θ plot. The data for Great Boiling and Mud Springs also lie along the same line in figure 11, implying that the thermal water at these springs has been affected by the same processes that have affected the water at the six playa wells.

TABLE 5.--*Apparent initial chloride and fractionation factors (alpha values) calculated using the Rayleigh distillation equation*

[The δD_i and $\delta^{18}O_i$ values used for the calculations, -128 and -17 permil, respectively, were selected on the basis of the trends shown in figure 10B.]

Sample sites used in calculations	δD (permil)	Chloride (milligrams per liter)	Alpha	Initial chloride (milligrams per liter)	$\delta^{18}O$ (permil relative to V-SMOW)	Alpha	Initial chloride (milligrams per liter)
(A) Calculations for major trend samples from playa wells							
Spring at T40N R24E S24ABD[1]	-125	52	[a]1.0079	34	-16.4	1.0016	36
Playa well GRB	-77	44,000		-5.6			
(B) Calculations for anomalous samples from playa wells							
Spring at T40N R24E S24ABD[1]	-125	52	1.0130	40	-16.4	1.0018	37
Playa well BR08	-69	7,200			-7.6		
Spring at T40N R24E S24ABD[1]	-125	52	1.0100	37	-16.4	1.0019	38
Playa well BR09	-78.5	9,400			-6.8		
Spring at T40N R24E S24ABD[1]	-125	52	1.0092	36	-16.4	1.0017	36
Playa well BR10	-86	6,100			-8.4		

[1] Located in the southeast corner of the northwest corner of the northeast corner of Township 40 North, Range 24 East, section 24.

[a] Calculated using playa wells BR06, GRB, GRD, GRL, GRL', BR11.

The three points that plot above the line in figure 11 represent water from the playa (the P sites) and are from wells in the topographically lowest part of the playa (wells BR08, 09, and 10 in fig. 1). Water at wells BR09 and 10 appparently could have evolved from water with a similar chloride and deuterium composition and an apparent alpha of about 1.01. An apparent alpha of about 1.013 would be required for water at well BR08 to have evolved from a similar recharge water.

Calculated apparent alpha values are lower for ground water in the Black Rock Desert than for lakes affected by evaporation in arid environments but are within the range that can be calculated for ground water, in other closed basins. Alpha values of about 1.05-1.08 for the Salton Sea, Owens Lake in eastern California lakes in the Grand Coulee in Washington, and two lakes in the northeastern Sahara Desert were determined by Friedman and others (1976) using a Rayleigh-type equation. This range in alpha values is for lakes containing water with the same general range in salinity as the water used for the apparent alpha determinations in this study; salinity can affect the fractionation process. Alpha values for lakes affected by evaporation are in fair agreement with experimentally determined equilibrium alpha values. An alpha range of 1.055-1.097 for temperatures of about 10-40 °C can be derived from a compilation by Friedman and O'Neil (1977, fig. 34). An apparent alpha value for ground water in the western Carson Desert (about 14 km to the south-southeast of Black Rock Desert) of about 1.005-1.007 can be calculated from chloride and stable-isotope data (for wells 8A, 49A, and 58B) presented by Olmsted and others (1984) by the same procedure described above.

The difference in laboratory-derived alpha values at equilibrium and for the Black Rock Desert yield greatly different slopes on log θ versus log (R/R_o) plot (fig. 11). Thus, the apparent volume of water lost through evaporation from the playa is much less than would be estimated on the basis of an apparent alpha value similar to that for evaporating surface water.

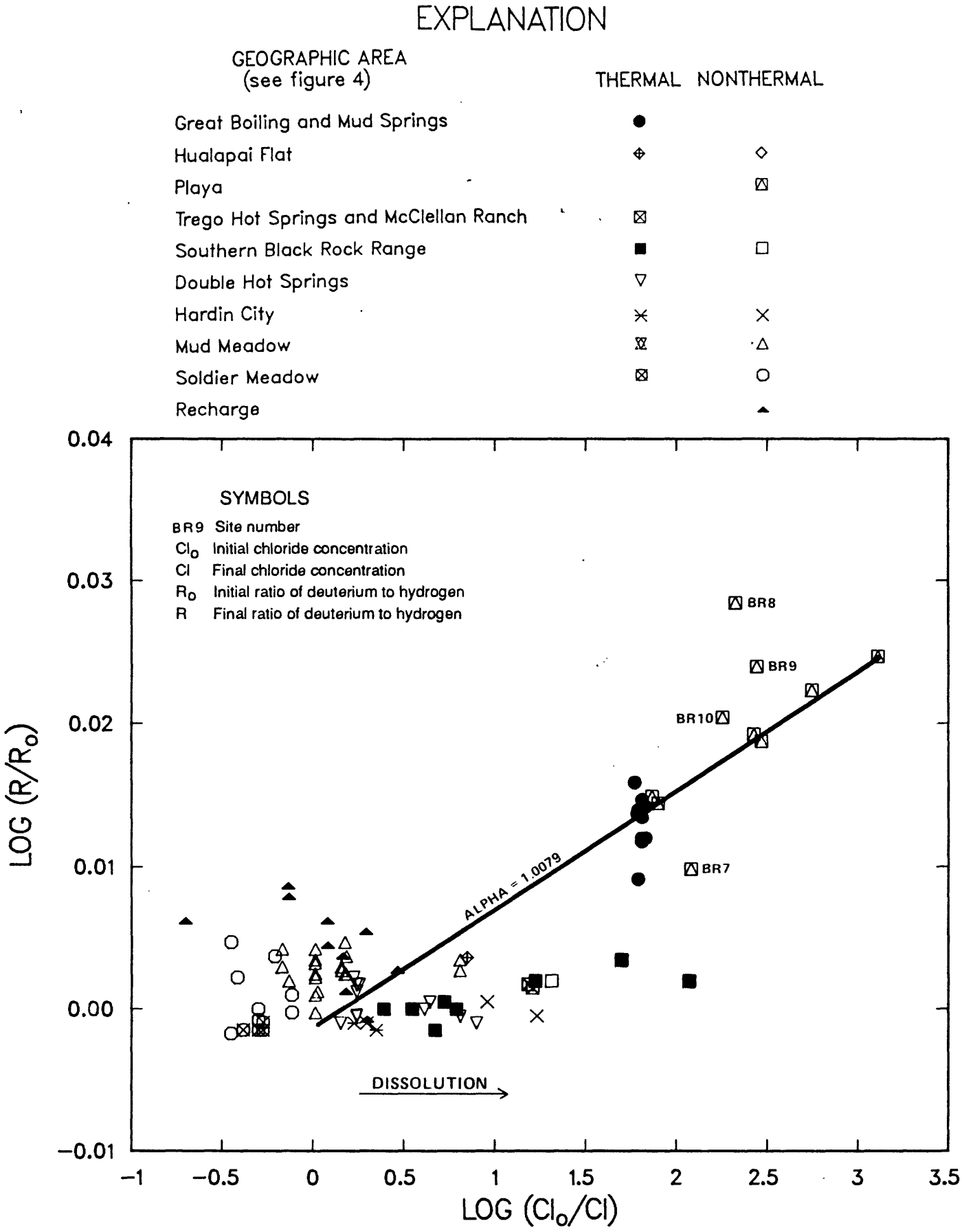

FIGURE 11.--Relation between parameters representing evaporation for hydrogen isotopes. Line, which passes through origin, was used to calculate apparent alpha for the hydrogen isotopes. Sampling sites are shown in figure 4.

The evaporation process was mathematically described by Craig and Gordon (1965) for a model consisting of a series of steps and includes molecular diffusion and fully turbulent flow above the evaporating liquid. The equation for isotopic fractionation for this model is given by Gat (1980, p. 36) (after making the variables compatible with those in this report) as:

$$\frac{\log\ (R_o/R)}{\log\ \theta} = \frac{h(R_s - R_a)/R_s - 1 + \alpha - \Delta E}{1 - h + \Delta E} \tag{29}$$

where R_s = isotopic concentration in the liquid,

R_a = isotopic concentration in the atmospheric moisture,

ΔE = kinetic excess separation factor, and

h = humidity in the fully turbulent atmosphere (normalized with respect to saturated vapor at the temperature of the liquid surface).

This equation shows that log (R/R_o) is linearly related to log θ. Since log (R/R_o) and log θ appear to be linearly related--as shown in figures 11 and 12--for both the hydrogen and oxygen isotopes (with chloride as a measure of θ) equation 29 is of a form that is consistent with data for the western Black Rock Desert.

One of the difficulties of applying this equation is that additional parameters are required--namely ΔE, humidity, and R_a. Estimates of these parameters may, however, be useful in determining whether the Craig and Gordon model may yield α values more in line with laboratory observations.

An α value may be calculated using the previous formula after rewriting in terms of the δ notation as (assuming $\delta_i = \delta_s$):

$$\alpha = \frac{\log\ [(\delta_i + 1,000)/(\delta_f + 1,000)]}{\log\ (Cl_o/Cl)} (1 - h + \Delta E) - h\frac{(\delta_i - \delta_a)}{(\delta_i - 1,000)} + 1 + \Delta E \tag{30}$$

The kinetic excess separation factor--which is the difference between the equilibrium and effective α--can be approximated from the formulas $\delta D = 15(1 - h)$ permil and $\delta\ ^{18}O = 13(1 - h)$ permil (Merlivat, 1978). The composition of the atmospheric moisture is difficult to estimate--the isotopic composition of rainfall, together with an equilibrium fractionation factor multiplied by 0.8, was adopted by Zimmerman and others (1967). This approach yields $\delta D = -190$.

The humidity of the atmosphere at the point where fully turbulent flow occurs also is difficult to evaluate. For high humidities, calculated a values approach laboratory values (using a ΔE calculated from the humidity and the δ_a values given alone). A normalized humidity of 0.75 yields an α of 1.046 at data well GRB and the spring at section 24 of township 40 N, range 24 E. This value is much closer to the equilibrium values observed in the laboratory (1.055 at 40 °C) than the value calculated using a Rayleigh model (1.00791). The calculated a is sensitive to the humidity value--a humidity of 0.50 yields an a of 1.022. It is not clear if the humidity is high in fine-grained sediments due to evaporation above ground water. The lines on figures 11 and 13 for an a equal to 1.00791 using a Rayleigh model are identical to those predicted by the molecular diffusion model of Craig and Gordon (1965) using the values given above. Thus, the positions of the plotted data cannot be used to distinguish between the two models. Further field or laboratory work is needed to evaluate the validity of either model in this type of setting.

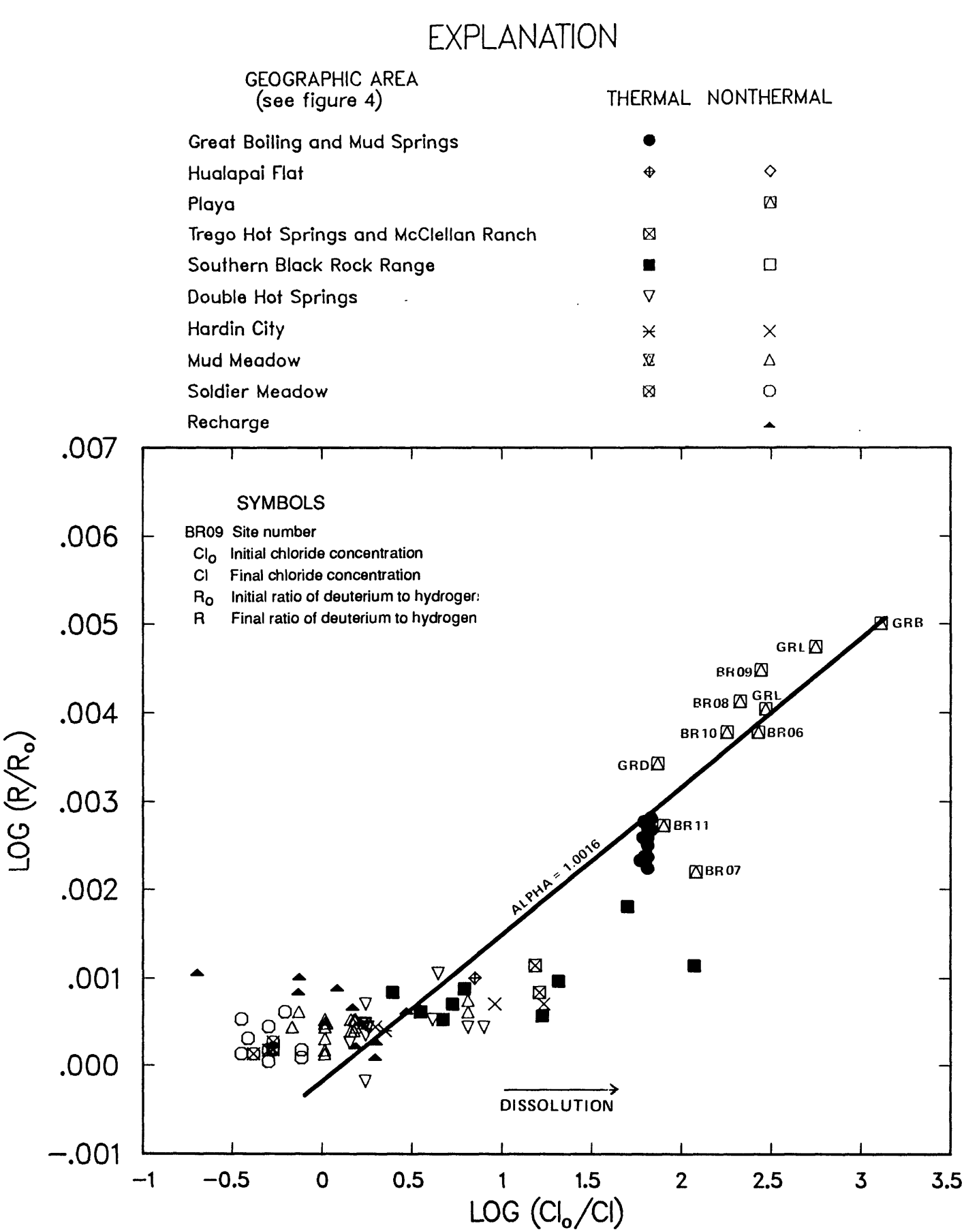

FIGURE 12.--Relation between parameters representing evaporation for oxygen isotopes. Line, which passes through origin, was used to calculate apparent alpha for oxygen isotopes. Sampling sites are shown in figure 4.

Water issuing from Great Boiling and Mud Springs appears to have undergone significant evaporation, as indicated by chloride and deuterium concentrations that plot along the same lines in figures 11 and 13, as do most wells sampled in the playa. An apparent alpha value (obtained using either the Rayleigh or Craig and Gordon, 1965 model) for these thermal springs that is in the same range as for most of the wells sampled in the playa could explain the observed deuterium and chloride concentrations at the thermal springs.

Figure 13 demonstrates that thermal springs near Gerlach are not a result of simple mixing of nonthermal, dilute recharge with water in the playa that has evolved with an apparent alpha value of about 1.008 for a Rayleigh model. Mixing of two waters would result in a plotting position along a line connecting points representing the composition end members. One example consists of recharge with a $\delta D = -128$ and a chloride con-centration of 34 mg/L and a water composition as represented by water at well GRL. Mixing of water from these sources would result in water with a composition represented by some point along the mixing line in figure 13.

The thermal water at Great Boiling and Mud Springs cannot be formed by simple mixing of two solutions along the line representing evolution of water with an apparent alpha value (from a Rayleigh model) of 1.008. Mixing of recharge with the same composition as described above ($\delta D = -128$ and chloride = 34 mg/L) with water from the central part of the playa could result in the composition measured at these thermal springs near Gerlach. This mixing scenario may not be hydrologically reasonable, however, assuming that the evolution of water with apparent alpha values of about 1.01 or greater is restricted to the central part of the playa. Because this area probably represents the most distal part of the ground-water flow system, deep recharge of water from this area is unlikely.

The oxygen-isotope data can be examined using the same approach as was described for hydrogen. One possible complicating factor is the exchange of oxygen isotopes between the water and aquifer materials. This oxygen shift is common in geothermal systems resulting in an isotopically heavier (less negative) water. A demonstrable oxygen shift is not apparent for systems examined in this study. This may, at least in part, be due to the fairly large apparent effect that evaporation has had on stable isotopes in the thermal water, which may make a small shift (of perhaps as much as 2-3 permil) impossible to detect.

The oxygen-isotope data show the same general features as the hydrogen-isotope data. The data for the water in the playa yield oxygen-alpha values for a Rayleigh model of 1.0016-1.0019 for the data shown in table 5. Application of the Craig and Gordon (1965) model yields an alpha value of about 1.002 for a normalized humidity value of 0.75 and an atmospheric $\delta^{18}O$ of -14.4 for the data from GRB and the spring at T. 40 N., R. 24 E. S24ABD. The actual atmospheric value is probably much lighter than 14.4 permil; thus, the a probably has little physical meaning. A more negative atmospheric value (lighter isotopic composition) yields unrealistic a values. The data for the water in the playa yield R/R_o and θ values which generally plot along the same line in figure 12. The data for Great Boiling and Mud Springs lie along this same line. Because these thermal springs lie along an evolutionary trend line with the same apparent oxygen alpha value as water in the playa (see figs. 12 and 14) a similar process is assumed to have affected the water in these two areas. As is the case for the hydrogen isotopes, a laboratory-derived alpha value (1.0093 at 25 °C from Friedman and O'Neil, 1977, fig. 9) does not agree with the observed data (fig. 12).

The magnitude of any oxygen shift, if present, for the thermal water appears to be small--about 2 permil or less. Thermal water that plots to the right of the meteoric water line (fig. 10B) is not proof that water/rock interaction is responsible for the shift to the right of the meteoric-water line (fig. 10) as ground water in arid and semiarid environments commonly is shifted toward a heavier oxygen-isotope composition (see, for example, Gat, 1971, fig. 5). Local recharge water (fig. 10A) has an oxygen-isotope composition about 1 permil heavier than the meteoric-water line. Because most of the thermal water (except for Great Boiling and Mud Springs) is offset from the meteoric-water line by about 2 permil or less, the oxygen shift appears to be no more than about 2 permil.

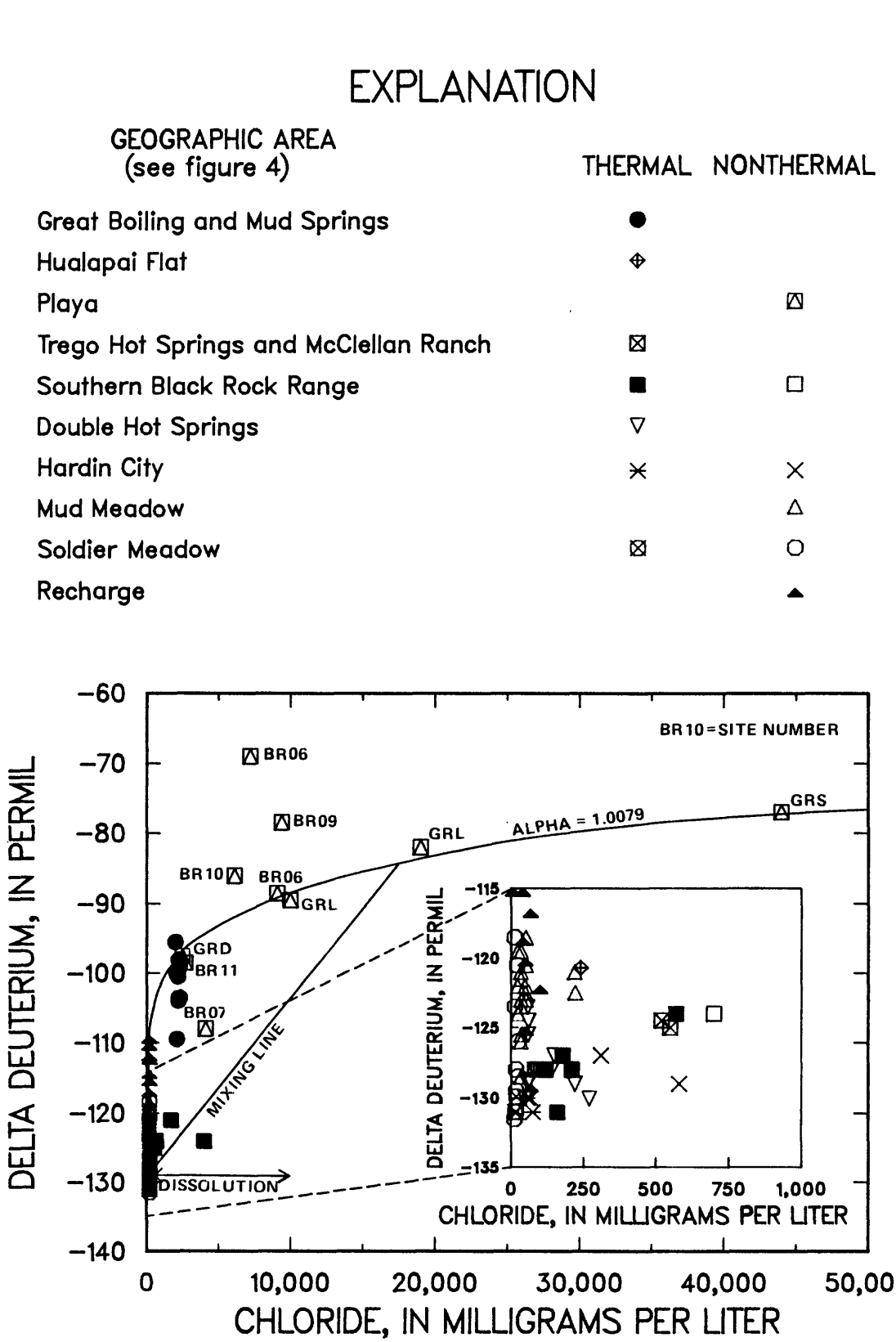

FIGURE 13.--Relations between the hydrogen isotopic composition and chloride. Sampling sites are shown in figure 4.

The close correlation for deuterium and oxygen isotopes between the nonthermal water in the playa and water at Great Boiling and Mud Springs implies little, if any, oxygen shift in the thermal water. If a significant oxygen shift were present, the data would not plot along the same trend lines in figures 12 and 14. Other geothermal systems in the northern Basin and Range with estimated (on the basis of chemical geothermometry) or measured temperatures greater than 150 °C and little (less than about 2 permil) or no oxygen shift are the Soda Lakes anomaly (Olmsted and others, 1984) and Leach Hot Springs (Welch and others, 1981). The apparent lack of a demonstrable oxygen shift at systems in the western part but away from the margin of the Basin and Range physiographic province (thus excluding the systems at Steamboat Springs, Nev., Coso Hot Springs and Long Valley, Calif.) appears to be a common feature of thermal water in the northern Basin and Range. The small oxygen shift may be a result of some combination of (1) flow in a fractured system that limits the water-rock interaction as a result of a high water volume to rock surface area ratio, and (2) a fairly great age for the system, thereby allowing the rock to be in isotopic equilibrium with the water. The proposition that the oxygen and hydrogen isotope and chloride data are controlled primarily by evaporation is based on a number of assumptions.

The preceding discussion assumes that the original isotopic composition of the thermal water is equal to that of the nonthermal water. Climatic change can, however, result in a change in the isotopic composition of recharge. If the thermal water was recharged about 10,000 years ago or earlier, then the effect that a pluvial climate might have had on the isotopic composition must be considered. For a change in mean annual temperature of about 1 °C, the δD would change by about 5 permil, according to a relation developed by Dansgaard (1964). If the pluvial climate was 2.8 °C cooler than present (as suggested by Mifflin and Wheat, 1979), the resulting effect would be a lighter hydrogen-isotope composition of about 14 permil. A lighter isotopic composition in recharge water is not, however, indicated by the data presently available, because the present-day recharge throughout most of the area is compositionally similar to that in the thermal water. The only area where a distinctly different composition is apparent is near Gerlach, where the recharge is lighter than the water issuing from Great Boiling and Mud Springs. A lighter isotopic composition in the recharge, which might have been present during a pluvial period, would imply that the water at these thermal springs would have evolved to an even greater extent than is implied by the composition of current recharge.

In the above discussion, a one-step process was considered--thus, some combination of evaporation and chloride dissolution was not discussed. Chloride dissolution may, in fact, be occurring. Possible examples are represented by points that plot to the right of most of the data and below the main playa-evaporation trend in figures 13 and 14.

The assumption that chloride concentrations at Great Boiling and Mud Springs are controlled primarily by shallow evaporation deserves consideration. Alternate sources of chloride are: (1) dissolution of halite and (2) mixing with shallow (nonthermal) chloride-rich water isotopically heavier than that in the thermal water.

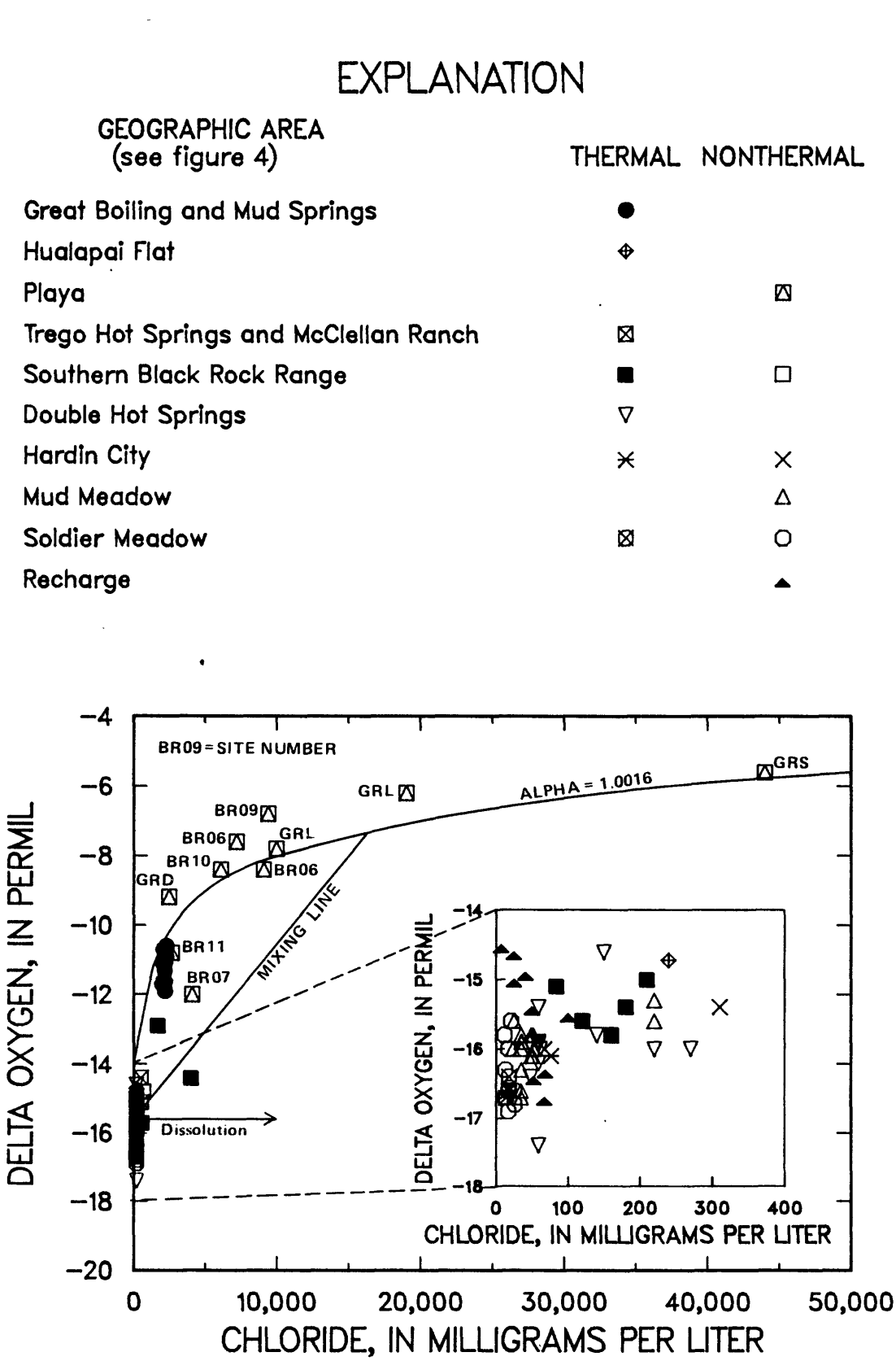

FIGURE 14.--Relations between the oxygen isotopic composition and chloride. Sampling sites are shown in figure 4.

Dissolution of chloride-bearing minerals (or leaching from aquifer materials) can increase chloride concentrations without affecting the stable-isotope composition. Water with an isotopic composition similar to that in local recharge, but with greater chloride concentrations, is probably a result of these processes. Samples plotting to the right of the recharge samples in figures 11-14, such as is the case for playa well BR07, are examples of increased chloride with no apparent change in isotopic composition. With the exception of Trego Hot Springs and Great Boiling and Mud Springs, chloride concentrations from major thermal springs are less than about 110 mg/L (which corresponds to a log θ of about 0.5, assuming a recharge chloride value of 34 mg/L). Water with log θ values greater than 0.5 along the western base of Black Rock Range (from the vicinity of Hardin City, Double Hot Springs, and the southern end of the range) is either nonthermal or from springs with low flow rates or shallow wells in areas with efflorescent salts. The presence of salts indicates a potential for dissolution of chloride salts. The similarity in isotopic composition between local recharge and the shallow thermal and nonthermal water along the base of the Black Rock Range is consistent with dissolution rather than evaporation being the primary process responsible for the greater chloride concentrations. The relatively high flow rates, low chloride concentrations (less than 100 mg/L), and isotopic compositions similar to those of local recharge water of thermal springs at Hardin City and Double Hot Springs indicate that the thermal water in these areas has not been greatly affected by evaporation.

High chloride concentration at Trego Hot Springs, combined with an isotopic composition similar to that of local recharge water, indicates that dissolution, rather than evaporation, is the primary process responsible for the observed chloride values. Although halite has not been reported in the playa sediments, its presence would not be considered unusual in a closed basin setting like the Black Rock Desert. Furthermore, only the uppermost part of a thick sequence of sedimentary fill has thus far been penetrated.

If dissolution is the predominant source of chloride at Great Boiling and Mud Springs, then another process needs to be identified to explain the heavier isotopic composition in these thermal waters. On the basis of present knowledge of the behavior of stable isotopes, the process of evaporation appears to be the only explanation for the heavier isotopic composition, other than mixing with isotopically heavier ground water.

The isotopically similar composition of thermal water in Soldier Meadow and Mud Meadow to local recharge and low chloride concentrations (>100 mg/L) indicate that the water was not subject to extensive evaporation prior to recharge or significant dissolution of chloride-bearing minerals. The chloride concentration at Fly Ranch (240 mg/L) and hydrogen-isotope composition are consistent with either limited shallow evaporation prior to deep recharge or incorporation of chloride as a result of reactions in the thermal aquifer.

Geothermometry

The temperature of deep thermal water commonly is estimated using chemical data. The most widely applied methods are based on the silica or relative cation concentrations in thermal water. Additional methods using gas and isotopic compositions also have been developed. The silica and cation methods have been applied to water analyses in the Black Rock Desert by Mariner and others (1974) and Anderson (1977). The sulfate-water oxygen-isotope method has been applied to one analysis for Great Boiling Springs by Nehring and Mariner (1979) and Nehring and others (1979).

The results of applying silica and cation geothermometer calculations to water with source temperatures greater than 25 °C in the study area are shown in appendix 4 and summarized in table 6.

TABLE 6.--*Summary of chemical geothermometry for the western arm of the Black Rock Desert*

[Temperature estimates are in degrees Celsius]

Location	Silica[1]	Sodium-potassium-calcium			Albite-microcline	Wairakite-microcline	Laumontite-microcline	Wairakite-albite	Laumontite-albite
		Uncorrected		Magnesium corrected					
Great Boiling and Mud Springs	149-170(A)	186-208	(β=1/3)	178-204	192-228	225-245	127-242	230-267	196-236
Trego Hot Springs	124-125(A)	124-126	(β=1/3)	120-124	121-123	174-176	118-120	219-227	95-118
McClellan Ranch	127-134(C)	134-169	(β=1/3)	134-164	114-156	144-197	38-60	193-204	171-201
Hualapai Flat (Fly Ranch)	124-128(A)	141-152	(β=1/3)	136-147	153-172	191-205	143-163	218-242	92-179
Southern Black Rock Range[2]	145(A)	148	(β=1/3)	144	166	194	146	216	86
Double Hot Springs[3]	133-137(A) 103-113(H)	123-125	(β=1/3)	96-131	127-131	166-173	106-116	199-211	48-75
Hardin City	113-127(A)	129-141	(β=1/3)	129-130	111-271	189-191	138-141	225-253	111-271
Mud Meadow[4]	110-124(C) 80-99(H)	171-203	(β=1/3)	79-129	232-294	163-192	102-143	127-151	--
Soldier Meadows	111-114(C) 60-85(H)	18-41	(β=4/3)	67-120	91-112	127-169	58-111	92-172	1

[1] Letters in parentheses indicate the silica geothermometer: (A), adiabatic quartz method; (C), conductive quartz method; (H), conductive chalcedony method. The adiabatic estimates are more applicable to samples with boiling and near-boiling measured temperatures. The conductive methods are applicable for the lower temperatures.

[2] Based on a single sample. See the geothermometry section for a discussion of this area.

[3] Based on data collected during this study only.

[4] Excludes data for well WW3922T2.

The chemical geothermometers are based on several assumptions as discussed by Fournier and others (1974). These assumptions are that: (1) temperature-dependent reactions occur at depth; (2) all constituents involved are sufficiently abundant; (3) water-rock equilibration take place in the thermal aquifer; (4) no change in composition occurs as the water moves from the thermal aquifer and the sampling point; and (5) the thermal water does not mix with nonthermal, shallow ground water. Plots like those in figure 15 can assist in evaluating the internal consistency of the various temperature estimates and may indicate whether any of the above assumptions have been violated.

Estimated temperature values for the Great Boiling-Mud Springs area plot in a fairly limited region below the equal temperature line (fig. 15). The adiabatic rather than conductive quartz estimate is probably more applicable for samples with source temperatures at or near boiling, as is the case for the major thermal springs in this study area. The magnesium-corrected cation estimate of Fournier and Potter (1979) is used rather than the uncorrected value because of a better agreement with the adiabatic quartz value. The corrected values are generally within 10 °C or less of the uncorrected values, a difference that does not affect the following discussions regarding the possible reasons for the discrepancies between the cation and quartz silica estimates. As discussed by Fournier and others (1979), possible reasons for plotting below the equal temperature line include precipitation of silica, precipitation of calcite, and mixing with nonthermal ground water. The presence of siliceous sinter in the spring area indicates that silica precipitation may be the cause of the lower temperature values estimated using the quartz geothermometer. Precipitation of calcite cannot be ruled out, although calcite has not been noted in the vicinity of thermal springs. The relatively narrow range in calcium concentration

(generally from 67 to 79 mg/L) in water with source temperatures from 46 °C to boiling indicates that if calcite is being precipitated, it is occurring at depth. The relative insensitivity of the cation estimate to the calcium concentration also indicates that calcite precipitation is not the main cause of the discrepancy between the geothermometers. For the analysis from Mud Springs orifice 1, a calcium concentration of more than 8,000 mg/L would be required to make the cation estimate agree with the 160 °C quartz-silica value. The possibility of mixing is not easy to eliminate entirely, although the relatively narrow range in chloride concentration (a constituent that probably would be conserved during mixing) and the fairly limited range in stable-isotope composition indicate that mixing is probably not occurring. If there is, in fact, no mixing or calcite precipitation, then the magnesium-corrected cation geothermometer indicates that the temperatures in the deep aquifer supplying water to the Great Boiling Spring-Mud Springs area is in the range of 178-204 °C. The uncorrected cation temperature estimates are somewhat higher, with a range of 186-208 °C.

Agreement between the cation and adiabatic quartz estimates for the data from Trego Hot Springs is favorable. The data indicate deep aquifer temperatures in the 120-125 °C range. Estimates based on previous sampling at McClellan Ranch (about 8.5 km west-southwest of Trego Hot Springs) are in good agreement for the one sample with a high (92 °C) measured temperature. A lower temperature is reported for a more recent sample with an analysis that yields a higher cation estimate in comparison to the earlier sampling. The reason for this discrepancy is difficult to assess although the lower measured temperature indicates that the more recent sample may be affected by mixing with nonthermal water. On the basis of higher temperature sample, the deep aquifer temperature is tentatively estimated to be in the 130-134 °C range.

Temperature estimates for samples from the Fly Ranch area of Hualapai Flat (section 1 of township 34 N, range 23 E) have a fairly narrow range based on the quartz and cation geothermometers (124-128 °C and 136-147 °C, respectively). However, the agreement between cation and quartz values is only fair. As was the case for the Great Boiling-Mud Spring area, temperature estimates for Fly Ranch plot below the equal temperature line in figure 15A. The large amount of calcite actively being precipitated in this area indicates that at least some of this disagreement between the cation and quartz values is due to a loss of calcium from the water subsequent to reaching equilibration in the deep thermal aquifer. Because the water is precipitating calcite, which affects the cation estimate, the quartz-silica range of 124-128 °C is a better estimate for this area.

Estimated temperature values for thermal water found along the western flank of the southern Black Rock Range generally plot above the equal temperature line in figure 15A. The water sample that contained the lowest chloride concentration in the group is in excellent agreement with values from the magnesium-corrected cation and adiabatic-quartz geothermometers. All the estimated temperature values for thermal water along the western flank of the southern Black Rock Desert plot above the equal temperature line. One exception is the relatively cool sample from well 51A, which has temperature values which plot well below the equal temperature line (perhaps as a result of silica precipitation in the shallow subsurface). The cation values may be low as a result of: (1) evaporation (as discussed by Fournier and others, 1979) or (2) resolution of efflorescent salts. The variability of the chloride concentration within this group combined with the common occurrence of a large, wet surface area and presence of efflorescent salts surrounding many of the springs with low-flow rates, imply that dissolution of salts is occurring.

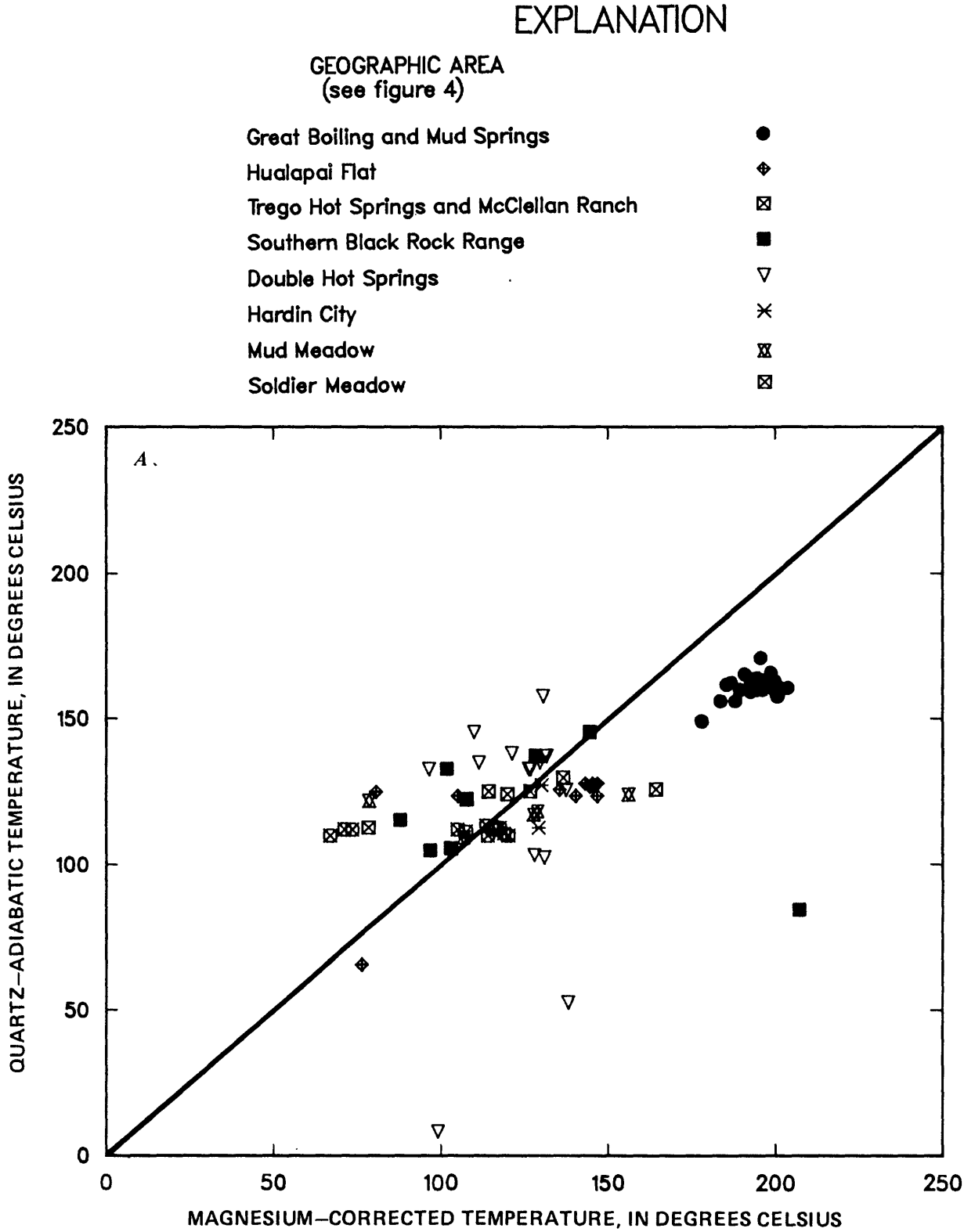

FIGURE 15.--Relations between magnesium-corrected temperatures and the following calculated temperatures: *(A)* quartz-adiabatic, *(B)* quartz-conductive, *(C)* albite-microcline, *(D)* laumontite-microcline, *(E)* wairakite-microcline, *(F)* wairakite-albite, and *(G)* laumontite-albite. Sampling sites are shown in figure 4.

The lack of direct correspondence between the chloride and silica concentrations, however, indicates that the silica is not a result of simple evaporative concentration or mixing with nonthermal water with a uniform composition. The chloride variability also may result from some combination of shallow mixing with nonthermal water of variable composition. The variable composition prevents the use of mixing models (Fournier, 1977). The best estimate of a deep aquifer temperature therefore is obtained when the cation and silica values are in good agreement. A relatively low chloride concentration (84 mg/L) indicates that water is affected little by near-surface processes, and the high measured temperature is consistent with little or no mixing with nonthermal water.

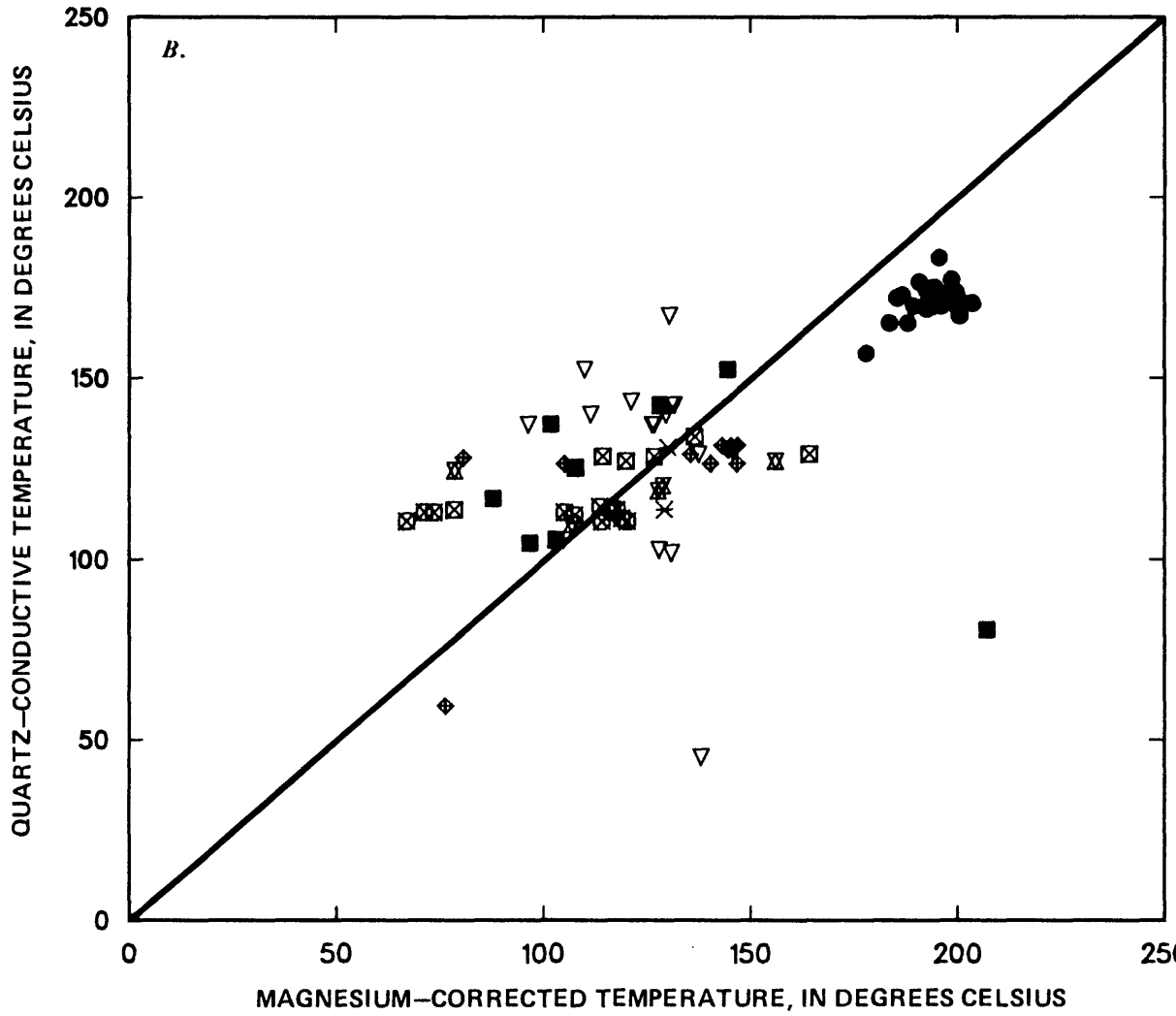

FIGURE 15.--Continued.

The geothermometry for Double Hot Springs indicates fair agreement between the cation and adiabatic quartz estimates. Data collected during the study indicate a fairly narrow range for the adiabatic quartz and Na-K-Ca methods of 133-137 °C and 123-125 °C, respectively. The chalcedony geothermometer values are in the range of 103-113 °C. The two silica values (based on quartz and chalcedony are within 10 °C of the cation values. The reliability of these silica methods, as applied to Double Hot Springs, is difficult to assess. The kinetics of quartz may be too slow in this temperature range (140 °C and less) to act as the control on silica concentrations. Because of this uncertainty, the cation method may be more reliable, in this case, a "best" estimate of 123-125 °C. If previously collected analytical data were included, a somewhat wider range (115-126 °C) would result.

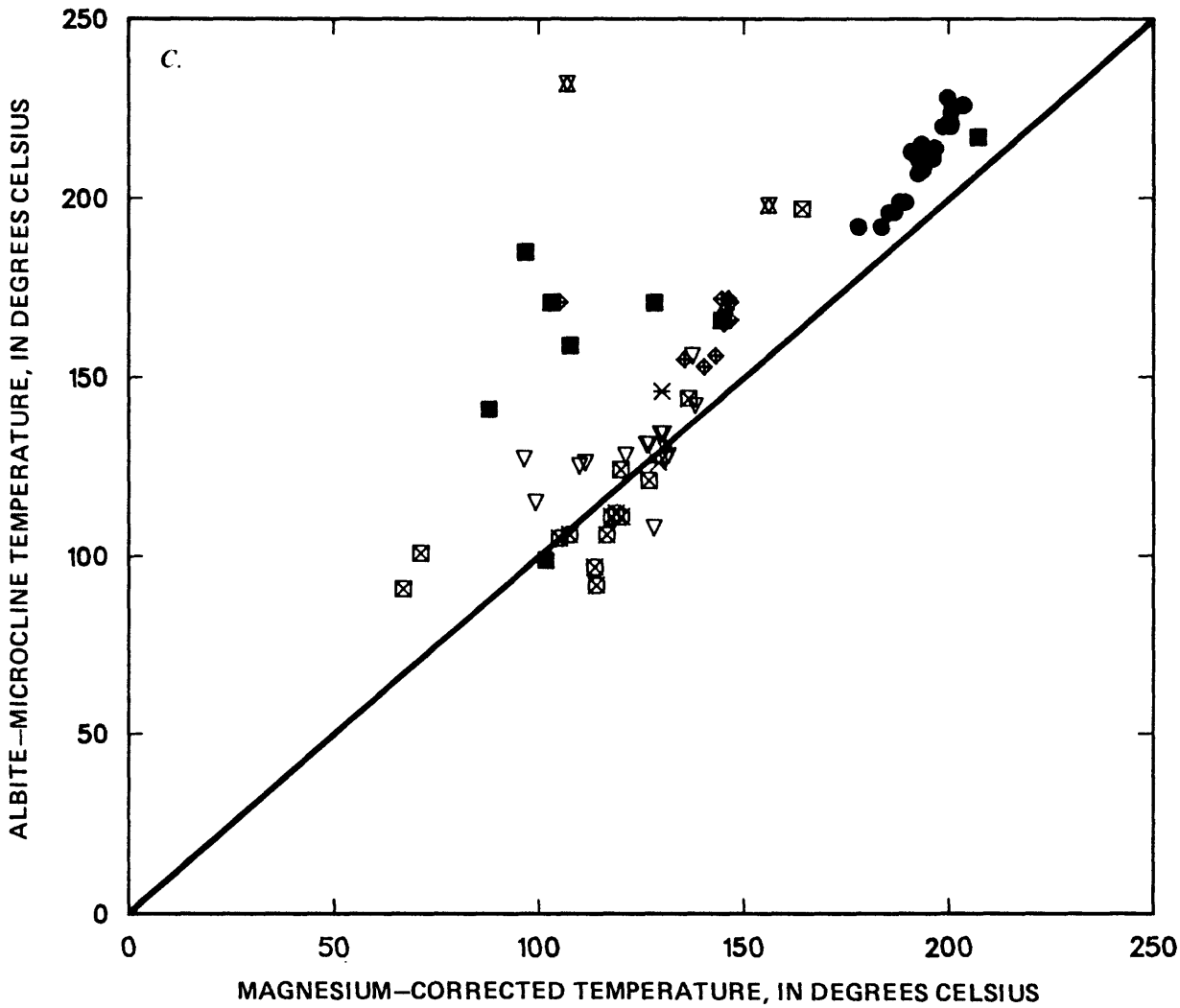

FIGURE 15.--Continued.

The estimates for the thermal water in the Hardin City area are in the same general range as that for Double Hot Springs. On the basis of limited sampling, the magnesium-corrected cation estimate is probably the most reliable, with a best estimate being 129-130 °C. The similar chloride concentrations in the combined Double Hot Springs and Hardin City areas, with the similar temperature estimates, imply that these areas may be fed by the same deep, thermal aquifer.

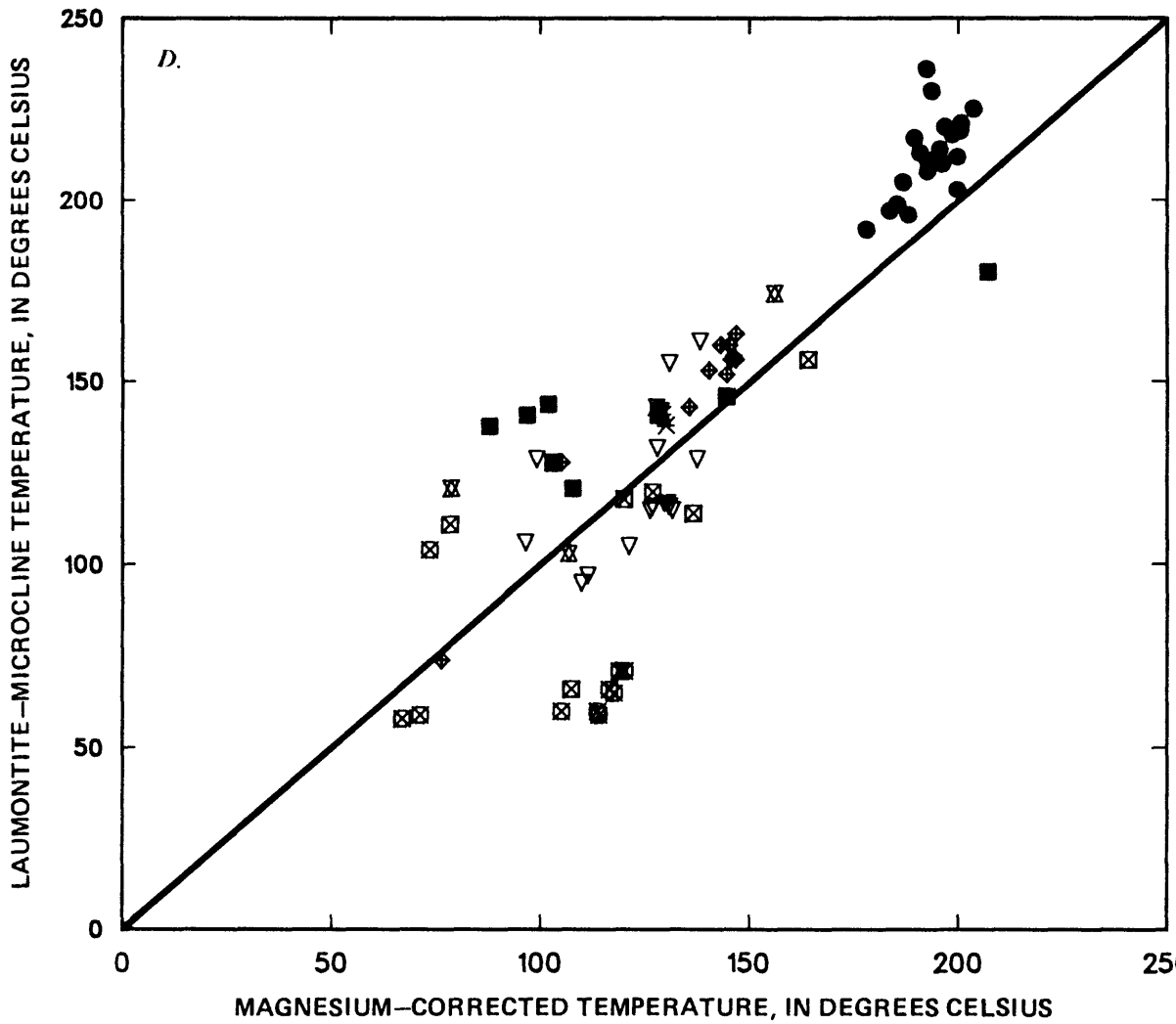

FIGURE 15.--Continued.

Temperature estimates for the Mud Meadow area vary widely. The Na-K-Ca method appears to give unrealistically high values, considering the measured temperatures and the conductive-quartz values. The magnesium-corrected values are, if not accurate, at least more consistent with the silica estimates. The two samples with the highest measured temperatures show reasonable agreement between the magnesium-corrected cation and conductive quartz values yielding a "best" estimate of 119-128 °C. The sample from well WW3922T2 plots below the equal temperature line in figure 15B. This may be due to mixing, supported by the fact that the chloride concentration is significantly higher than that in the other thermal samples. For this reason, the geothermometry estimates for this well are not included in table 6.

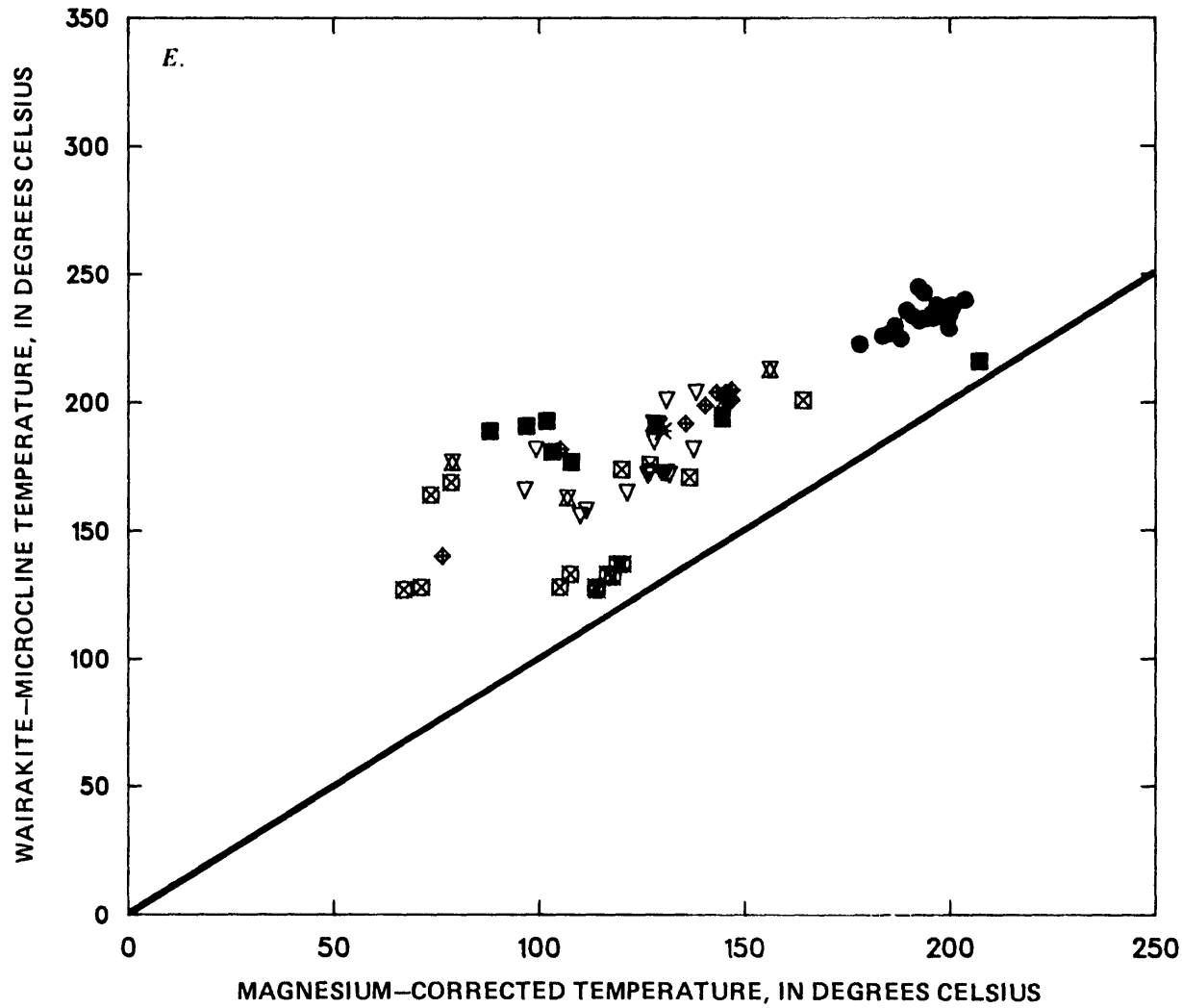

FIGURE 15.--Continued.

The water from Soldier Meadow, although agreement between the silica and cation methods is poor, appears to yield the lowest temperature estimates of any areas discussed in this section. The cation method with $\beta = 4/3$ (as recommended by Fournier and Truesdell, 1973, for estimates less than 100 °C) yields unrealistically low values, as the maximum estimated value is 16 °C lower than the highest measured temperature. Because of the lack of a reliable criterion for selecting one conductive silica method over another, the quartz may be used only as an apparent maximum value of 110-114 °C. If the chalcedony values are accurate, then a range of 60-85 °C is indicated which, in some cases, is only slightly above the measured values.

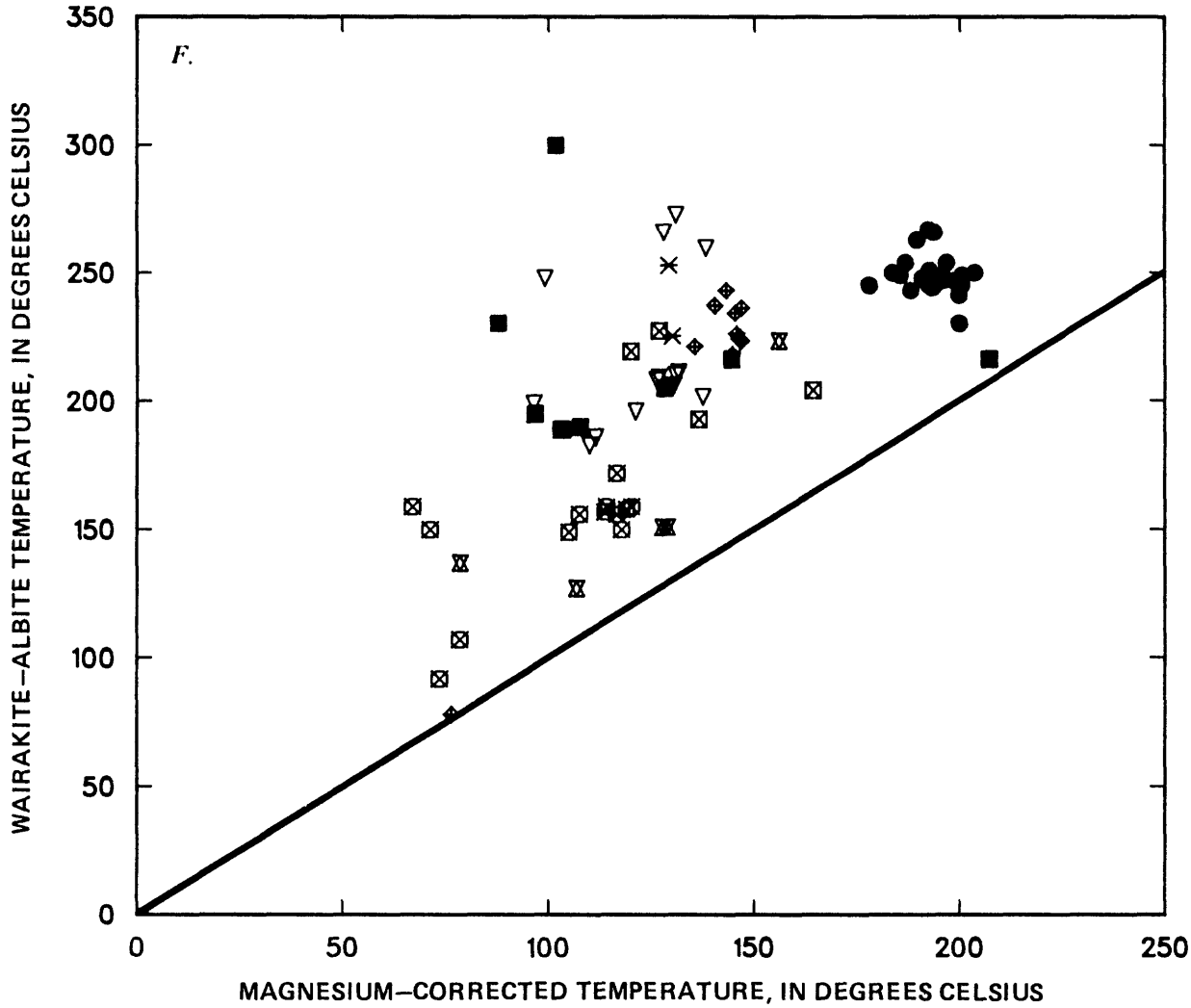

FIGURE 15.--Continued.

Evaluating the geothermometers on the basis of thermodynamic data is difficult because the true deep thermal temperatures of the various systems are unknown. For the purpose of evaluating qualitatively thermodynamically based geothermometers, one of the more commonly applied geothermometers, the magnesium-corrected alkali method, is used as a standard for comparison (figs. 15C-G). The relations between the activities and temperature for the various reactions at equilibrium are shown in figures 16A-C. Although agreement between a thermodynamically based value and the alkali method does not necessarily indicate that the thermodynamic method is valid, a comparison of results should be useful in deciding whether the new approach is worth further evaluation.

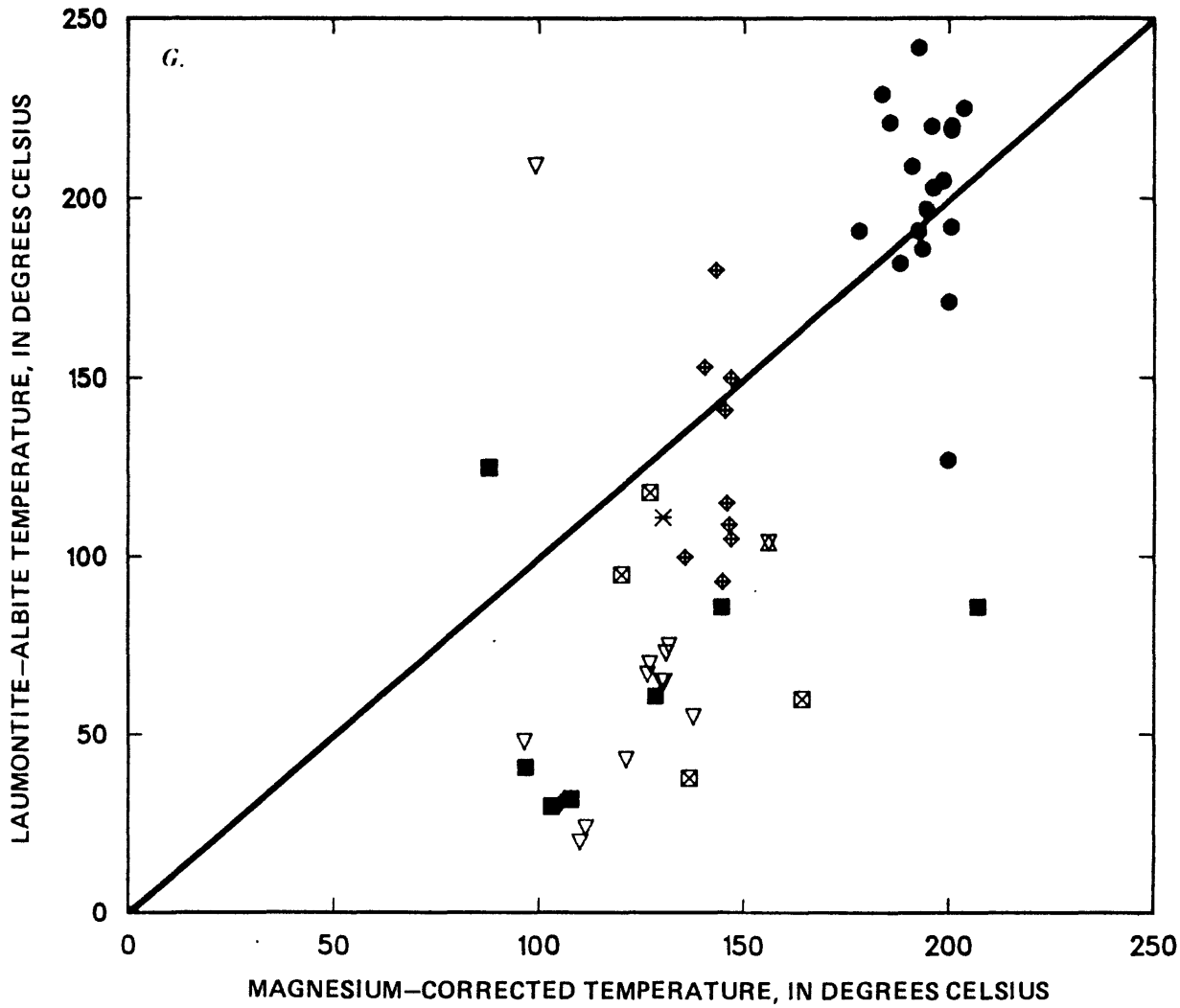

FIGURE 15.--Continued.

The results of the microcline-albite geothermometry agree with the alkali results within about 20 °C for water with alkali values greater than 140 °C (fig. 15C). Microcline-albite values for samples from the area south of Double Hot Springs, the Mud Meadow area, and one sample from Hualapai Flat are in poor agreement with the cation estimates. As disscussed earlier in this section, most of the alkali and silica temperature values for samples from the southern part of the Black Rock Range are in poor agreement. As was the case for the silica and alkali methods, the temperature estimates from the alkali and microcline-albite methods for the thermal water with the lowest chloride concentration along the southern Black Rock Range are in reasonable agreement. The water from the Mud Meadow area is relatively cool; source temperatures are less than 55 °C and may be too low for albite and microcline to be in equilibrium.

The agreement between the microcline-laumontite and the alkali methods is fairly good, particularly for samples with alkali values greater than about 120 °C (fig. 15D). In general, except for some of the samples from Soldier Meadow, the agreement is within about 15 °C. The agreement between the wairakite-microcline and alkali methods is generally not good, although most of the data plotted in figure 15E form a general 1:1 slope. This offset may indicate that the thermodynamic data are in error. Deep aquifer temperature measurements and mineralogic data would help in more closely evaluating the geothermometer.

The agreement between the wairakite-albite and the alkali values is only fair; wairakite-albite values are about 30 °C greater than the alkali values (fig. 15F). Despite considerable scatter, the data for the Great Boiling and Mud Springs area and Soldier Meadow could be joined to form a line with a 1:1 slope, which indicates that the disagreement may be related to the accuracy of the thermodynamic data. Comparison of the albite-laumontite and the alkali values (fig. 15G) shows considerable scatter although the results for Great Boiling and Mud Springs are in reasonable agreement.

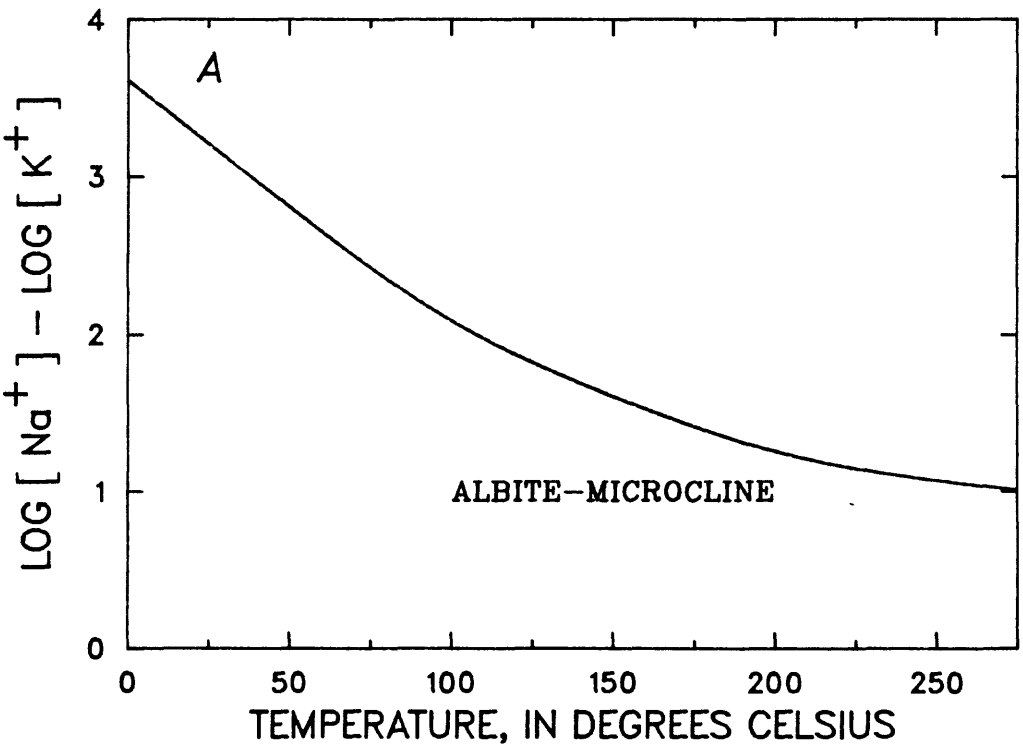

FIGURE 16.--Relation between temperature and the equilibrium activity ratios for *(A)* $\log[Na^+] - \log[K^+]$, *(B)* $\log[Ca^{2+}] - 2\log[K^+]$, and *(C)* $\log[Ca^{2+}] - 2\log[Na^+]$.

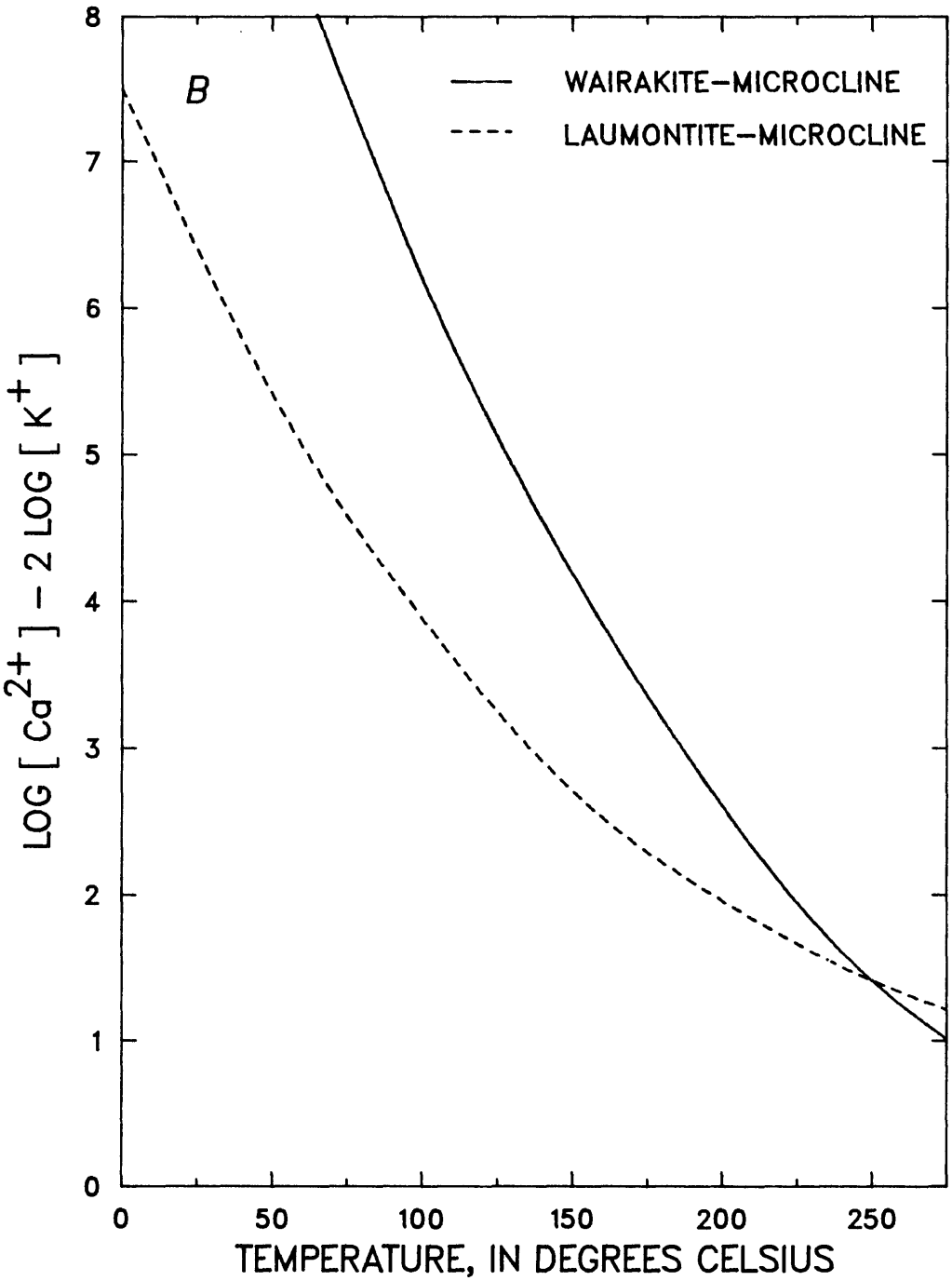

FIGURE 16.--Continued.

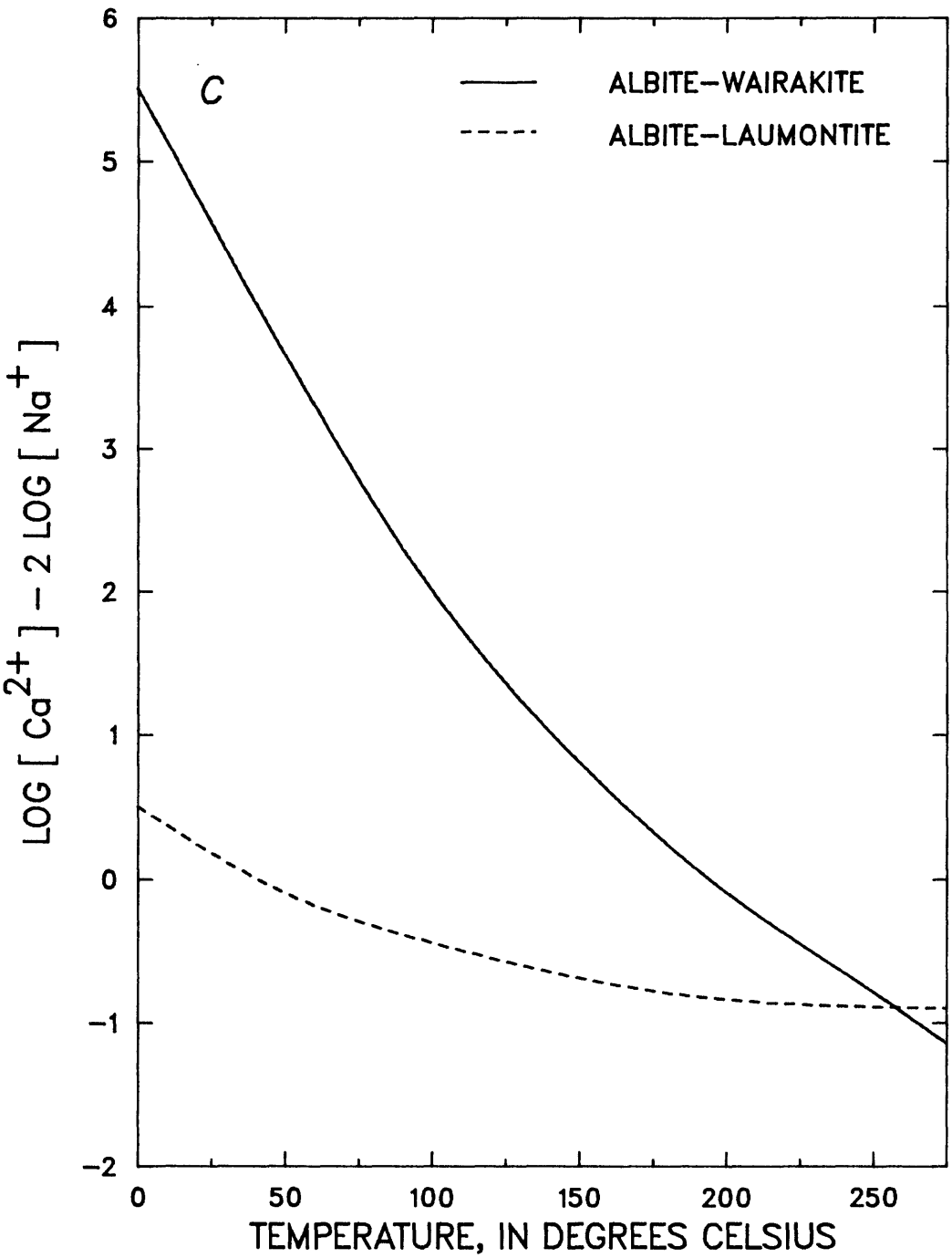

FIGURE 16.--Continued.

In summary, estimated temperatures in the deep thermal aquifers are generally higher from north to south along the ground-water flow direction. Exceptions are Trego Hot Springs, which may receive flow from the eastern area of the Black Rock Desert or recharge from the mountains to the south, and Hualapai Flat, which receives recharge from the Granite Range to the west or flow through the basin-fill sediments. The highest temperatures are associated with Great Boiling and Mud Springs and may exceed 200 °C at depth.

The application of thermodynamically based geothermometry shows considerable promise for systems such as the western Black Rock Desert where deep aquifer temperature measurements and mineralogic data are unavailable. More work is clearly needed to evaluate these geothermometers.

Dissolved Gases

Aquifer temperatures in the Black Rock Desert estimated using isotopic and gas composition data, generally do not agree well with the alkali and silica values. The composition of gas collected at selected orifices and associated temperature estimates (using the method of D'Amore and Panichi, 1980), are presented in table 7. This method is the only gas geothermometer that does not require a knowledge of the gas-water ratio (which cannot be determined for these thermal springs). The estimated temperatures are all lower than the "best" estimates shown in table 6. Several reasons for this difference are possible:

1. Equilibrium has not been attained at depth with the phases ($CaCO_3$, $CaSO_4$, FeS_2, Fe_3O_4, C, CO_2, CH_4, H_2O, H_2S, H_2, and O_2) used in the model by D'Amore and Panichi (1980). A lack of knowledge concerning the phases present at depth makes evaluation of this factor difficult.

2. The methane might be from a deep source, such as magma or the upper mantle. Ratios of methane to carbon dioxide for all the spring gases shown in table 7 are greater than in the 34 geothermal systems considered by D'Amore and Panichi (1980). Because the estimated temperature is inversely related to this ratio, an additional source of methane could result in an estimated temperature less than that which would be calculated if equilibrium were achieved. A deep source of reduced carbon is consistent with the observation by Barnes and others (1978) that high carbon fluxes correspond to areas of tectonic activity and the suggestion by Barnes and Mariner (1979) that carbon in some carbon dioxide rich springs is primarily from the mantle.

TABLE 7.--*Gas compositions and associated temperature estimates for thermal springs*

[Compositions are in volume percent and temperatures are in degrees Celsius. Analyses were performed by W.C. Evans, U.S. Geological Survey, Menlo Park, Calif.]

Sample site	Oxygen	Argon	Nitrogen	Carbon dioxide	Methane	Ethane	Helium	Hydrogen	Temperature[1]
Great Boiling Spring	<0.04	1.37	79.00	15.12	4.78	0.04	0.02	0.39	113
Trego Hot Springs	.01	1.81	93.59	1.25	3.11	<.01	.05	<.01	72
Black Rock Hot Springs	3.42	1.27	74.34	18.66	2.24	<.01	.09	<.005	(2)
Double Hot Springs Orifice 1	.43	1.77	89.48	4.83	3.13	.01	.12	.005	73
Double Hot Springs Orifice 2	.40	1.80	89.66	4.88	3.21	.01	.11	.005	72

[1] The temperatures were calculated using the gas geothermometer of D'Amore and Panichi (1980).
[2] The estimated temperature is not given as the >3 percent oxygen is believed to indicate atmospheric contamination. It is not known whether the oxygen is a result of contamination associated with sampling or shallow mixing at the spring.

3. Lack of analytical data for hydrogen sulfide required the use of an estimated value, in this case, 0.001 percent, following the suggestion of D'Amore and Panichi (1980, p. 554). A greater concentration might reasonably be expected, as indicated by the semiquantitative field measurements of dissolved hydrogen sulfide. A greater hydrogen sulfide concentration results in lower temperature estimates, which makes the agreement with the "best" estimates even poorer.

HEAT FLOW

The magnitude and distribution of heat flow in the shallow subsurface can be used to evaluate conceptual models of the geothermal system in the western Black Rock Desert. Heat-flow data collected during the course of this study represent an areal extension and expansion of the work by Olmsted and others (1975), Sass, Kennelly, and others (1979), Sass, Zoback, and Galanis (1979), and Mase and Sass (1980).

Heat is lost from geothermal systems through radiation, advection, conduction, and convection. Heat lost through radiation is believed to be small, compared with the other components. Radiation from warmed ground is included in the estimates of conductive heat discharge. Other sources of heating, such as radioactive decay, frictional heating from ground-water flow, and chemical reaction are considered to be negligible.

Advective heat discharge, as considered in this study, is the heat removed by water flowing out of the heat-flow budget area. Because the amount of water moving out of the area is considered to be small, advective heat loss also is considered to be small. Permeable materials at the base of the valley-fill deposits, such as coarse alluvial fan deposits or fractured volcanics, may allow some thermal water to flow out of the area near Gerlach; however, lack of information about the deep thermal system prevents thorough evaluation of this possibility. Thus, for the purposes of this report, heat loss resulting from advection is considered negligible and is not discussed further.

Advection of heat into the heat-flow budget area may be occurring and may represent a major source of heat. The presence of thermal water in the vicinity of Wheeler Ranch (fig. 1) makes this a strong possibility. Heating of water in the surrounding mountain ranges also could supply heat to the area and would not be accounted for in this analysis. However, the heat flow in the mountains is not known and the temperature and flow rate of the water entering the area from the north are not well defined.

Heat lost by conduction through near-surface materials is defined as the conductive part of the total heat budget. Heat lost from the area as a result of rising nonthermal water and pure conduction are included in this component of the heat-flow budget. Because some heat flow is supplied by shallow, lateral movement of thermal water, areas with conductive-heat flow values greater than 400 mW/m^2 (milliwatts per square meter; shown in fig. 17) are excluded from the conductive component of the total heat-flow budget. This cutoff value is somewhat arbitrary and was selected to coincide with heat-flow values from areas where thermal water is rising or moving laterally. Areas of upward or laterally moving thermal water are indicated in the field by the presence of warm ground, thermal springs, and large, variable thermal gradients in wells (notably BR02, 03, 05, and 12) as observed by Mase and Sass (1980, p. 8).

The distribution of heat flow shown in figure 17 represents a modification of previous work (primarily by Mase and Sass, 1980) and includes additional information of the area along the western base of the Black Rock Range. The equal heat-flow lines are based on temperature profiles in shallow wells (less than about 100 m) and measured or estimated thermal conductivity data. The conductive heat flow as shown in figure 17 is, at least in part, a result of shallow lateral movement of thermal water that has risen along basin-bounding faults. Conductive heat flow resulting from pure conduction for the area shown in figure 17 is estimated to average about 76 mW/m^2 in areas not affected by shallow flow of thermal water (Mase and Sass, 1980, p. 10). Conductive heat loss from the area (about 940 km^2) outlined in figure 17 is about 81 mW (milliwatts).

Upward movement of ground water in the playa sediments also contributes to the total heat discharge. This contribution to the total heat discharge can be estimated using the method described by Lachenbrach and Sass (1977) (also see Olmsted and others, 1984, p. 107-108). Heat-flow contribution from upward flow is, however, negligible, adopting the upward hydraulic gradients, indicated in appendix 5, estimated hydraulic conductivities, and the average thermal conductivity for playa sediments (see the section on shallow ground-water flow) presented by Mase and Sass (1980). Thus, the upward flow of nonthermal water through the playa sediments (the only part of the heat-budget area with a documented upward component of flow) is not considered to represent an appreciable addition to the total heat flow and is not discussed further.

Convective heat discharge is defined as the heat lost through evapotranspiration of thermal water. The heat removed from the system as a result of geothermal heating input is the heat content of the thermal water above that of recharge water and may be estimated by using spring flow and the corresponding deep aquifer temperatures obtained from the geothermometry. The amount of geothermal heating is estimated to be equal to the difference between the estimated recharge enthalpy (11 cal/g estimated on the basis of upper altitude "recharge" water) lost from the study area and the thermal water. A previous estimate for Great Boiling and Mud Springs (from Olmsted and others, 1975, p. 144) is adapted as it was based on a more detailed analysis of heat discharge from those spring systems. Heat-discharge values in table 8 (other than for Great Boiling and Mud Springs) are probably underestimated as most hot spring systems are associated with some lateral ground-water flow that does not reach the surface in discrete, measurable springs. Unaccounted for flow represents additional heat discharge.

The total convective heat discharge for the heat-flow budget area (which excludes Mud and Soldier Meadows) is about 52 MW (table 8), which combined with the conductive-heat discharge of 81 MW, yields a total heat discharge of about 133 MW. This amount of heat discharge averaged over the heat-budget area (940 km^2) yields an average heat flow of about 140 mW/m^2. A heat flow of 140 mW/m^2 is in the high range compared with other estimates for the Battle Mountain heat-flow high (which may include the western Black Rock Desert; fig. 18). Other studies of heat flow on a basinwide scale in the Battle Mountain area indicate lower average values--in southern Grass Valley, about 140 mW/m^2 (Welch and others, 1981); near Whirlwind Valley, 120-140 mW/m^2 (Franklin H. Olmsted and F. Eugene Rush, U.S. Geological Survey, written commun., 1985).

The high value of 140 mW/m^2 does not appear to be a result of shallow heat sources such as shallow magmatic intrusion. The youngest volcanism in the area has been assigned an age of late Miocene to early Pliocene (Schaefer and others, 1983, p. 8), which corresponds to an absolute age of about 4 million years. This age generally is considered too old to supply significant quantities of heat to active geothermal systems. One possible reason for the apparently high heat flow is that heat is being advected into the area, as previously discussed in this section.

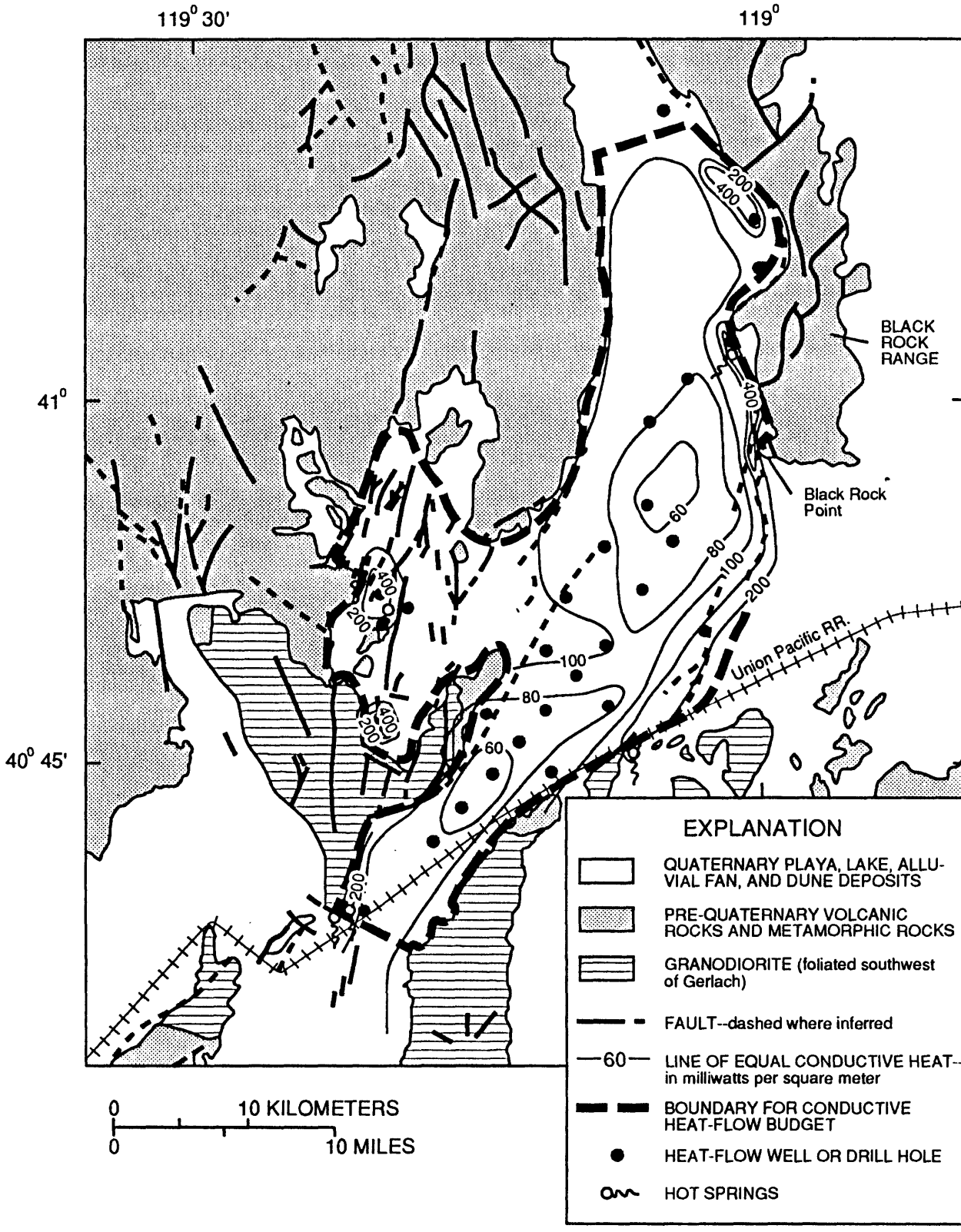

FIGURE 17.--Conductive heat flow in the western arm of the Black Rock Desert. Modified from Mase and Sass (1980).

TABLE 8.--*Estimated convective heat flux*

Area or spring name	Discharge of thermal water[1] (cubic meters per minute)	Amount of geothermal heating[2] (calories per gram)	Heat discharge (megawatts)
Great Boiling and Mud Springs	--	--	[a]23
Trego Hot Springs	0.075	164 - 11 = 153	.8
Hualapai Flat (Fly Ranch)	[b].48	153 - 11 = 142	4.8
Base of the Black Rock Range	1.9	181 - 11 = 170	23
Heat budget area from figure 17	--	--	52
Areas outside heat-budget area			
Mud Meadow	6.0	156 - 11 = 145	61
Soldier Meadows	5.9	120 - 11 = 109	45

[1] See table 1 for sources of the data.
[2] Defined here as the amount of heat supplied by geothermal heating. Calculated as

$$H = T_f - T_i \ ,$$

where H = heat supplied,
T_f = deep aquifer temperature (the maximum magnesium-correct cation value from table 6 was used), and
T_i = temperature of the recharge.

The heat supplied can be estimated using temperatures as in the range 0-200 °C, the enthalpy is numerically about the same as the temperature. The flow volumes were not corrected for the lower density of the heated water.

[a] From Method B of Olmsted and others (1973, p. 144).
[b] Thermal water discharge from Brook and others (1979). The discharge indicated in table 1 (p. 8, herein) includes a nonthermal component.

In addition to allowing an analysis of total heat flow, conductive heat flow data can give insight to the flow regime in the playa sediments. As previously noted, the conductive heat loss through the playa sediments is low. Additionally, the lowest heat flow values generally are associated with greater depths to bedrock (fig. 19), as indicated by the work by Schaefer and others (1983, pl. 4). This general inverse correspondence (greater depths to bedrock corresponding to areas of low heat flow) led Sass and his coworkers (Sass, Zoback, and Galanis, 1979; Mase and Sass, 1980) to suggest that recharge might be supplied by downward flow through the playa sediments. A major argument against this suggestion is the upward hydraulic gradient present in the shallow part of the playa. If recharge is taking place through the playa sediments, then it must be at depths greater than 100 m. Upward hydraulic gradients in the shallow subsurface and downward gradients at greater depth have been documented for basin-fill deposits in the Carson Desert (Olmsted and others, 1984). Thus, downward flow in the playa sediments cannot be ruled out.

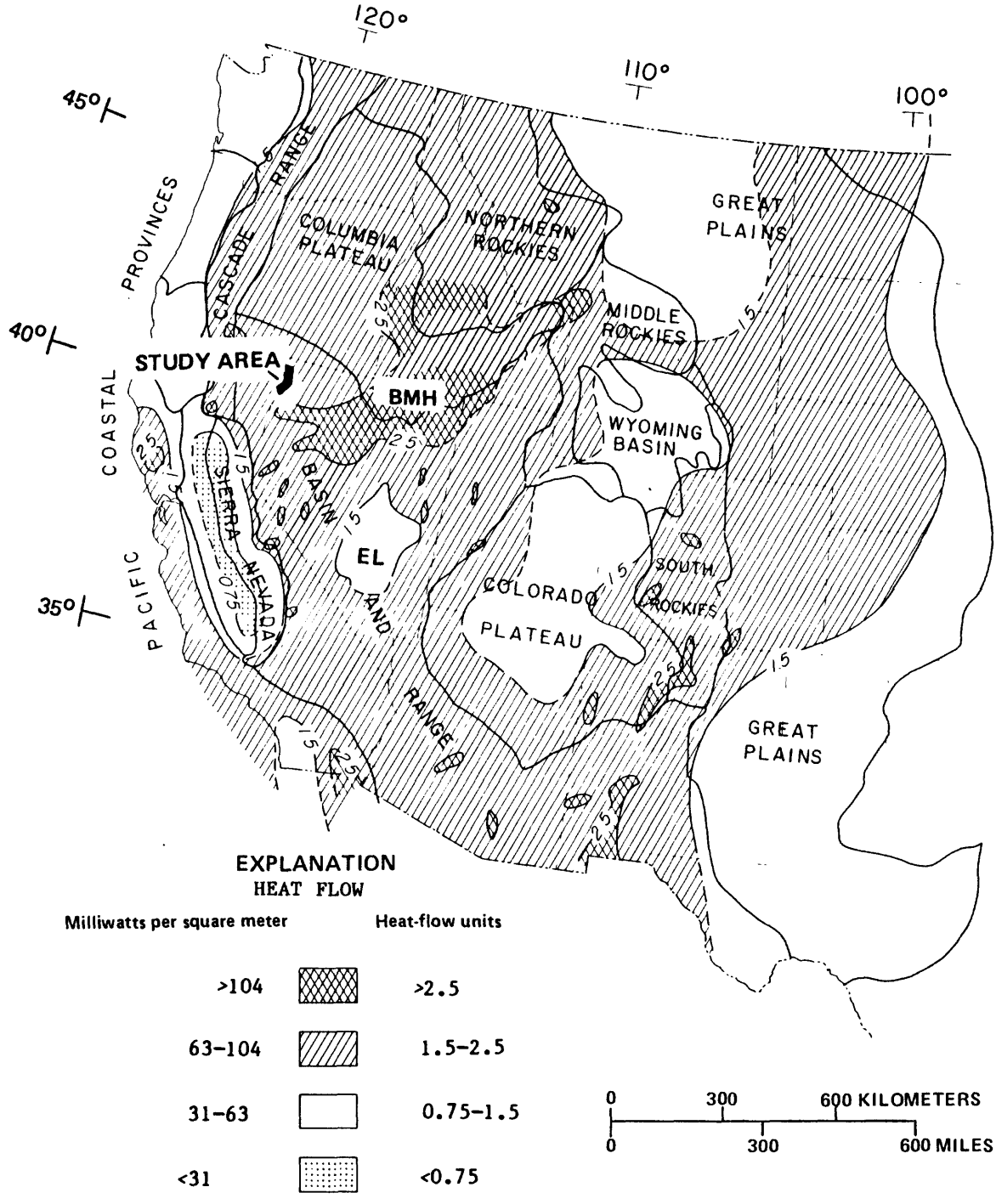

FIGURE 18.--Heat flow in the western United States. Modified from Lachenbruch and Sass (1978).

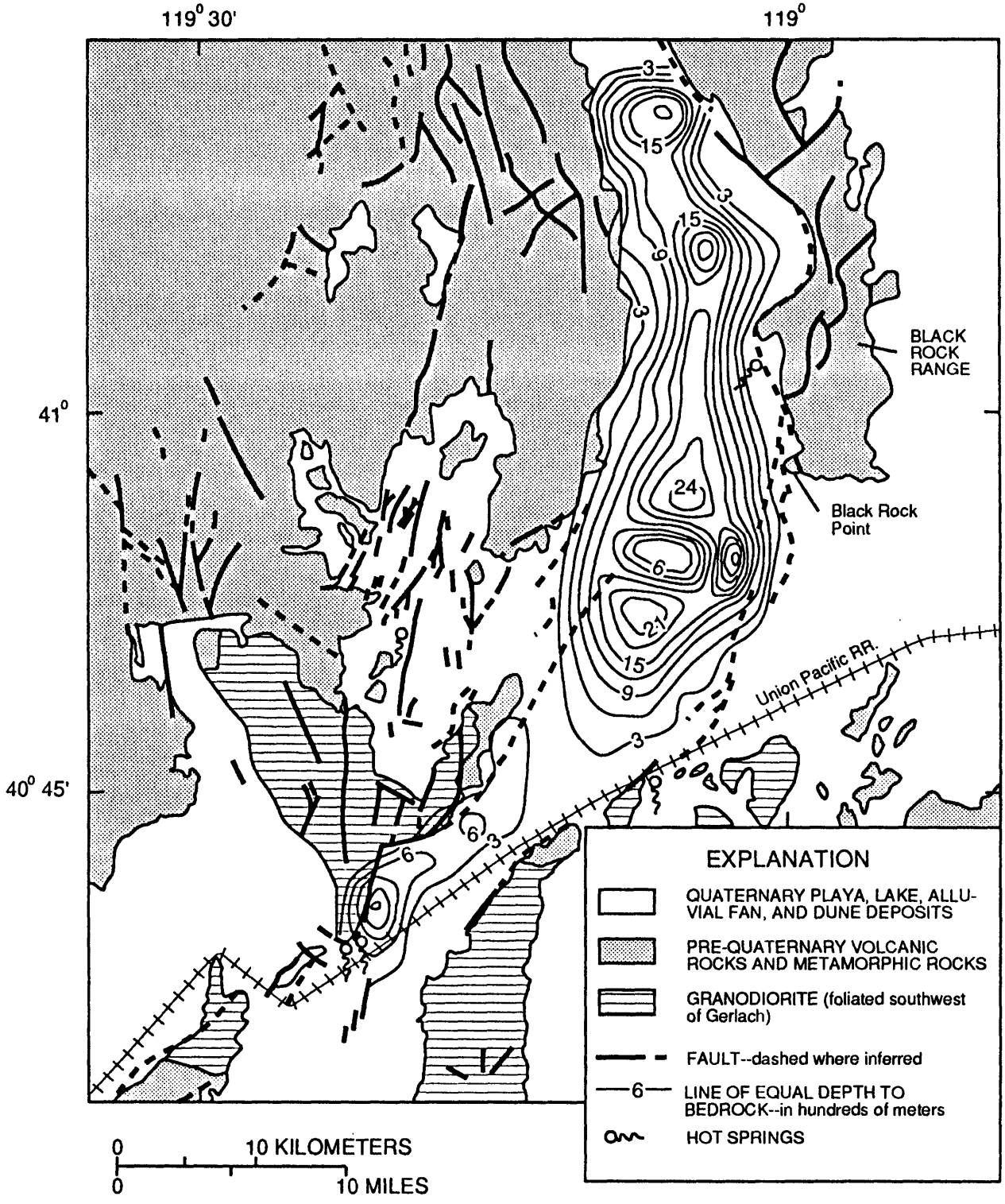

FIGURE 19.--Approximate depth to bedrock in the western arm of the Black Rock Desert. Adapted from Schaefer and others (1983).

Keller and Grose (1978b) suggested that the playa might be acting as an insulating cover of low-conductivity material, resulting in the high water temperatures. Estimated temperatures of less than 40 °C at the base of the valley fill do not appear to support this proposition, at least within 30 km of Gerlach (fig. 20). The temperatures were calculated using the average thermal conductivity adopted by Sass, Zoback, and Galanis (1979) for the playa sediments (1.05 W/m-K), the depth to bedrock (fig. 19), and the heat flow value defined by Mase and Sass (1980). Near the southern Black Rock Range, temperatures may approach 200 °C, which is within a range that could reasonably be expected for thermal water in that area. Temperatures at the base of the fill may, in some cases, be great enough to provide the observed geothermal temperatures. Near Great Boiling and Mud Springs, the indicated temperatures at the base of the valley-fill deposits are much less than estimated thermal temperatures. Thus flow to depths greater than the base of the valley fill is required to reach the estimated temperatures.

The low heat flow through basin-fill sediments in the northern Basin and Range also has been interpreted as an artifact of thermal refraction by Blackwell (1983) who also discussed other complicating factors, including sedimentation, extension, and variations in radioactive-heat production. The effect of ground-water movement on shallow heat flow has yet to be fully evaluated.

CONCEPTUAL MODEL OF GEOTHERMAL SYSTEM

Integration of geochemical, geophysical, and hydrologic information can help place limits on conceptual models of the geothermal system. Hydrologic models that have been used to describe recharge to other geothermal systems in the Basin and Range have, until recently, consisted of either direct recharge to the mountain blocks or into basin-bounding faults by surface or shallow ground water (fig. 21). Recent work by Olmsted and others (1984) in the western Carson Desert, a Pleistocene Lake Lahontan basin with many hydrologic features that are similar to those in the western Black Rock Desert, has led to the hypothesis that recharge occurs within the basin-fill sediments. The major-element chemistry, stable-isotope composition of Great Boiling and Mud Springs, regional heat flow, and hydrogeologic features appear consistent with a model conceptually similar to that proposed for the western Carson Desert.

Recharge to geothermal systems in the northern Basin and Range is not well understood. Arguments for recharge models generally are based on patterns of heat flow or hydrogeologic and hydraulic considerations. Although a detailed consideration of all studies that present arguments for recharge models is beyond the scope of this study, a brief overview is presented to provide a framework within which the systems in the western Black Rock Desert may be discussed.

The association between basin-bounding faults and thermal springs was recognized by Russell (1885, p. 47, 48). During the century since the work by Russell, many other investigators have confirmed that many geothermal systems in the northern Basin and Range are associated with faults. Recent workers have considered a model that incorporates downflow, or recharge, deep lateral flow, and discharge occurring largely within a fault zone at the margin of a basin. This model, shown schematically in figure 21A, has a limited area for heat capture, owing to the steep dip of most basin-bounding faults. The results of numerical modeling of a geothermal system in northern Nevada indicated a maximum age of about 10,000 years if a temperature of 180 °C were to be maintained (see Welch and others, 1981, p. 152-164). A reliable estimate for the age of a geothermal system is difficult to obtain; thus, the limitation on age is difficult to assess. Additionally, the depth of circulation and the length of the fault segment associated with a geothermal system are difficult to determine. For Leach Hot Springs, the system considered by Welch and others (1981), the age may be greater than 250,000 years, on the basis of geologic interpretation by Brogan and Birkhahn (1981, p. 88). Age estimates are not available for the systems in the western Black Rock Desert but, if the Leach Hot Springs system is typical, then the age may make the fault-plane model unrealistic for areas with high aquifer temperatures.

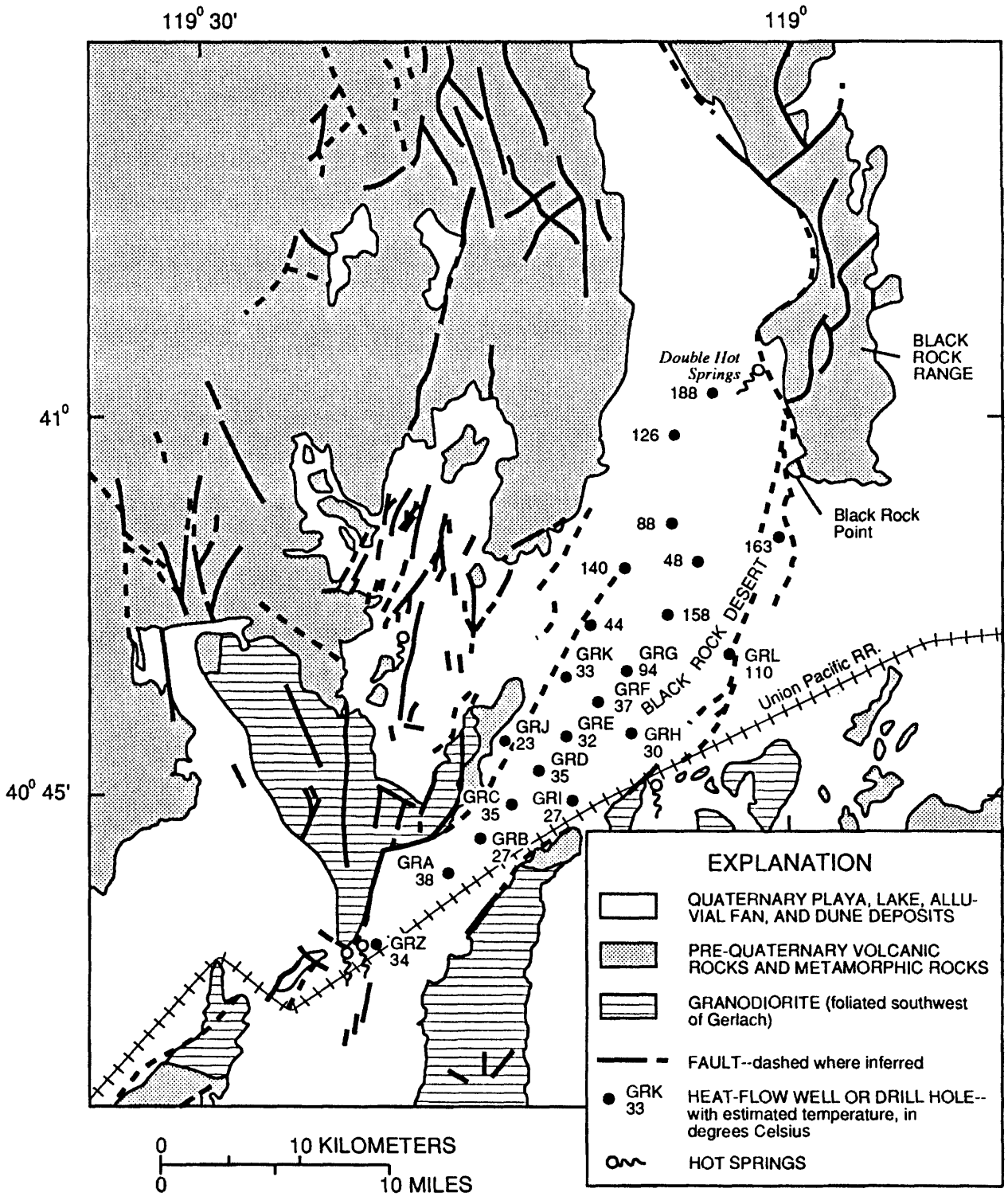

FIGURE 20.--Temperatures at the base of the valley fill estimated from temperature gradients and thermal conductivities.

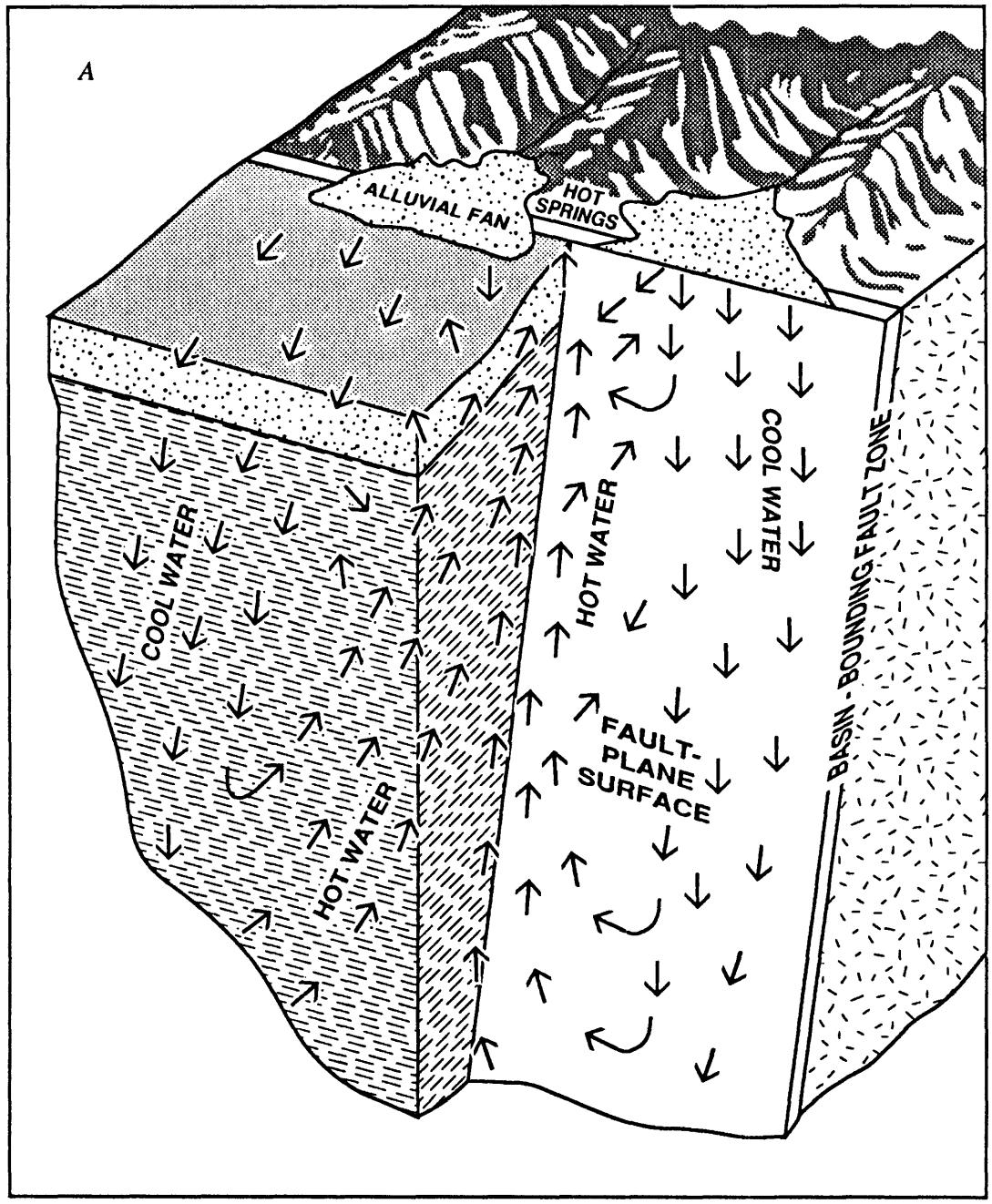

FAULT-PLANE MODEL

EXPLANATION

SHALLOW ALLUVIUM/ COLLUVIUM SEDIMENT

CONSOLIDATED ROCK

BASIN FILL

DIRECTION OF GROUND-WATER FLOW

FIGURE 21.--Schematic diagrams of *(A)* fault-plane and *(B)* mountain-block conceptual models of recharge to a geothermal system in the Basin and Range Province.

Recharge into alluvial fans along the mountain front also may be an important mechanism for recharging the deeper system. Recharge into alluvial fans is indicated by loss of flow as streams traverse the coarse alluvium and, in some cases, low temperatures encountered at shallow depths (Campana and others, 1980). Although recharge to nonthermal aquifers by infiltration into alluvial fans appears an accepted and well-established fact in the northern Basin and Range, the connection to geothermal systems has not been established. Nonetheless, recharge through alluvial fans may be an important water source water for thermal aquifers.

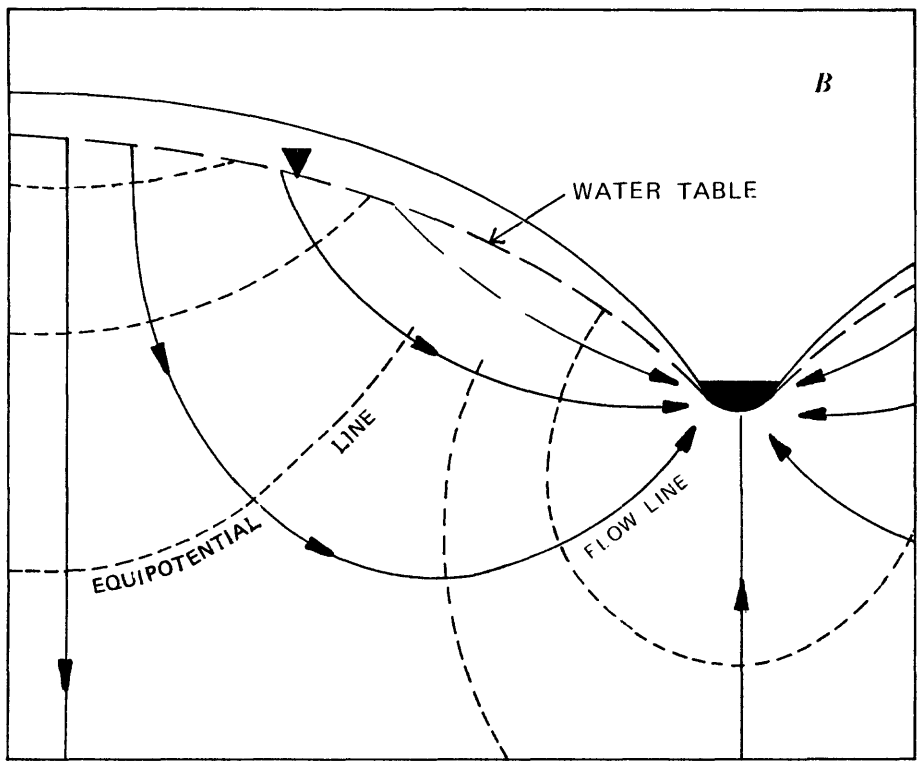

MOUNTAIN-BLOCK MODEL

FIGURE 21.--Continued.

The mountain-block model has as an essential element recharge directly into a mountain block, as shown in figure 21B. In contrast to the fault-plane model, the recharge is diffuse rather than confined to the much smaller cross section of a fault zone. This model is similar to the conceptual work by Toth (1962) and the general description of nonthermal ground-water flow in desert basins by Maxey (1968). A system like that depicted by the mountain-block model would have a much greater area that could supply heat than the fault-plane model and may, therefore, be more reasonable for systems that are old or that have reached thermal steady state. Low heat-flow values in the mountains presumably would be a consequence of the recharge. Low heat flow would appear to be in conflict with the data used by Sass and others (1971) to define the Battle Mountain heat-flow high (heat-flow data were obtained primarily in mountainous areas) and a study of heat flow in a basin in northern Nevada (Welch and others, 1981). Thus, the Battle Mountain heat-flow high must either represent an area of even higher heat flow than has been previously suggested, or mountain recharge is not a general feature in the northern Basin and Range. A hybrid model with diffuse recharge in the mountains with the upflow restricted to a fault zone also is possible. The apparent problem with high heat-flow values in the mountains also applies to this hybrid.

Recharge of dilute water in upland areas is implied by both the mountain-block (fig. 21B) and the fault-plane (fig. 22) models. Although dissolution could occur in mountainous areas composed in part of evaporite minerals, the chemical data collected in recharge areas in the western Black Rock Desert do not support this alternative. Additionally, evaporite minerals have not been reported in the local mountains. Uplands in the Soldier Meadow area are composed predominately of volcanic rocks that are generally able to accept rapid infiltration, which thereby decreases the amount of runoff. Thus, in the Soldier Meadow area, a mountain-block model is considered to be an acceptable alternative. The dilute and slightly thermal water in the Mud Meadow area may be supplied by either surface water from Mud Meadow Creek, which is an ephemeral stream, or from precipitation in the surrounding mountains. The Mud Meadow geothermal water does not appear to be associated with major recent faults, unlike most, if not all the other areas. The area appears to be underlain by a laterally extensive clastic-rock aquifer.

Chloride concentrations in thermal water along the western base of the Black Rock Range increase to the south, which may reflect an increasing proportion of water from the playa. The isotopic similarity of water along the base of the southern Black Rock Range and in Soldier Meadow indicates that deep flow from the north could be supplying water, as represented schematically in figure 22, by the flow rising in the east. Recharge to the Black Rock Range also may be supplying flow to the system. At most of the sampling sites, evapotranspiration probably is affecting the geochemistry where, with the exception of Double Hot Springs, the flow rates are fairly small and the area from which evapotranspiration is occurring is fairly large. The estimated depths to bedrock to the west of Double Hot Springs and the Black Rock Spring appear to be sufficient to reach the temperatures estimated on the basis of measured temperature gradients. Flow in an aquifer composed of volcanic or coarse sedimentary rocks near the base of the basin-fill deposits may be supplying the thermal springs.

Thermal water at Fly Ranch in Hualapai Flat, which may reach temperatures of about 130 °C at depth, may be recharged after some near-surface evapotranspiration, as indicated by the somewhat evolved stable-isotope composition (fig. 10). The chloride concentration of 240 mg/L is consistent with some evaporative concentration. The water at Trego Hot Springs and McClellan Ranch is similar to that at Hualapai Flat in terms of the chloride and possibly, an evolved stable-isotope composition.

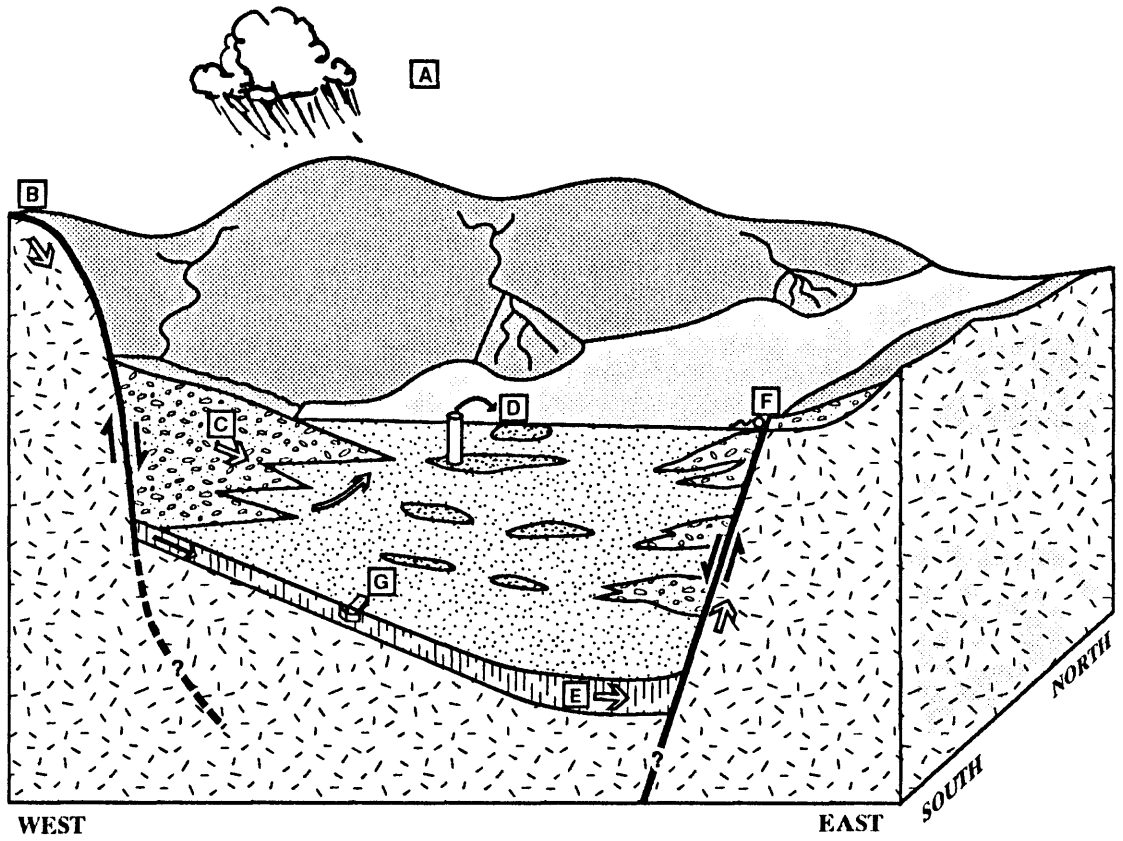

FIGURE 22.--Schematic block diagram showing conceptual model of thermal ground-water flow in the northern part of the western arm of the Black Rock Desert. Precipitation in the mountains (A) recharges thermal aquifers through fractured bedrock (B) and alluvial-fan deposits (C). Discharge of warm water from confined basin-fill aquifers occurs through open wells (D). Hot (greater than 100 °C) water flows near the base of the valley fill, perhaps within volcanic rocks (E), with surface discharge localized along major basin-bounding faults in the eastern part of the basin (F). Flow from north to south within the basin-fill and volcanic aquifers (G) also occurs.

Thermal water in the western Black Rock Desert is derived from local recharge, as indicated by the stable-isotope composition. The most saline thermal water in the area, at Great Boiling and Mud Springs, has a stable-isotope composition that appears to be a result of an evolutionary trend similar to that for nonthermal water in the playa sediments. Although the water at Trego Hot Springs and thermal springs along the western base of the Black Rock Range are not evolved isotopically, the salinity of these springs also may be primarily a result of evaporative concentration rather than dissolution of halite, incorporation of fluid inclusions, or mixing of saline and dilute water. If the chloride concentration in water at Great Boiling and Mud Springs is primarily a result of evaporative concentration, then only limited net mass transfer from the aquifer to the aqueous phase is required (except for silica) to account for the observed total dissolved-solids concentrations. Although the cation composition changes as a result of temperature-dependent reactions occurring at depth, the increase in total cations appears to be minor or essentially nonexistent.

SUMMARY AND CONCLUSIONS

This report describes the results of a study to examine the basic hydrologic and geochemical data and to evaluate the valididy of integrated conceptual models of the geothermal resources in the western arm of the Black Rock Desert, northern Great Basin. The most significant aspects of the study were: (1) the hydrologic connection, if any, between and among the various known thermal areas; (2) probable recharge paths to these thermal areas; and (3) controls on the aqueous geochemistry that can be deduced from information derived from springs and shallow wells. A multidisciplinary approach was used, with emphasis on geochemistry and isotopic hydrology. Such an approach would incorporate hydrologic, geochemical, and isotopic analyses and, thus, would constrain any conceptual heat- and mass-flow models more effectively than a limited study.

In summary, the stable-isotope and chemical composition of thermal water in the Black Rock Desert, when considered with the same kinds of data for local nonthermal water, indicate that:

1. Based on the stable isotopes of water, the source of recharge to the geothermal systems is local meteoric water.

2. Several distinct geothermal systems that attain different temperatures at depth are present. Although the head relations indicate potential for a general southward flow, hydraulic connection between the various known thermal discharge areas cannot be demonstrated. The differing geochemical and isotopic compositions of the water indicate that the various major discharge areas do not represent upflow from a single geothermal system, at least not without significant recharge between the discharge areas.

3. The hydrothermal system that discharges at Great Boiling and Mud Springs appears to have been recharged by water that was affected by shallow evapotranspiration prior to deep circulation. This implies that recharge is occurring through basin-fill sediments or, perhaps, along basin-bounding faults. The system at Trego and perhaps Fly Ranch also may be receiving water that has been affected by shallow evaporation prior to recharge. Thermal water issuing along the western base of the Black Rock Range, in Soldier and Mud Meadows, was recharged by water that was not extensively affected by evaporation prior to recharge.

4. The cation chemistry appears to be controlled by temperature-dependent reactions. The observed cation compositions appear to be consistent with recent compilations of thermodynamic data for minerals in other active geothermal systems. Polynomial equations applied here may be useful in estimating deep aquifer temperatures in other systems.

The use of thermodynamically based geothermometry allows the incorporation of geologic and mineralogic information into the estimation of deep aquifer temperatures. The application of this approach may be hindered by inadequate thermodynamic data or, as is the case in this study, a lack of mineralogic information on the deep geothermal system.

5. The amount of net mass transfer from the thermal aquifer matrix to the aqueous phase is minor (with the exception of an increase in silica concentrations). Although the relative proportions of cations are modified by the temperature-dependent reactions, the molar sum of the cations does not appear to increase greatly at the deep aquifer temperatures. The limited water-rock interaction is consistent with the small or nonexistent oxygen shift and a large water to rock-surface-area ratio such as in a fault-controlled or fractured system.

REFERENCES CITED

Anderson, J.P., 1977, A geological and geochemical study of the southwest part of the Black Rock Desert and its geothermal areas; Washoe, Pershing, and Humboldt Counties, Nevada: Colorado School of Mines, unpublished M.S. thesis, 86 p.

Arnorsson, Stefan, Gunnlaugsson, Einar, and Svavarsson, Hordur, 1983, The chemistry of geothermal waters in Iceland. III: Chemical geothermometry in geothermal investigations: Geochimica et Cosmochimica Acta, v. 47, p. 567-577.

Arnorsson, Stefan, Sigurdsson, Sven, and Svavarrson, Hordur, 1982, The chemistry of geothermal waters in Iceland. I: Calculation of aqueous speciation from 0-370 °C: Geochimica et Cosmochimica Acta, v. 46, p. 1513-1532.

Barnes, Ivan, Irwin, W.P., and White, D.E., 1978, Global distribution of carbon dioxide discharges and major zones of seismicity: U.S. Geological Survey Open-File Report 78-39, 12 p.

Barnes, Ivan, and Mariner, R.H., 1979, Geochemical evidence on the nature of the basement rocks of the Sierra: Geological Society of America, Annual Meeting, Abstracts with Programs, v. 11, no. 7, p. 68.

Blackwell, D.D., 1983, Heat flow in the northern Basin and Range province, *in* The role of heat in the development of energy and mineral resources in the northern Basin and Range province: Davis, Calif., Geothermal Resources Council Special Report No. 13, p. 81-92.

Brogan, G.E., and Birkhahn, P.C., 1981, Faults and occurrence of geothermal anomalies: Final report for contract no. 14-08-001-16310 supported by U.S. Geological Survey geothermal research program, 93 p.

Brook, C.A., Mariner, R.H., Mabey, D.R., Swanson, J.R., Guffanti, Marianne, and Muffler, L.J.P., 1979, Hydrothermal convection systems with reservoir temperatures 90 degrees Centigrade, *in* Muffler, L.J.P., ed., Assessment of geothermal resources of the United States, 1978: U.S. Geological Survey Circular 790, p. 18-85.

Brown, R.H., 1963, Estimating the transmissibility of an artesian aquifer from the specific capacity of a well, *in* Bentall, Ray, compiler, Methods of determining permeability, transmissibility and drawdown: U.S. Geological Survey Water-Supply Paper 1536-I, p. 336-338.

Campana, M.E., Jacobson, R.L., and Ingraham, N.L., 1980, Chap. 6, Shallow temperature survey, *in* Geothermal reservoir assessment case study, northern Basin and Range province, northern Dixie Valley, Nevada: University of Nevada, Reno, Mackay Minerals Resources Research Institute, p. 187-205.

Craig, Harmon, 1961, Isotopic variations in meteoric waters: Science, v. 133, no. 3465, p. 1702-1703.

Craig, Harmon, and Gordon, L.I., 1965, Deuterium and oxygen-18 variations in the ocean and the marine atmosphere, *in* Pisa, T.E., ed., Stable isotopes in oceanographic studies and paleotemperatures: Consiglio Nazionale della Ricerche, Laboratorio di Geologia Nucleare, p. 1-122.

D'Amore, F., and Panichi, C., 1980, Evaluation of deep temperatures of hydrothermal systems by a new gas geothermometer: Geochimica et Cosmochimica Acta, v. 44, p. 549-556.

Dansgaard, W., 1964, Stable isotopes in precipitation: Tellus, v. 16, p. 436-464.

Ellis, A.J., 1970, Quantitative interpretation of chemical characteristics of hydrothermal systems: United Nations Symposium on the Development and Utilization of Geothermal Resources, PISA, v. 2, Part 1, p. 516-528.

Eugster, H.P., and Hardie, L.A., 1978, Saline Lakes, Chapter 8, *in* Lerman, Abraham, ed., Lakes--chemistry, geology, physics: New York, Springer-Verlag, p. 237-249.

Eugster, H.P., and Jones, B.F., 1979, Behavior of major solutes during closed-basin brine evolution: American Journal of Science, v. 279, p. 609-631.

Fouillac, Christian, and Michard, Gil, 1981, Sodium/lithium ratio in water applied to the geothermometry of geothermal waters: Geothermics, v. 10, p. 55-70.

Fournier, R.O., 1977, Chemical geothermometers and mixing models for geothermal systems: Geothermics, v. 5, p. 41-50.

Fournier, R.O., and Potter, R.W. II, 1979, Magnesium correction to the Na-K-Ca chemical geothermometer: Geochimica et Cosmochimica Acta, v. 43, p. 1543-1550.

Fournier, R.O., Sorey, M.L., Mariner, R.H., and Truesdell, A.H., 1979, Chemical and isotopic prediction of aquifer temperatures in the geothermal system at Long Valley, California: Journal of Volcanology and Geothermal Research, v. 5, p. 17-34.

Fournier, R.O., and Truesdell, A.H., 1973, An empirical Na-K-Ca geothermometer for natural waters: Geochimica et Cosmochimica Acta, v. 37, p. 1255-1275.

Fournier, R.O., White, D.E., and Truesdell, A.H., 1974, Geochemical indicators of subsurface temperature--Part I, basic assumptions: U.S. Geological Survey Journal of Research, v. 2, no. 3, p. 259-262.

Freeze, R.A., and Cherry, J.A., 1979, Groundwater: Englewood Cliffs, N.J., Prentice-Hall, Inc., 604 p.

Friedman, Irving, and O'Neil, J.R., 1977, Compilation of stable isotope fractionation factors of geochemical interest: U.S. Geological Survey Professional Paper 440-K, 12 p.

Friedman, Irving, Smith, G.I., and Hardcastle, K.G., 1976, Studies of Quaternary saline lakes--II. Isotopic and compositional changes during desiccation of the brines in Owens Lake, California, 1969-1971: Geochimica et Cosmochimica Acta, v. 40, p. 501-511.

Garside, L.J., and Schilling, J.H., 1979, Thermal waters of Nevada: Nevada Bureau of Mines and Geology Bulletin 91, 163 p.

Gat, J.R., 1971, Comments on the stable isotope method in regional groundwater investigations: Water Resources Research, v. 7, p. 980-993.

-----1980, The isotopes of hydrogen and oxygen in precipitation, *in* Fritz, P., and Fontes, J.C., eds., Handbook of environmental isotope geochemistry: New York, Elsevier Scientific Publishing, v. 1, ch. 1, 545 p.

Giggenbach, W.F., Gonfiantini, R., Jangi, B.L., and Truesdell, A.H., 1983, Isotopic and chemical composition of Parbati Valley geothermal discharges, NW Himalaya, India: Geothermics, v. 12, p. 199-122.

Gonfiantini, R., 1978, Standards for stable isotope measurements in natural compounds: Nature, v. 271, p. 534-536.

Harbeck, G.E., 1962, A practical field technique for measuring reservoir evaporation utilizing mass-transfer theory: U.S. Geological Survey Professional Paper 272-E, p. 101-105.

Hardman, George, 1936, Nevada precipitation and acreages of land by rainfall zones: University of Nevada Agriculture Experimental Station mimeographed report and map, 10 p.

Harrill, J.R., 1969, Hydrologic response to irrigation pumping in Hualapai Flat, Washoe, Pershing, and Humboldt Counties, Nevada, 1960-67: Nevada Department of Conservation and Natural Resources, Water Resources Bulletin 37, 75 p.

Helgeson, H.C., 1969, Thermodynamics of hydrothermal systems at elevated temperatures and pressures: American Journal of Science, v. 267, p. 729-804.

Helgeson, H.C., Delany, J.M., Nesbitt, H.W., and Bird, D.K., 1978, Summary and critique of the thermodynamic properties of rock-forming minerals: American Journal of Science, v. 278-A, p. 1-229.

Helgeson, H.C., and Kirkham, D.H., 1974, Theoretical prediction of the thermodynamic behavior of aqueous electrolytes at high pressures and temperatures: II. Debye-Huckel parameters for activity coefficients and relative partial molal properties: American Journal of Science, v. 274, p. 1199-1261.

Helgeson, H.C., Kirkham, D.H., and Flowers, G.C., 1981, Theoretical prediction of the behavior of aqueous electrolytes at high pressures and temperatures: IV. Calculation of activity coefficients, osmotic coefficients, and apparent molal and standard and relative partial molal properties to 600 °C and 5 kb: American Journal of Science, v. 281, p. 1249-1493.

Henley, R.W., and Ellis, A.J., 1983, Geothermal systems, ancient and modern: A geochemical review: Earth Science Reviews, v. 19, p. 1-50.

Henley, R.W., Truesdell, A.H., and Barton, P.B. Jr., 1984, Fluid-mineral equilibria in hydrothermal systems: Missouri, Reviews in Economic Geology, Society of Economic Geologists, v. 1, 267 p.

Jacob, C.E., and Lohman, S.W., 1952, Non-steady flow to a well of constant drawdown in an extensive aquifer: American Geophysical Union Transactions, v. 33, no. 4, p. 559-569.

Jones, B.F., and Weir, A.H., 1983, Clay minerals of Lake Abert, an alkaline, saline lake: Clays and Clay Mineralogy, v. 31, no. 3, p. 161-172.

Kharaka, Y.K., and Barnes, Ivan, 1973, SOLMNEQ-solution mineral equilibrium computations: U.S. Geological Survey, Computer contribution, 81 p.; available only from U.S. Department of Commerce, National Technical Information Service, Springfield, VA 22161, as Report PB-215 899.

Kharaka, Y.K., and Mariner, R.H., 1977, Solution-mineral equilibrium in natural water-rock systems, *in* Paquet, H., and Tardy, Y., eds., Second International Symposium on Water-Rock Interaction, Strasbourg, Austria, August 17-25, 1977, Proceedings, Section IV, p. IV66-IV75.

Kharaka, Y.K., Specht, D.J., and Carothers, W.W., 1985, Low to intermediate subsurface temperatures calculated by chemical geothermometers: American Association of Petroleum Geologists Bulletin, v. 69/2, p. 273.

Keller, G.V., and Grose, L.T., eds., 1978a, Studies of a geothermal system in northwestern Nevada - part 1: Colorado School of Mines Quarterly, v. 73, no. 3, 84 p.

Keller, G.V., and Grose, L.T., eds., 1978b, Studies of a geothermal system in northwestern Nevada - part 2: Colorado School of Mines Quarterly, v. 73, no. 4, 76 p.

Lachenbruch, A.H., and Sass, J.H., 1977, Heat flow in the United States and the thermal regime of the crust, *in* Heacock, J.G., ed.: American Geophysical Union Monograph 20, p. 626-675.

-----1978, Models of an extending lithosphere and heat flow in the basin and range province: Geological Society of America Memoir 152, p. 209-250.

Mariner, R.H., Presser, T.S., and Evans, W.C., 1976, Chemical data for eight springs in northwestern Nevada: U.S. Geological Survey Open-File Report, 13 p.

Mariner, R.H., Presser, T.S., Rapp, J.B., and Willey, L.M., 1975, The minor and trace elements, gas, and isotope compositions of the principal hot springs of Nevada and Oregon: U.S. Geological Survey Open-File Report, 27 p.

Mariner, R.H., Rapp, J.B., Willey, L.M., and Presser, T.S., 1974, Chemical composition and estimated minimum thermal reservoir temperatures of the principal hot springs of northern and central Nevada: U.S. Geological Survey Open-File Report, 32 p.

Mase, C.W., and Sass, J.H., 1980, Heat flow from the western arm of the Black Rock Desert, Nevada: U.S. Geological Survey Open-File Report 80-1238, 38 p.

Maxey, G.B., 1968, Hydrogeology of desert basins: Ground Water, v. 6, no. 5, p. 10-22.

Merlivat, L., 1978, Molecular diffusivities of water $H_2{}^{16}O$, $HD^{16}O$ and $H_2{}^{18}O$ in gases: Journal of Chemical Physics, v. 69, p. 2864-2871.

Mifflin, M.D., and Wheat, M.M., 1979, Pluvial lakes and estimated pluvial climates of Nevada: Nevada Bureau of Mines and Geology Bulletin 94, 57 p.

Morris, D.A., and Johnson, A.I., 1967, Summary of hydrologic properties of rock and soil materials, as analyzed by the Hydrologic Laboratory of the U.S. Geological Survey, 1948-60: U.S. Geological Survey Water-Supply Paper 1839-D, 42 p.

Nehring, N.L., and Mariner, R.H., 1979, Sulfate water isotopic equilibrium temperatures for thermal springs and wells of the Great Basin: Geothermal Resources Council, Transactions, v. 3, p. 485-488.

Nehring, N.L., Mariner, R.H., White, L.D., Huebner, M.A., Roberts, E.D., Harmon, Karen, Bowen, P.A., and Tanner, Lane, 1979, Sulfate geothermometry of thermal waters in the western United States: U.S. Geological Survey Open-File Report 79-1135, 11 p.

Olmsted, F.H., Glancy, P.A., Harrill, J.R., Rush, F.E., and Van Denburgh, A.S., 1973, Sources of data for evaluation of selected geothermal areas in northern and central Nevada: U.S. Geological Survey Water-Resources Investigations 44-73, 78 p.

-----1975, Preliminary hydrogeologic appraisal of selected hydrothermal systems in northern and central Nevada: U.S. Geological Survey Open-File Report 75-56, 267 p.

Olmsted, F.H., Welch, A.H., Van Denburgh, A.S., and Ingebritsen, S.E., 1984, Geohydrology, aqueous geochemistry, and thermal regime of the Soda Lakes and Upsal Hogback geothermal systems, Churchill County, Nevada: U.S. Geological Survey Water-Resources Investigations Report 84-4054, 166 p.

Paces, Thomas, 1972, Chemical characteristics and equilibrium in natural water-felsic rock-CO_2 systems: Geochimica et Cosmochimica Acta, v. 36, p. 217-240.

Robie, R.A., Hemingway, B.S., and Fisher, J.R., 1978, Thermodynamic properties of minerals and related substances at 298.15 K and 1 bar (10^5 Pascals) pressure and at higher temperatures: U.S. Geological Survey Bulletin 1452, 456 p.

Russell, I.C., 1885, Geological history of Lake Lahontan: U.S. Geological Survey Monograph 11, 288 p.

Sanders, J.W., and Miles, M.J., 1974, Mineral content of selected geothermal waters: University of Nevada, Desert Research Institute Project Report 26, 37 p.

Sass, J.H., Kennelly, J.P., Jr., Wendt, W.E., Moses, T.H. Jr., and Ziagos, J.P., 1979, *In situ* determination of heat flow in unconsolidated sediments: U.S. Geological Survey Open-File Report 79-593, 73 p.

Sass, J.H., Lachenbruch, A.H., Munroe, R.J., Greene, G.W., and Moses, T.H., Jr., 1971, Heat flow in the western United States: Journal of Geophysical Research, v. 76, no. 26, p. 6376-6413.

Sass, J.H., Zoback, M.L., and Galanis, S.P. Jr., 1979, Heat flow in relation to hydrothermal activity in the southern Black Rock Desert, Nevada: U.S. Geological Survey Open-File Report 79-1467, 30 p.

Schaefer, D.H., Welch, A.H., and Maurer, D.K., 1983, Geothermal resources of the western arm of the Black Rock Desert, northwestern Nevada--Part 1, Geology and geophysics: U.S. Geological Survey Open-File Report 81-918, 37 p.

Sinclair, W.C., 1962, Ground-water resources of Hualapai Flat, Washoe, Pershing, and Humboldt Counties: Nevada Department of Conservation and Natural Resources, Ground-Water Resources - Reconnaissance Report 11, 16 p.

-----1963, Ground-water appraisal of the Black Rock Desert area, northwestern Nevada: Nevada Department of Conservation and Natural Resources, Ground-Water Resources - Reconnaissance Report 20, 32 p.

Thiem, G., 1906, Hydrologisch methoden (Hydrologic methods): Gebhardt, Leipzig, 56 p.

Toth, J., 1962, A theory of groundwater motion in small drainage basins in central Alberta, Canada: Journal of Geophysical Research, v. 67, no. 11, p. 4375-4387.

Truesdell, A.H., 1976, Summary of section III, Geochemical techniques in exploration: Second United Nations Symposium on the Development and Use of Geothermal Resources, San Francisco, 1975, Proceedings, v. 1, p. liii-lxxix.

U.S. Geological Survey, 1982, Water resources data for Nevada, water year 1981: U.S. Geological Survey Water-Data Report NV-81-1, 404 p.

Waring, G.A., 1965, Thermal springs of the United States and other countries of the world - a summary: U.S. Geological Survey Professional Paper 492, 383 p.

Welch, A.H., Sorey, M.L., and Olmsted, F.H., 1981, The hydrothermal system in southern Grass Valley, Pershing County, Nevada: U.S. Geological Survey Open-File Report 81-915, 193 p.

Wood, W.W., 1976, Guidelines for collection and field analysis of ground-water samples for selected unstable constituents: U.S. Geological Survey Techniques of Water-Resources Investigations Book 1, Chapter D2, 24 p.

Zimmerman, U., Ehhalt, D., and Munnich, K.O., 1967, Soil-water movement and evapotranspiration: Changes in the isotopic composition of the water: International Atomic Energy Agency Symposium on Isotopes in Hydrology, Vienna, 1966, Proceedings, p. 567-584.

(PAGE 77 FOLLOWS)

APPENDICES

APPENDIX 1.--*Chemical, isotopic, and related data for ground-water samples collected prior to 1979*

[All units are in milligrams per liter, except as noted. Abbreviations: °C, degrees Celsius; µS/cm, microsiemens per centimeter at 25 °C; µg/L, micrograms per liter.]

No.	Location	Site name	Latitude	Longitude	Temperature (°C)	pH (units)	Specific conductance (µS/cm)	Calcium	Magnesium	Sodium
1	N36 E26 04D	DOUBLE HOT SPRINGS	41.0464	119.0264	80.0	7.9	902	4.8	0.1	180
2	N36 E26 04D	DOUBLE HOT SPRINGS	41.0464	119.0264	76.0	7.6	--	4.8	.2	180
3	N36 E26	DOUBLE HOT SPRINGS	41.0492	119.0275	77.6	7.9	910	15	.1	230
4	N36 E26	DOUBLE HOT SPRINGS, ORIFICE 2	41.0492	119.0275	68.5	7.1	--	17	.1	230
5	N36 E26	DOUBLE HOT SPRINGS, ORIFICE 3	41.0492	119.0275	73.5	6.9	--	15	.2	260
6	N36 E26	DOUBLE HOT SPRINGS, ORIFICE 4	41.0492	119.0275	68.5	7.1	--	18	.2	270
7	N32 E23 15B	BORAX SPRING	40.6608	119.3650		8.2	--	78	1.3	1,600
8	N32 E23 15B	GREAT BOILING SPRING, ORIFICE 3	40.6608	119.3650	86.0	7.1	7,610	68	1.2	1,400
9	N32 E23 15B	GREAT BOILING SPRING, ORIFICE 3	40.6608	119.3650		7.4	--	67	1.4	1,300
10	N32 E23 15B	GREAT BOILING SPRING, ORIFICE 9	40.6608	119.3650	75.0	7.6	8,150	73	2.0	1,600
11	N32 E23 15B	GREAT BOILING SPRING, ORIFICE 18	40.6608	119.3650	58.0	8.3	7,600	73	2.5	1,600
12	N32 E23 15B	GREAT BOILING SPRING, ORIFICE 19	40.6608	119.3650	98.0	7.4	7,600	70	1.0	1,400
13	N32 E23 15B	GREAT BOILING SPRING, ORIFICE 22	40.6608	119.3650	55.3	8.2	8,100	75	2.5	1,800
14	N32 E23 15B	GREAT BOILING SPRING, ORIFICE 23	40.6608	119.3650	35.1	--	--	150	12	1,900
15	N32 E23 15B	GREAT BOILING SPRING, ORIFICE 24	40.6608	119.3650	93.5	7.6	7,800	73	2.0	1,600
16	N32 E23 15B	GREAT BOILING SPRING, ORIFICE 27	40.6608	119.3650	63.0	7.8	--	75	2.2	1,600
17	N32 E23 15B	GREAT BOILING SPRING, ORIFICE 28	40.6608	119.3650	95.5	7.1	7,620	68	2.8	1,600
18	N32 E23 15B	GREAT BOILING SPRING, ORIFICE 37	40.6608	119.3650	65.0	7.7	--	70	2.2	1,400
19	N32 E23 15B	GREAT BOILING SPRING, ORIFICE 43	40.6608	119.3650	45.8	6.8	7,600	69	2.3	1,800
20	N32 E23 15B	GREAT BOILING SPRING, ORIFICE 46	40.6608	119.3650	83.8	7.6	7,600	96	2.3	1,400
21	N32 E23 15B	GREAT BOILING SPRING, ORIFICE 55	40.6608	119.3650	78.0	7.0	--	73	2.3	1,600
22		GREAT BOILING SPRING	40.6614	119.3675	92.0	8.0	7,300	72	1.2	1,500
23	N32 E23 15BBA	GERLACH HOT SPRINGS	40.6614	119.3650	84.0	--	7,830	89	1.0	1,500
24	N32 E23 10A1	DITCH SPRING	40.6733	119.3550	97.0	7.2	--	73	2.2	1,400
25		MUD SPRINGS, ORIFICE 1	40.6508	119.3839	60.5	7.8	--	75	2.8	1,500
26		MUD SPRINGS, ORIFICE 2	40.6508	119.3839	74.0	7.2	--	74	2.5	1,500
27	N32 E23 16D	MUD SPRING, ORIFICE 9	40.6508	119.3839	84.3	7.0	8,000	73	2.4	1,500
28	N32 E23 16D	MUD SPRING, ORIFICE 13	40.6508	119.3839	42.0	7.1	7,600	50	2.3	1,600
29	N32 E23 15A	HORSE SPRING	40.6586	119.3536	63.0	7.6	--	74	1.0	1,400
30		LAKE	--	--	--	--	--	2.9	1.4	860
31	N33 E25	TREGO HOT SPRINGS	40.7700	119.1100	86.0	8.2	2,300	11	.2	450
32	N34 E25	TREGO HOT SPRINGS	40.7672	119.1108	86.0	8.4	2,300	25	.2	460
33	N33 E25 10A	MCCLELLAN RANCH WELL	40.7436	119.1608	36.3	8.6	2,150	21	.2	320
34	N33 E25 10B	MCCLELLAN RANCH WELL	40.7447	119.1730	92.0	7.4	1,410	13	.6	270
35	N33 E24 30	PLAYA WELL	40.6958	119.2997	17.0	8.1	8,700	6.0	16	2,100
36	N34 E25 16D	COYOTE SPRING	40.8092	119.1794	22.0	7.8	5,150	12	19	1,200
37	N32 E23 18D	GODEY SPRING	40.6514	119.4217	20.0	9.7	--	2.0	.2	1,000
38	N33 E23 26D	UNNAMED WELL	40.7103	119.3367	16.0	7.4	1,110	18	5.0	310
39	N33 E22 27B	DEEP SPRING	40.7180	119.4833	18.0	8.1	--	1.0	3.0	74
40	N33 E25 10B	UNNAMED WELL	40.7447	119.1730	20.0	8.4	1,980	15	4.0	270
41	N34 E22	SQUAW SPRING	40.8244	119.4847	10.0	8.1	--	30	3.0	300
42	N40 E24	SOLDIER MEADOW SPRING 1	41.3580	119.2178	54.0	8.5	360	4.0	1.0	74
43	N40 E24	SOLDIER MEADOW SPRING 2	41.3580	119.2178	48.0	7.6	357	2.4	1.5	76
44	N40 E24	SOLDIER MEADOW SPRING 2	41.3580	119.2178	54.0	8.6	363	3.1	< .1	74
45	N35 E23 25B	UNNAMED WELL	40.8064	119.3244	13.0	--	703	30	9.5	110
46	N34 E24 03BB	WELL USGS H-7	40.8658	119.2483	15.0	8.4	4,200	18	17	800
47	N35 E23 26DB	SAND SPRING LAND CO. WELL	40.8847	119.3333	--	8.2	480	39	14	53
48	N34 E23	FLY RANCH WARDS HOT SPRINGS	40.8667	119.3483	87.0	8.1		18	4.0	320
49	N35 E23 24DB	JOHN FITZ WELL	40.8867	119.3150	25.0	8.3	420	31	13	42
50	N35 E24 06CC	RICHARD BAILEY WELL	40.9422	119.3044	26.0	8.1	480	1.8	.9	82
51	N36 E24 16A	CAINE SPRING	41.0133	119.2547	21.0	--	323	23	13.4	74
52	N34 E23 02	WELL AT FLY RANCH	40.7808	119.3775	80.0	7.9	1,800	31	4.2	340
53	N34 E23 34A	GRANITE CREEK	40.7939	119.3342	26.0	7.5	229	19	3.8	18
54	N34 E23 10A	UNNAMED SPRING	40.8503	119.3514	22.0	7.2	755	72	21	54
55	N34 E23 01	WESTERN SPRING	40.8605	119.3181	96.0	8.4	1,800	22	.2	390
56	N34 E23 01	HUALAPAI FLAT SPRING 1	40.8605	119.3181	32.4	8.4	2,100	28	.2	380
57	N34 E25 01	HUALAPAI FLAT SPRING 3	40.8605	119.3181	35.0	8.4	2,100	24	.2	380
58	N34 E23 01	HUALAPAI FLAT SPRING 16	40.8605	119.3181	94.0	7.2	1,950	22	.2	410
59	N34 E23 01	HUALAPAI FLAT SPRING 18	40.8605	119.3181	91.0	7.1	2,300	28	.2	400
60	N34 E23 01	HUALAPAI FLAT SPRING 41	40.8605	119.3181	33.5	7.9	2,060	17	.2	440
61	N34 E23 01	HUALAPAI FLAT SPRING 50	40.8605	119.3181	32.0	7.9	2,100	18	.2	430
62	N34 E23 01	HUALAPAI FLAT SPRING 63	40.8605	119.3181	82.0	7.1	2,250	24	.2	410
63	N34 E23 01	HUALAPAI FLAT SPRING 82	40.8605	119.3181	32.0	8.0	2,100	20	.2	400
64	N34 E24 06BB	JACKSON WELL	40.8658	119.3055	16.0	7.9	409	27	10	38
65	N35 E24 31AB	JACKSON WELL	40.8797	119.2958	17.0	7.7	366	26	9.7	33
66	N35 E23 25AC	JACKSON WELL	40.8914	119.3150	21.0	7.3	509	44	14	35
67	N35 E23 23AD	SAND SPRINGS LAND CO. WELL	40.9055	119.3292	24.0	8.2	440	34	13	44
68	N35 E23 13DB	HAROLD FERRIS WELL	40.9169	119.3156	18.4	7.8	339	25	9.0	32
69	N35 E23 10B	NEGRO WELL	40.9361	119.3608	23.0	7.4	288	9.0	4.0	21
70	N36 E23 36A	UNNAMED WELL	40.9592	119.3325	13.0	7.2	559	46	20	40
71	N37 E25 09D	UNNAMED WELL	41.1136	119.1319	15.5	7.3	451	18	6.9	66
72	N37 E25 10D	UNNAMED WELL	41.1142	119.1167	36.1	7.8	446	9.6	2.8	78

APPENDIX 1.--*Chemical, isotopic, and related data for ground-water samples collected prior to 1979*--Continued

No.	Potassium	Bicarbonate	Carbonate	Chloride	Sulfate	Fluoride	Silica	Total dissolved solids (calculated)	Cation-anion balance	Site	Date (year-month-day)	Reference
1	4.5	260	2	59	120	10	110	616	-0.02	Spring	74-01-01	Mariner & others, 1974 & 197
2	4.0	420	0	53	83	--	170	675	-0.11	Spring	78-01-01	WATSTORE
3	5.0	260	2	80	120	10	110	692	0.08	Spring	75-01-01	Anderson, 1977
4	5.0	280	0	110	120	10	130	762	0.03	Spring	75-01-01	Anderson, 1977
5	6.0	280	0	120	140	10	110	801	0.05	Spring	75-01-01	Anderson, 1977
6	10	280	0	120	140	10	86	784	0.08	Spring	75-01-01	Anderson, 1977
7	134	75	0	2100	370	--	170	4450	0.06	Spring	75-01-01	Anderson, 1977
8	130	83	<1	2200	400	4.5	170	4430	-0.03	Spring	74-01-01	Mariner & others, 1974 & 197
9	67	100	0	1800	340	--	280	4410	0.03	Spring	78-01-01	WATSTORE
10	110	90	0	2100	360	--	180	4430	0.05	Spring	75-01-01	Anderson, 1977
11	135	84	0	2200	380	--	190	4600	0.03	Spring	75-01-01	Anderson, 1977
12	140	90	0	2100	370	4.5	170	4330	-0.01	Spring	75-01-01	Anderson, 1977
13	128	88	0	2400	380	--	180	5010	0.05	Spring	75-01-01	Anderson, 1977
14	270	88	0	5000	1400	--	170	8850	-0.28	Spring	75-01-01	Anderson, 1977
15	135	66	0	2100	360	--	170	4450	0.06	Spring	75-01-01	Anderson, 1977
16	148	82	0	2200	380	--	180	4590	0.04	Spring	75-01-01	Anderson, 1977
17	134	160	0	2200	410	--	170	4610	0.02	Spring	75-01-01	Anderson, 1977
18	133	90	0	2300	350	--	190	4550	-0.05	Spring	75-01-01	Anderson, 1977
19	130	88	0	2200	360	4.4	170	4770	0.09	Spring	75-01-01	Anderson, 1977
20	136	83	0	2400	400	4.8	170	4560	-0.06	Spring	75-01-01	Anderson, 1977
21	140	85	0	2100	360	--	180	4530	0.06	Spring	75-01-01	Anderson, 1977
22	110	85	0	2200	370	5.5	160	4460	-0.00	Spring	77-05-08	WATSTORE
23	113	91	0	2200	390	5.5	170	4596	0.01	Spring	74-02-19	Sanders and Miles, 1974
24	121	84	0	2200	390	--	180	4400	-0.03	Spring	75-01-01	Anderson, 1977
25	135	75	0	2100	380	3.8	170	4430	0.03	Spring	75-01-01	Anderson, 1977
26	134	70	0	2100	370	--	170	4400	0.03	Spring	75-01-01	Anderson, 1977
27	143	70	0	2100	380	--	170	4390	0.03	Spring	75-01-01	Anderson, 1977
28	131	74	0	2400	370	--	170	4760	-0.01	Spring	75-01-01	Anderson, 1977
29	130	74	0	1900	360	4.1	180	4080	0.04	Spring	75-01-01	Anderson, 1977
30	15	--	--	620	230	12	--	--	--	Well	--	USGS unpublished data
31	9.0	190	0	280	86	4.4	85	1020	0.23	Spring	75-01-01	Anderson, 1977
32	9.3	150	0	520	86	--	85	1260	0.06	Spring	74-01-01	Mariner and others, 1976
33	21	100	15	290	140	3.0	86	943	0.07	Well	75-01-01	Anderson, 1977
34	8.4	93	0	280	160	2.8	94	871	-0.01	Well	61-06-12	Sinclair, 1963
35	75	1450	0	1700	10	--	61	4620	0.14	Well	75-01-01	Anderson, 1977
36	15	1210	0	1200	5.8	1.5	58	3040	0.01	Spring	61-05-03	Sinclair, 1963
37	47	460	0	690	280	.2	30	2280	0.15	Spring	75-01-01	Anderson, 1977
38	10	360	48	160	79	--	44	847	0.04	Well	45-04-09	Sinclair, 1963
39	5.0	150	0	110	38	--	50	348	-0.27	Spring	75-01-01	Anderson, 1977
40	9.0	88	14	270	160	--	100	893	0.00	Well	47-09-02	Sinclair, 1963
41	4.0	230	0	26	9.0	.2	32	516	0.51	Well	75-01-01	Anderson, 1977
42	1.0	90	3	18	35	12	63	256	0.11	Spring	75-01-01	Anderson, 1977
43	0	96	0	21	39	12	65	266	0.08	Spring	61-05-06	Sinclair, 1963
44	1.1	92	3	18	41	12	63	--	0.06	Spring	74-01-01	Mariner & others, 1974 & 197
45	2.2	220	0	86	41	.1	36	424	-0.00	Well	61-12-13	Harrill, 1969
46	23	550	45	760	390	--	--	--	-0.03	Well	67-08-03	Harrill, 1969
47	13	200	0	48	62	--	35	364	-0.05	Well	67-07-25	Harrill, 1969
48	13	260	0	280	48	--	84	1115	0.08	Spring	78-01-01	WATSTORE
49	17	170	0	38	56	--	--	--	-0.05	Well	67-09-28	Harrill, 1969
50	39	170	0	44	77	--	--	--	-0.09	Well	67-06-16	Harrill, 1969
51	10	110	0	32	22	.1	74	298	0.23	Spring	61-12-12	Harrill, 1969
52	17	460	4	240	46	7.0	82	1000	0.04	Well	74-01-01	Mariner & others, 1974 & 197
53	3.5	280	0	21	9.0	.1	18	234	-0.47	Well	61-12-13	Harrill, 1969
54	10	220	0	93	67	.1	89	516	-0.03	Spring	61-12-13	Harrill, 1969
55	17	460	0	250	250	--	88	1240	-0.04	Spring	75-01-01	Anderson, 1977
56	17	460	0	240	240	--	89	1210	-0.04	Spring	75-01-01	Anderson, 1977
57	17	460	0	280	190	7.0	90	1210	-0.03	Spring	75-01-01	Anderson, 1977
58	17	460	0	250	210	--	90	1210	0.01	Spring	75-01-01	Anderson, 1977
59	18	440	0	250	200	--	88	1200	0.01	Spring	75-01-01	Anderson, 1977
60	16	460	0	260	220	--	90	1270	0.02	Spring	75-01-01	Anderson, 1977
61	15	450	0	250	210	--	82	1230	0.03	Spring	75-01-01	Anderson, 1977
62	14	440	0	260	390	7.0	86	1400	-0.08	Spring	75-01-01	Anderson, 1977
63	17	470	0	250	160	--	82	1160	0.02	Spring	75-01-01	Anderson, 1977
64	8.8	180	0	27	20	.1	69	287	-0.04	Well	61-12-12	Harrill, 1969
65	7.1	160	0	25	20	.2	66	266	-0.04	Well	61-05-03	Harrill, 1969
66	8.9	180	0	46	42	.1	60	339	-0.05	Well	67-05-12	Harrill, 1969
67	16	170	0	48	61	--	34	336	-0.07	Well	67-07-25	Harrill, 1969
68	4.7	150	0	23	16	.2	61	244	-0.03	Well	61-05-03	Harrill, 1969
69	7.0	75	0	13	12	.1	64	167	-0.02	Well	75-01-01	Anderson, 1977
70	5.1	200	0	33	69	.1	42	357	-0.03	Well	67-05-12	Harrill, 1969
71	5.4	150	0	42	32	1.2	84	328	-0.00	Well	61-06-14	Sinclair, 1963
72	11	170	0	28	38	1.8	79	329	-0.01	Well	61-06-14	Sinclair, 1963

APPENDIX 1.--*Chemical, isotopic, and related data for ground-water samples collected prior to 1979*--Continued

No.	Boron (µg/L)	Barium (µg/L)	Iron (µg/L)	Lithium (µg/L)	Manganese (µg/L)	Strontium (µg/L)	Zinc (µg/L)	Delta deuterium (permil)	Delta oxygen (permil)	Plotting symbol
1	1800	--	<20	60	<20	90	--	-128.8	-15.93	D
2	1800	<100	48	70	<10	730	13	--	--	D
3	2000	--	--	--	--	--	--	--	--	D
4	2100	--	--	--	--	--	--	--	--	D
5	2000	--	--	--	--	--	--	--	--	D
6	1800	--	--	--	--	--	--	--	--	D
7	--	--	--	--	--	--	--	--	--	G
8	9900	--	20	1600	30	2600	--	-100.5	-10.83	G
9	7650	230	<30	1640	22	2100	--	--	--	G
10	1100	--	--	--	--	--	--	--	--	G
11	1300	--	--	--	--	--	--	--	--	G
12	1800	--	--	--	--	--	--	--	--	G
13	1500	--	--	--	--	--	--	--	--	G
14	900	--	--	--	--	--	--	--	--	G
15	--	--	--	--	--	--	--	--	--	G
16	--	--	20	--	20	--	--	--	--	G
17	1600	--	--	--	--	--	--	--	--	G
18	1700	--	--	--	--	--	--	--	--	G
19	1500	--	--	--	--	--	--	--	--	G
20	1500	--	--	--	--	--	--	--	--	G
21	--	--	--	--	--	--	--	--	--	
22	--	<40	90	3520	18	408	135	--	--	G
23	--	--	--	--	--	--	--	--	--	G
24	--	--	--	--	--	--	--	--	--	G
25	2100	--	--	--	--	--	--	--	--	G
26	--	--	--	--	--	--	--	--	--	G
27	1100	--	--	--	--	--	--	--	--	G
28	1200	--	--	--	--	--	--	--	--	G
29	1800	--	--	--	--	--	--	--	--	G
30	--	--	--	--	--	--	--	--	--	L
31	5000	--	--	--	--	--	--	--	--	T
32	--	--	--	--	--	--	--	-124.5	-14.40	T
33	600	--	--	--	--	--	--	--	--	T
34	--	--	--	--	--	--	--	--	--	T
35	4800	--	--	--	--	--	--	--	--	P
36	4500	--	--	--	--	--	--	--	--	P
37	100	--	--	--	--	--	--	--	--	R
38	--	--	--	--	--	--	--	--	--	R
39	--	--	--	--	--	--	--	--	--	R
40	0.6	--	--	--	--	--	--	--	--	R
41	100	--	--	--	--	--	--	--	--	R
42	600	--	--	--	--	--	--	--	--	S
43	820	--	--	--	--	--	--	--	--	S
44	640	--	<20	170	<20	<50	--	-129.9	-16.56	S
45	400	--	--	--	--	--	--	--	--	U
46	--	--	--	--	--	--	--	--	--	U
47	--	--	--	--	--	--	--	--	--	U
48	2.2	170	130	440	<10	830	6	--	--	U
49	--	--	--	--	--	--	--	--	--	U
50	--	--	--	--	--	--	--	--	--	U
51	100	--	--	--	--	--	--	--	--	U
52	1900	--	130	460	<20	1100	--	-120.7	-14.72	U
53	100	--	--	--	--	--	--	--	--	U
54	100	--	--	--	--	--	--	--	--	U
55	900	--	--	--	--	--	--	--	--	U
56	--	--	--	--	--	--	--	--	--	
57	--	--	--	--	--	--	--	--	--	U
58	500	--	--	--	--	--	--	--	--	U
59	--	--	--	--	--	--	--	--	--	U
60	6600	--	--	--	--	--	--	--	--	U
61	5400	--	--	--	--	--	--	--	--	U
62	600	--	--	--	--	--	--	--	--	U
63	5200	--	--	--	--	--	--	--	--	U
64	100	--	--	--	--	--	--	--	--	U
65	200	--	--	--	--	--	--	--	--	U
66	100	--	--	--	--	--	--	--	--	U
67	--	--	--	--	--	--	--	--	--	U
68	100	--	--	--	--	--	--	--	--	U
69	100	--	--	--	--	--	--	--	--	U
70	--	--	--	--	--	--	--	--	--	U
71	0	--	--	--	--	--	--	--	--	M
72	--	--	--	--	--	--	--	--	--	M

(PAGE 82 FOLLOWS)

APPENDIX 2.--*Chemical, isotopic, and related data for ground-water samples collected from 1979 to 1982*

[All units are in milligrams per liter, except as noted. Abbreviations: °C, degrees Celsius; µS/cm, microsiemens per centimeter at 25 °C; µg/L, micrograms per liter.]

No.	Location	Site name	Latitude	Longitude	Temperature (°C)	pH (units)	Specific conductance (µS/cm)	Calcium	Magnesium
1	N35 E27 30CAC	TH SP #1 SULPHUR 2NW QD	40.9530	118.9994	89.0	7.0	6,620	23	3.4
2	N36 E26 09DAC	TH SP#1 SOLD CR 4SE QUA	40.9533	118.9992	45.5	8.2	2,360	23	4.7
3	N36 E26 34BAB	BLACK ROCK SPRING	40.9739	119.0069	77.0	7.5	2,130	14	3.0
4	N36 E26 22CBD	WELL BRD51A	40.9950	119.0089	28.0	8.0	12,300	200	.2
5	N36 E26 27BCA	WELL BRD52B	40.9855	119.0092	24.0	9.8	4,110	1.4	.1
6	N36 E26 21AA	TH SP #4 ORA SOLDIER CR 4S	41.0033	119.0161	87.0	7.3	1,670	24	2.1
7	N36 E26 16DA	TH SP #3 ORA SOLDIER CR SE	41.0150	119.0164	78.0	7.3	1,320	19	2.4
8	N36 E26 16DAC	TH SP #3 ORG SOLDIER CR 4S	41.0125	119.0153	46.5	7.1	1,540	25	3.6
9	N36 E26 16AA	TH SP#2 ORE SOLDIER CR 4SE	41.0236	119.0144	91.0	7.9	1,140	9.4	.5
10	N36 E26 09ABD	WELL BRD57A	41.0372	119.0189	40.5	9.3	1,160	2.0	< .1
11		DOUBLE HOT SPRINGS, ORIFICE 1	41.0492	119.0275	82.0	8.1	854	5.4	.1
12		DOUBLE HOT SPRINGS, ORIFICE 2	41.0492	119.0275	78.0	8.2	871	5.6	.1
13					--	--	--	--	--
14		DOUBLE HOT SPRINGS, ORIFICE 3	41.0492	119.0275	84.0	7.8	835	4.9	< .1
15		DOUBLE HOT SPRINGS, ORIFICE 4	41.0492	119.0275	60.0	8.4	850	5.7	.3
16		DOUBLE HOT SPRINGS, ORIFICE 5	41.0492	119.0275	78.0	8.1	876	6.0	1.0
17	N36 E26 04D	DOUBLE HOT SPRINGS, ORIFICE 6	41.0492	119.0275		8.1	851	6.4	< .1
18	N36 E26 04BAB	WELL DHS4	41.0542	119.0267	35.0	8.2	1,860	3.8	.1
19	N36 E26 04BAB	WELL DHS4	41.0542	119.0267	37.0	8.3	1,580	2.8	.2
20	N36 E26 04BBA	WELL DHS5	41.0542	119.0269	36.0	9.5	691	2.0	<1.0
21	N36 E26 04BBA	WELL DHS6	41.0542	119.0272	25.5	9.6	1,240	2.1	.5
22		GREAT BOILING SPRING, ORIFICE 23	40.6625	119.3653	100.5	7.2	7,430	74	1.2
23					--	--	--	--	--
24		GREAT BOILING SPRING, ORIFICE 46	40.6608	119.3650	88.5	7.3	7,530	70	1.1
25		GREAT BOILING SPRING, ORIFICE 48	40.6617	119.3653	94.0	7.2	7,400	67	1.5
26	N32 E23 10A	DITCH	40.6733	119.3550	90.0	8.1	7,320	56	.9
27					--	--	--	--	--
28		MUD SPRINGS, ORIFICE 1	40.6508	119.3839	79.0	7.1	7,330	77	2.6
29		MUD SPRINGS, ORIFICE 2	40.6508	119.3839	91.5	7.7	7,460	79	2.8
30					--	--	--	--	--
31	N37 E26 28DBA	WELL BR04	41.0753	119.0181	24.5	9.0	2,700	2.7	.5
32	N37 E26 10DCA	TH SP HARDIN CITY SE QD	41.1156	119.0008	51.0	8.8	914	1.5	< .1
33	N37 E26 03DB	WELL BR12	41.1317	119.0000	24.5	10.0	827	2.0	< .1
34	N38 E26 33C	TH SP #1 OR B SOLDIER CR 4N	41.1478	119.0203	70.0	8.8	776	1.9	.3
35	N37 E26 27BA	WELL BRD53B	41.0831	119.0056	21.0	9.5	3,010	3.2	1.0
36		TREGO HOT SPRINGS, ORIFICE A	40.7717	119.1158	86.5	8.3	2,250	14	< .1
37	N33 E24 21CA	WELL GRB'	40.7267	119.2650	12.0	9.3	93,000	1.7	1.8
38	N33 E24 01CB	WELL GRD	40.7717	119.2167	11.5	11.7	8,470	89	< .1
39	N34 E26 08CB	WELL GRL	40.8450	119.0500	13.0	9.8	32,200	3.0	.4
40	N34 E26 08CB	WELL GRL'	40.8450	119.0500	13.5	9.5	47,700	6.1	15
41	N36 E25 23CDA	WELL BR06	40.9928	119.0994	17.0	7.6	26,500	21	140
42	N36 E26 18BAC	WELL BR07	41.0217	119.0633	16.0	7.7	15,000	19	76
43	N35 E26 05BBA	WELL BR08	40.9358	119.0983	14.0	7.5	20,100	34	320
44	N35 E25 13BBB	WELL BR09	40.9064	119.1375	15.0	7.6	25,700	34	240
45	N35 E26 30AAA	WELL BR10	40.8775	119.1030	13.0	7.3	18,200	110	450
46	N35 E25 27BDD	WELL BR11	40.8725	119.1689	15.0	8.4	10,300	4.0	6.1
47	N33 E23 15BCC	GRANITE BASIN SPRING	40.7433	119.3672	14.5	--	--	--	--
48	N33 E23 06ACB	SUMMIT SPRING	40.7744	119.4150	10.5	--	--	--	--
49	N33 E22 13ACD	RAILROAD SPRINGS	40.7428	119.4361	12.0	8.0	448	47	5.7
50	N40 E25 22CAC	MIDDLE MUSTANG SPRING	41.3555	119.1158	23.0	--	--	--	--
51	N40 E24 24ACD	SP#1 ORB MUD MDW QD NE2	41.3605	119.1944	10.5	7.3	767	7.4	1.5
52	N40 E24 24ABD	SP#2 MUD MDW QD NE 24	41.3644	119.1947	11.0	7.5	599	6.4	1.3
53	N40 E24 03ACC	SP#1 SOLD MDW QD CHU GU	41.4030	119.2381	12.0	6.9	155	10	3.8
54	UNSURVEYED	SPR #1 DONNELLY CR. QUA	41.0414	119.1472	14.0	7.5	707	59	15
55	N37 E25 19DDAC	SP#2 DONNELLY CR QD SE1	41.0858	119.1672	17.0	7.6	452	37	3.4
56	N37 E25 09DC	DONNELLY CREEK	41.1142	119.1333	6.5	7.9	286	19	6.8
57					--	--	--	--	--
58	N39 E26 30BBC	SP BELOW LITTLE BIG MTN	41.2567	119.0619	15.0	--	--	--	--
59	N39 E25 17BCC	WHEELER SPRING	41.2867	119.1694	18.0	8.0	678	27	5.5
60					--	--	--	--	--

APPENDIX 2.--*Chemical, isotopic, and related data for ground-water samples collected from 1979 to 1982*--Continued

No.	Location	Site name	Latitude	Longitude	Temperature (°C)	pH (units)	Specific conductance (µS/cm)	Calcium	Magnesium
61	N39 E25 12CDD	RUNNING WATER SPRING	41.2905	119.0730	9.5	--	--	--	--
62	N39 E24 01BB	SP#3 ORB MUD MDW QD NW1	41.3219	119.2064	24.5	8.3	321	11	1.4
63	N40 E25 29CCC	TH SP #5 MUD MDW QD SW2	41.3383	119.1678	27.0	7.2	290	3.0	.1
64	N40 E24 25DDCA	TH SP#10 ORB MUD MDWSE2	41.3389	119.1919	53.5	8.8	362	3.1	.1
65	N40 E24 23DCCD	THERMAL SP NO.2 MUDMEAD	41.3525	119.2167	53.0	8.8	374	3.1	.1
66	N40 E24 23CCDA	TH SPR #3 MUD MDW QUAD	41.3539	119.2236	44.0	8.7	355	3.9	.1
67		TH SPR #1 MUD MDW QUAD	41.3569	119.1878	57.0	8.9	345	3.1	.9
68					--	--	--	--	-
69	N40 E24 23BCDA	TH SPR #6 OR A MUD MDW	41.3608	119.2233	51.0	8.8	336	3.9	.1
70	N40 E24 23ABCD	TH SPR #9 MUD MEADOW QU	41.3636	119.2164	35.5	9.0	357	3.2	< .1
71	N40 E25 18BBC	TH SP#4 SOLD MDW QD NW1	41.3797	119.1872	55.0	8.8	364	2.8	.2
72	N40 E25 18BACA	TH SP #1 ORA SLDR MDW Q	41.3800	119.1808	38.5	8.9	381	13	3.5
73	N40 E25 05CCCD	TH SP #3 SLDR MDW QD SW	41.3975	119.1664	30.0	7.5	198	10	3.0
74	N36 E25 16ADC	A. JACKSON RANCH WELL	41.0181	119.1297	17.0	8.2	1,530	9.3	4.3
75	N36 E25 16ADC	A. JACKSON RANCH WELL			--	--	--	--	--
76	N37 E24	WW3921	41.0547	119.1136	20.5	9.1	930	1.2	.2
77					--	--	--	--	--
78	N37 E24	WW3922T1	41.0733	119.1097	24.0	8.9	603	2.7	.2
79	N37 E24	WW3922T1	41.0733	119.1097	--	--	--	--	--
80	N37 E24	WW3922T2	41.0742	119.1097	26.0	8.6	584	3.0	.3
81					--	--	--	--	--
82	N37 E24	WW 3922T3	41.0828	119.1050	24.0	9.0	553	2.0	.1
83					--	--	--	--	--
84	N37 E24	WW3922T4	41.0831	119.1042	23.0	9.1	573	2.0	.1
85	N37 E25 11BDB	PW290	41.1208	119.1017	38.5	8.2	453	8.9	1.4
86					--	--	--	--	--
87	N37 E25 11BDB	PW1636	41.1211	119.1014	38.5	8.1	451	8.5	1.4
88					--	--	--	--	--
89	N37 E25 3CCD	FL WL WW3985T1 SO CR 4N	41.1272	119.1247	15.0	8.2	465	17.0	2.3
90	N37 E24	WELL AT WAGNER SPRINGS	41.1358	119.1378	32.0	7.9	352	9.6	1.4
91					--	--	--	--	--
92	N37 E24	WELL NO. 2 3989T	41.1442	119.1272	13.5	8.5	480	6.8	.7
93					--	--	--	--	--
94	N38 E25 07AB	CALICO MOUNTAINS SPRING	41.1597	119.1836	--	--	--	--	--

APPENDIX 2.--*Chemical, isotopic, and related data for ground-water samples collected from 1979 to 1982*--Continued

No.	Sodium	Potassium	Bicar-bonate	Carbon-ate	Chloride	Sulfate	Fluoride	Silica	Cation-anion balance	Site	Date
1	1,500	19	930	0	1700	280	5.8	100	-0.96	Spring	80-07-08
2	420	26	120	1	570	180	1.1	54	-0.99	Spring	80-06-10
3	460	14	900	1	180	130	9.4	70	-0.99	Spring	80-06-24
4	900	77	510	3	4000	340	0.9	31	-0.97	Well	81-06-16
5	930	38	860	290	700	40	7.9	1.9	-0.98	Well	81-06-30
6	330	16	430	0	210	160	11	115	-0.99	Spring	80-06-17
7	270	11	400	0	120	150	11	80	-0.99	Spring	80-06-16
8	300	15	480	0	160	140	9.4	55	-0.99	Spring	80-06-16
9	240	10	320	1	84	160	13	130	-0.99	Spring	80-06-10
10	260	7.2	230	23	140	140	9.0	12	-0.99	Well	80-12-09
11	200	4.7	260	2	59	130	12	110	-0.99	Spring	79-12-05
12	200	4.7	260	2	59	130	11	115	-0.99	Spring	79-12-05
13	--	--	--	--	--	--	--	--	--	Spring	79-12-85
14	200	4.5	250	1	58	130	11	115	-0.99	Spring	79-12-05
15	210	4.9	270	3	59	130	11	130	-0.99	Spring	79-12-05
16	210	4.8	250	2	61	130	12	115	-0.99	Spring	79-12-05
17	200	4.4	250	2	57	130	11	110	-0.99	Spring	79-12-05
18	390	8.6	370	3	270	110	9.4	50	-0.99	Well	80-08-07
19	350	5.2	370	4	220	110	10	55	-0.99	Well	80-11-13
20	150	2.7	180	28	48	96	12	37	-1.00	Well	80-08-07
21	270	4.5	280	58	150	130	12	2.2	-0.99	Well	80-11-15
22	1,500	120	100	0	2200	380	4.7	170	-0.96	Spring	80-01-17
23	--	--	--	--	--	--	--	--	--	Spring	80-01-17
24	1,400	120	96	0	2100	380	5.1	210	-0.96	Spring	80-01-28
25	1,500	100	84	0	2300	370	5.1	160	-0.96	Spring	80-01-16
26	1,400	110	68	0	2000	370	4.6	160	-0.96	Spring	79-11-28
27	--	--	--	--	--	--	--	--	--	Spring	79-11-28
28	1,400	120	120	0	2200	390	5.0	190	-0.96	Spring	80-02-05
29	1,500	100	120	0	2200	380	4.6	140	-0.96	Spring	80-01-18
30	--	--	--	--	--	--	--	--	--	Spring	80-01-18
31	660	18	810	38	310	130	13	65	-0.98	Well	81-04-08
32	210	4.4	280	9	76	120	0.1	60	-0.99	Spring	80-07-09
33	180	4.0	140	73	67	97	11	5.3	-1.00	Well	81-05-06
34	170	5.2	190	5	57	110	12	90	-1.00	Spring	80-07-21
35	640	34	460	76	580	110	3.2	1.7	-0.98	Well	81-07-01
36	470	10	140	1	550	170	4.4	87	-0.99	Spring	80-04-28
37	31,000	170	9560	900	44000	3400	6.9	16	-0.56	Well	80-11-12
38	2,300	130			2500	400	0.1	2.0		Well	80-12-04
39	7,300	56	2220	670	10000	92	6.6	1.0	-0.84	Well	80-11-11
40	11,000	150	2550	390	19000	130	10	17	-0.78	Well	80-11-10
41	5,600	72	2960	6	9100	22	1.1	60	-0.87	Well	80-08-04
42	3,400	61	2820	7	4100	40	0.9	63	--	Well	80-07-28
43	3,800	85	2270	4	7200	14	0.7	54	-0.90	Well	80-07-17
44	4,900	86	2160	5	9400	23	0.9	63	-0.88	Well	80-07-16
45	3,500	50	1050	1	6100	100	0.3	66	--	Well	80-10-08
46	2,300	7.5	1480	19	2700	12	1.7	51	--	Well	80-07-15
47	--	--	--	--	--	--	--	--	--	Spring	79-08-22
48	--	--	--	--	--	--	--	--	--	Spring	79-08-22
49	22	6.2	92	0	67	32	0.1	13	-1.00	Spring	80-01-10
50	--	--	--	--	--	--	--	--	--	Spring	79-08-22
51	160	4.5	170	0	68	120	11	73	-1.00	Spring	80-04-30
52	130	4.3	140	0	52	140	8.8	75	-1.00	Spring	80-05-13
53	15	3.0	74	0	6.8	9.4	0.5	43	-1.00	Spring	80-05-27
54	55	20	190	0	100	69	0.4	77	-1.00	Spring	80-04-21
55	44	10	140	0	50	34	0,3	66	-1.00	Spring	80-05-12
56	26	4.4	110	0	25	20	0.2	43	-1.00	Stream	80-02-06
57	--	--	--	--	--	--	--	--	--	Stream	80-02-06
58	--	--	--	--	--	--	--	--	--	Spring	79-08-22
59	120	9.6	230	1	41	110	7.6	58	-1.00	Spring	80-03-05
60	--	--	--	--	--	--	--	--	--	Spring	80-03-05

APPENDIX 2.--*Chemical, isotopic, and related data for ground-water samples collected from 1979 to 1982*--Continued

No.	Sodium	Potassium	Bicar-bonate	Carbon-ate	Chloride	Sulfate	Fluoride	Silica	Cation-anion balance	Site	Date
61	--	--	--	--	--	--	--	--	--	Spring	79-08-22
62	55	5.4	110	1	17	30	5.6	63	-1.00	Spring	80-05-26
63	75	0.9	120	0	21	46	11	46	-1.00	Spring	80-03-12
64	71	1.2	93	3	17	38	12	69	-1.00	Spring	80-05-14
65	73	1.2	95	3	17	38	3.8	64	-1.00	Spring	80-01-02
66	72	1.2	90	2	12	37	11	66	-1.00	Spring	80-01-09
67	77	0.8	94	4	26	41	13	60	-1.00	Spring	80-01-01
68	--	--	--	--	--	--	--	--	--	Spring	80-01-01
69	69	1.0	88	3	14	34	12	66	-1.00	Spring	80-04-22
70	73	1.1	88	4	18	39	13	66	-1.00	Spring	80-04-29
71	75	0.8	89	3	18	39	12	60	-1.00	Spring	80-05-27
72	40	9.8	94	4	13	18	1.9	99	-1.00	Spring	80-03-04
73	23	7.6	80	0	12	14	0.5	64	-1.00	Spring	80-03-11
74	340	20.0	540	4	220	40	4.7	75	-0.99	Well	80-02-29
75	--	--	--	--	--	--	--	--	--	Well	80-02-29
76	240	5.6	490	31	49	17	8.6	74	-0.99	Well	79-12-04
77	--	--	--	--	--	--	--	--	--	Well	79-12-04
78	150	8.7	220	8	52	49	2.3	90	-1.00	Well	79-12-13
79	--	--	--	--	--	--	--	--	--	Well	79-12-13
80	140	9.4	220	4	51	50	2.0	90	-1.00	Well	79-12-13
81	--	--	--	--	--	--	--	--	--	Well	79-12-13
82	130	6.4	230	11	35	44	2.6	87	-1.00	Well	79-12-19
83	--	--	--	--	--	--	--	--	--	Well	79-12-19
84	130	7.6	240	15	36	39	3.2	87	-1.00	Well	79-12-13
85	80	13	160	1	35	40	1.8	75	-1.00	Well	80-01-29
86	--	--	--	--	--	--	--	--	--	Well	80-01-29
87	78	13	160	1	23	39	2.0	75	-1.00	Well	80-01-29
88	--	--	--	--	--	--	--	--	--	Well	80-01-29
89	80	8.0	180	1	25	45	2.9	75	-1.00	Well	81-04-07
90	56	6.1	120	0	35	27	0.8	70	-1.00	Well	79-12-27
91	--	--	--	--	--	--	--	--	--	Well	79-12-77
92	94	7.8	140	2	35	69	6.4	69	-1.00	Well	80-01-30
93	--	--	--	--	--	--	--	--	--	Well	80-01-30
94	--	--	--	--	--	--	--	--	--	Spring	79-08-22

APPENDIX 2.--*Chemical, isotopic, and related data for ground-water samples collected from 1979 to 1982*--Continued

No.	Boron (µg/L)	Barium (µg/L)	Lithium (µg/L)	Strontium (µg/L)	Zinc (µg/L)	Delta deuterium (permil)	Delta oxygen (permil)	Plotting symbol
1	--	170	720	2,000	16	-121	-12.9	B
2	--	50	68	310	6	-124	-15.7	B
3	--	140	160	720	4	-127	-15.4	B
4	--	--	1,800	17,500	--	-124	-14.4	B
5	--	180	330	190	26	-124	-14.8	B
6	--	130	230	550	<3	-128	-15.0	B
7	--	110	190	580	<3	-128	-15.6	B
8	--	100	230	550	18	-131	-15.8	B
9	--	130	110	0.4	<3	-128	-15.1	B
10	--	40	39	51	18	-128	-15.8	D
11	1,900	--	9	--	--	[a]-121	[a]-15.6	D
12	1,900	--	70	--	--	-129	-16.2	D
13	--	--	--	--	--	[a]-121	[a]-17.1	D
14	--	20	60	81	<3	--	--	D
15	2,000	--	90	--	--	[a]-120	[a]-15.1	D
16	1,900	--	80	--	--	[a]-120	[a]-15.7	D
17	--	20	60	82	<3	[a]-119	[a]-15.6	D
18	--	40	30	86	5	-130	-16.0	D
19	--	50	26	65	5	-129	-16.0	D
20	--	30	29	60	180	-130	-16.4	D
21	--	30	58	78	8	-127	-14.6	D
22	--	90	1,600	2,800	<3	-98.0	-11.6	G
23	--	--	--	--	--	[a]-99.0	[a]-11.0	G
24	8,200	--	1,700	--	--	[a]-105	[a]-10.4	G
25	--	80	1,500	2,700	4	[a]-99.0	[a]-10.6	G
26	--	140	1,600	2,400	6	[a]-99.5	[a]-11.6	G
27	--	--	--	--	--	[a]-91.0	[a]-11.4	G
28	7,900	--	1,700	--	--	[a]-95.0	[a]-11.3	G
29	--	130	1,600	3,000	12	-99.5	-11.1	G
30	--	--				[a]-95.5	[a]-10.8	G
31	--	40	18	130	65	-127	-15.4	H
32	--	6	32	36	<3	-131	-16.1	H
33	--	120	24	27	120	-130	-16.0	H
34	--	30	53	38	3	-130	-15.9	H
35	--	180	130	140	16	-129	-15.4	H
36	--	50	280	770	<8	-125	-15.1	T
37	--	--	30	450	--	-77.0	-5.6	P
38	--	40	1,500	2,500	63	-97.5	-9.2	P
39	--	--	260	600	--	-89.5	-7.8	P
40	--	--	110	1,000	--	-82.0	-6.2	P
41	--	--	460	2,900	--	-88.5	-8.4	P
42	--	800	310	1,400	69	-108	-12.0	P
43	--	--	280	4,000	--	-69.0	-7.6	P
44	--	--	470	3,300	--	-78.5	-6.8	P
45	--	2,900	490	7,900	120	-86.0	-8.4	P
46	--	240	80	700	50	-98.5	-10.8	P
47	--	--	--	--	--	-114	-14.8	R
48	--	--	--	--	--	-109	-14.8	R
49	--	10	9	250	<3	[a]-112	[a]-16.4	R
50	--	--	--	--	--	-124	-16.1	R
51	--	40	180	56	35	-129	-16.3	R
52	--	40	140	47	15	-125	-16.4	R
53	--	60	9	78	40	-115	-14.5	R
54	--	110	16	560	99	-122	-15.5	R
55	--	20	17	90	13	-120	-15.4	R
56	90	--	10	--	--	-110	-15.0	R
57	--	--	--	--	--	[a]-107	[a]-14.3	R
58	--	--	--	--	--	-127	-16.7	R
59	1,100	--	50	--	--	-115	-14.9	R
60	--	--	--	--	--	[a]-114	[a]-14.6	R

APPENDIX 2.--*Chemical, isotopic, and related data for ground-water samples collected from 1979 to 1982*--Continued

No.	Boron (µg/L)	Barium (µg/L)	Lithium (µg/L)	Strontium (µg/L)	Zinc (µg/L)	Delta deuterium (permil)	Delta oxygen (permil)	Plotting symbol
61	--	--	--	--	--	-118	-15.1	R
62	--	20	1000	58	6	-128	-16.0	S
63	900	--	150	--	--	[a]-116	[a]-15.3	S
64	--	10	160	12	<3	-131	-16.6	S
65	--	7	160	14	<3	[a]-125	[a]-16.6	S
66	--	7	170	24	6	[a]-127	[a]-16.4	S
67	--	3	190	20	<3	-126	-16.6	S
68	--	--	--	--	--	[a]-124	[a]-16.5	S
69	--	6	170	22	6	-131	-16.7	S
70	--	10	170	4	<3	-131	-16.4	S
71	--	10	190	21	<3	-131	-16.6	S
72	190	--	30	--	--	[a]-119	[a]-16.0	S
73	80	--	10	--	--	[a]-114	[a]-15.5	S
74	3,400	--	30	--	--	-121	-15.6	M
75	--	--	--	--	--	[a]-118	[a]-15.0	M
76	1,200	--	7	--	--	-122	-15.8	M
77	--	--	--	--	--	[a]-118	[a]-15.8	M
78	640	--	30	--	--	-123	-15.8	M
79	--	--	--	--	--	[a]-116	[a]-15.7	M
80	610	--	20	--	--	-123	-15.8	M
81	--	--	--	--	--	[a]-114	[a]-15.8	M
82	640	--	10	--	--	-123	-16.0	M
83	--	--	--	--	--	[a]-115	[a]-15.7	M
84	670	--	20	--	--	[a]-121	[a]-15.6	M
85	500	10	21	53	<3	-121	-15.9	M
86	--	--	--	--	--	[a]-119	[a]-15.5	M
87	470	8	17	53	<3	-122	-16.0	M
88	--	--	--	--	--	[a]-115	[a]-15.7	M
89	--	120	73	210	21	-124	-15.6	M
90	--	5	15	64	<3	-123	-16.0	M
91	--	--	--	--	--	[a]-117	[a]-16.4	M
92	990	--	20	--	--	-126	-16.6	M
93	--	--	--	--	--	[a]-124	[a]-16.0	M
94	--	--	--	--	--	-112	-16.6	M

[a] Stable-isotope analysis by University of Arizona.

APPENDIX 3.--*Data for wells in the western arm of the Black Rock Desert*

Name of test well	Latitude (north)	Longitude (west)	Altitude of land surface (meters)	Height of measuring point above land surface (meters)	Depth of casing, screen, or cap at bottom[1] (meters)	Nominal inside diameter of casing[2] (millimeters)	Type of completion[3]	Other data available[4]
GRA[5]	40 42 18	119 17 24	1,190	-0.09	102*	32	Sh	T,TC,W
GRB[5]	40 43 36	119 15 54	1,190	- .12	90*	32	Sh	T,TC
GRC[5]	40 45 00	119 14 30	1,190		95*	32	Sh	T,TC
GRD[5]	40 46 18	119 13 00	1,190	~- .11	125*	32	Sh	T,TC
GRE	40 47 36	119 11 36	1,190		95*	32	Sh	T,TC
GRF	40 49 00	119 10 06	1,190		128*	32	Sh	T,TC
GRG	40 50 12	119 08 36	1,190		102*	32	Sh	T,TC
GRH[5]	40 48 00	119 07 36	1,190	~- .23	102*	32	Sh	T,TC,W
GRI[5]	40 46 06	119 10 42	1,191	- .10	102*	32	Sh	T,TC,W
GRJ	40 46 18	119 15 06	1,190		93*	32	Sh	T,TC
GRK[5]	40 49 42	119 12 00	1,190		96*	32	Sh	T,TC
GRL[5]	40 50 42	119 03 00	1,191	~- .10	98*	32	Sh	T,TC
DHS1	41 03 13	119 01 34	1,210	- .52	14.9-16.2	51	Sl	L
DHS2	41 03 15	119 01 34	1,210	.75		102	Sl	
DHS3	41 03 16	119 01 35	1,210	- .15	126.2-127.4	102	Sc	L
DHS4	41 03 15	119 01 36	1,210	.50	213.1-214.3	102	Sc	L,W
DHS5	41 03 15	119 01 36	1,210	~- .50	153.9-155.1	102	Sc	L,W
DHS6	41 03 15	119 01 38	1,210		232.6-233.8	102	Sc	L
BR01A	41 12 19	119 04 58	1,250	.80	68.9-70.1	51	Sc	T,L,TC,W
BR01B	41 12 19	119 04 58	1,250		28.7-29.9	51	Sc	L
BR02	41 05 50	118 59 29	1,231					T,TC
BR03	41 05 52	118 59 30	1,230					T
BR04	41 04 31	119 01 05	1,209	.51	89.6-90.8	51	Sc	T,L,TC,W
BR05	41 03 06	119 01 24	1,216					T,TC
BR06	40 59 34	119 05 58	1,190		87.2-88.4	51	Sc	T,L,W
BR07	41 01 18	119 03 48	1,191		95.7-96.9	51	Sc	T,L,F,W
BR08	40 56 09	119 05 54	1,190		96.3-97.5	51	Sc	T,L,F,W
BR09[5]	40 54 23	119 08 15	1,190		41.5-42.7	51	Sc	T,L,F,W
BR10[5]	40 52 39	119 06 11	1,190		96.3-97.5	51	Sc	T,L,F,W
BR11	40 52 21	119 10 08	1,190		96.3-97.5	51	Sc	T,L,F,W
BR12	41 07 54	119 00 00	1,228	.88	45.1	38	Sc	T,W
BR13	40 57 53	119 09 30	1,204		5.8-7.0	51	Sc	L,W
BR14	40 44 04	119 10 56	1,212		6.1-7.3	51	Sc	L
BR15A	40 40 25	119 16 23	1,218		43.0-44.2	51	Sc	L
BR15B	40 40 25	119 16 23	1,218		25.3-26.5	51	Sc	L
BRD51A	40 59 42	119 00 32	1,202	.37	85.0-86.3	102	Sc	L,W
BRD51B	40 59 42	119 00 33	1,202	~ .62	84.1-85.3	51	Sc	T,L,W
BRD52A	40 59 08	119 00 32	1,200	.72	89.9-91.1	102	Sc	L
BRD52B	40 59 08	119 00 33	1,200	.36	90.2-91.4	51	Sc	T,L
BRD53A	41 04 58	119 00 20	1,233	.38	90.2-91.4	102	Sc	L,W
BRD53B	41 04 59	119 00 20	1,233	~ .12	59-7-61.0	51	Sc	T,L,W
BRD53C	41 04 57	119 00 20	1,234		9.8-10.1	102	Sl	L
BRD57A	41 02 14	119 01 08	1,211	.47	78.3-79.6	102	Sc	L,W
BRD57B	41 02 14	119 01 09	1,211		78.3-79.6	51	Sc	L,W
PW1	41 07 38	119 07 29	1,215	~ .12	(234.47)	95		F
PW2	41 07 37	119 07 30	1,215	~ .03	(221.52)	95		F
PW3	41 07 36	119 07 28	1,215	- .05	(36.14)	95		F
PW4	41 07 34	119 07 27	1,215	- .09	(43.38)	95		F
PW290	41 07 15	119 06 06	1,214	.0	(26.9)	152		L,F
PW1635	41 07 05	119 08 02	1,232	~ .15	308.5	357 254 203	O	L,W
PW1636	41 07 16	119 06 05	1,214	.0	81.7 (88.9)	254	O	L,F
PW289[5]	41 07 03	119 07 34	1,220	.0	82.9 (140.4)	102	O	L,W

[1] Value in parenthesis is the sounded or reported total depth of hole. Value with asterisk (*) derived from temperature profile of the well.

[2] Well cased with more than one casing diameter where indicated.

[3] Sc = screen, Sl = slotted, Sh = shot, P = perforated, O = open casing.

[4] There is also a shallow well of approximately 6.1 m depth and screened at this well site. These are designated GRB', GRD', etc.

[5] Correlation with available drilling logs somewhat uncertain. Log No. 289 in the office of the State Engineer may not be correct for this well.

APPENDIX 4.--*Geothermometer temperatures for water with measured source temperatures greater than 25 °C*

[Estimates were calculated by the program SOLMNEQ (Kharaka and Barnes, 1973). All temperatures are in degrees Celsius.]

Site name	Chloride (milligrams per liter)	Quartz		Na/K	Sodium-potassium-calcium	
		Conductive	Adiabatic		β=1/3	Magnesium-corrected
PLOTTING SYMBOL B						
TH SP #1 SULPHUR 2NW QD	1,700	137	133	26	117	102
TH SP#1 SOLD CR 4SE QUAD	570	105	105	134	170	97
BLACK ROCK SPRING	180	117	115	77	141	88
WELL BRD51A	4,000	81	84	166	181	207
TH SP #4 ORA SOLD CR 4SE	210	143	137	112	153	128
TH SP #3 ORG SOLD CR 4SE	160	105	106	115	153	103
TH SP #3 ORA SOLD CR SE	120	125	122	99	144	108
TH SP#2 ORE SOLD CR 4SE	84	152	145	100	148	144
PLOTTING SYMBOL D						
WELL BRD57A	140	45	53	71	143	138
DOUBLE HOT SPRINGS	59	140	135	64	126	130
DOUBLE HOT SPRINGS	53	167	158	57	122	130
DOUBLE HOT SPRINGS	80	140	135	57	117	111
WELL DHS2	110	152	145	56	115	110
WELL DHS3	120	144	138	59	120	121
WELL DHS4	120	129	126	93	140	138
DOUBLE HOT SPRINGS, ORIFICE 1	59	137	133	60	125	127
DOUBLE HOT SPRINGS, ORIFICE 2	59	137	133	60	124	126
DOUBLE HOT SPRINGS, ORIFICE 3	58	143	137	58	123	132
DOUBLE HOT SPRINGS, ORIFICE 4	59	143	137	60	125	131
DOUBLE HOT SPRINGS, ORIFICE 5	61	137	133	59	123	96
DHS #4	270	102	103	56	134	131
DHS #4	220	103	103	34	118	128
DHS #5	48	88	91	45	116	0
DHS #6	150	--	8	40	121	99
PLOTTING SYMBOL G						
GREAT BOILING SPRING, ORIFICE 3	2,200	167	158	175	205	201
GREAT BOILING SPRING, ORIFICE 9	2,100	172	162	146	190	185
GREAT BOILING SPRING, ORIFICE 18	2,230	175	164	167	202	194
GREAT BOILING SPRING, ORIFICE 19	2,100	171	161	182	208	204
GREAT BOILING SPRING, ORIFICE 22	2,400	173	162	147	193	187
GREAT BOILING SPRING, ORIFICE 23	2,200	169	159	159	197	192
GREAT BOILING SPRING, ORIFICE 24	2,080	170	160	165	201	196
GREAT BOILING SPRING, ORIFICE 27	2,180	171	161	176	207	200
GREAT BOILING SPRING, ORIFICE 28	2,180	170	160	167	202	192
GREAT BOILING SPRING, ORIFICE 37	2,340	177	166	176	205	199
GREAT BOILING SPRING, ORIFICE 43	2,230	170	160	151	196	189
GREAT BOILING SPRING, ORIFICE 46	2,350	170	160	184	205	200
GREAT BOILING SPRING, ORIFICE 46	2,100	183	171	166	200	196
GREAT BOILING SPRING, ORIFICE 48	2,300	165	156	141	187	183
GREAT BOILING SPRING, ORIFICE 55	2,130	173	162	169	203	197
GREAT BOILING SPRING	2,200	165	156	150	192	188
DITCH	2,150	174	164	164	199	192
MUD SPRINGS, ORIFICE 1	2,100	170	160	170	203	193
MUD SPRINGS, ORIFICE 1	2,200	176	165	166	199	191
MUD SPRINGS, ORIFICE 2	2,075	170	160	168	202	194
MUD SPRINGS, ORIFICE 2	2,200	157	149	141	186	178
MUD SPRINGS, ORIFICE 9	2,130	167	158	181	208	200
MUD SPRINGS, ORIFICE 13	2,400	170	160	162	203	194
HORSE	1,915	174	163	177	205	200

APPENDIX 4.--*Geothermometer temperatures for water with measured source temperatures greater than 25 °C*--Continued

Site name	Chloride (milligrams per liter)	Quartz		Na/K	Sodium-potassium-calcium	
		Conductive	Adiabatic		β=1/3	Magnesium-corrected
---------- PLOTTING SYMBOL H ----------						
TH SP HARDIN CITY SE QD	76	114	113	53	129	129
TH SP #1 OR B SOL CR 4NE	57	131	127	78	141	130
---------- PLOTTING SYMBOL M ----------						
WW3922T2	51	127	124	142	173	156
UNNAMED WELL	28	124	122	228	192	79
PW290	35	120	118	248	201	129
PW1636	23	119	117	252	203	128
WELL AT WAGNER SPRINGS	35	110	109	193	171	107
---------- PLOTTING SYMBOL O ----------						
TREGO HOT SPRINGS	280	128	125	51	124	127
TREGO HOT SPRINGS ORIFICE A	550	127	124	54	126	120
TREGO HOT SPRINGS	520	128	125	51	119	114
MCCLELLAN RANCH WELL	290	129	126	141	169	164
MCCLELLAN RANCH WELL	278	134	130	78	134	136
---------- PLOTTING SYMBOL R ----------						
GRANITE CREEK	21	60	65	277	176	76
---------- PLOTTING SYMBOL S ----------						
TH SP #5 MUD MDW QD SW29	21	114	113	23	90	113
TH SP#10 ORB MUD MDWSE25	17	111	111	41	102	119
THERMAL SP NO. 2 MUDMEADO	17	111	110	40	101	120
TH SPR #3 MUD MDW QUAD	12	114	113	40	100	118
TH SPR #1 MUD MDW QUAD	26	111	110	16	85	67
SOLDIER MEADOW SPRING 1	18	113	112	29	93	71
SOLDIER MEADOW SPRING 2	18	113	112	34	97	117
TH SPR #6 OR A MUD MDW Q	14	113	112	33	94	105
TH SPR #9 MUD MEADOW QUA	18	112	111	35	98	107
TH SP #4 SOLD MDW QD NW18	18	111	110	18	87	114
TH SP #1 ORA SLDR MDW QD	13	114	113	319	208	78
TH SP #3 SLDR MDW QD SW5	12	113	112	384	218	73
---------- PLOTTING SYMBOL U ----------						
FLY RANCH WARDS HOT SPRINGS	275	128	125	98	147	81
WELL NEAR GERLACH	240	126	124	115	153	105
HUALAPAI FLAT SPRING 1	250	130	127	106	150	145
HUALAPAI FLAT SPRING 3	240	131	127	106	152	146
WESTERN SPRING	275	131	128	105	152	147
HUALAPAI FLAT SPRING 16	250	131	128	101	150	145
HUALAPAI FLAT SPRING 18	245	130	127	106	152	146
HUALAPAI FLAT SPRING 41	260	131	128	90	147	143
HUALAPAI FLAT SPRING 50	250	126	124	87	144	140
HUALAPAI FLAT SPRING 63	255	129	126	86	141	136
HUALAPAI FLAT SPRING 82	245	126	124	102	152	147

APPENDIX 5.--*Selected piezometric heads and flow measurements for wells in the western arm of the Black Rock Desert*

Name of test well	Altitude of land surface (meters)	Static water level (meters)	Static pressure (meters of water)	Open flows (liters per second)	Date of measurement
GRA	1,190	2.02			10-07-80
GRB	1,190		*		10-07-80
GRB'	1,190	2.79			10-07-80
GRD	1,190		*		10-07-80
GRD'	1,190	1.27			10-07-80
GRH	1,190	~ .25			10-07-80
GRI	1,191	.13			10-07-80
GRI'	1,191	1.47			10-07-80
GRL	1,191		*		10-07-80
GRL'	1,191	2.10			10-07-80
BR01A	1,250	31.73			12-11-80
BR04	1,209	3.97			11-05-80
BR06	1,190		2.56		12-13-79
BR07	1,191		9.60	0.002	7-28-80
BR08	1,190		0.94	.006	7-17-80
BR09	1,190		1.31	.006	8-07-80
BR10	1,190		3.11		12-17-79
BR10'	1,190	.96			10-09-80
BR11	1,190		4.45	.022	8-07-80
BR12	1,228	1.09			11-05-80
BR13				5.1	12-20-79
DHS4	1,210		1.07		6-16-80
DHS5	1,210		2.87		6-17-80
BRD51A	1,202	.73			1-19-81
BRD51A	1,202	.61			4-28-81
BRD51A	1,202	.77			6-16-81
BRD51B	1,202	*			4-28-81
BRD52A	1,200	7.81			4-21-81
BRD52B	1,200	30.98			6-30-81
BRD53A	1,233	5.83			11-05-80
BRD53B	1,233	~27.74			5-06-81
BRD53B	1,233	~27.57			7-01-81
BRD57A	1,211	- .45			11-04-80
BRD57B	1,211		~2.90		4-30-81
PW1	1,215			~ .28	4-07-81
PW2	1,215			~ .06	4-07-81
PW3	1,215			~ .85	4-29-81
PW4	1,215			3.40	4-29-81
PW289	1,220	6.68			11-12-80
PW290				5.1	12-20-79
PW1635	1,232	~17.72			4-08-81
PW1636	1,214			~28	12-20-79

* Well flowing but no pressure measurements taken.